Assessment of Distribution System with Integration of Distributed Energy Resources and Electric Vehicles

Thesis Submitted for the Award of the Degree of

DOCTOR OF PHILOSOPHY

In

Electrical Engineering

By

Dharavat Nagaraju

Registration Number: 11916763

Supervised By

Dr. Suresh Kumar Sudabattula (21628)

Power System (Associate Professor)

Lovely Professional University, Punjab

Co-Supervised by

Dr. Velamuri Suresh

Electronics and Telecommunication

(Assistant Professor)

Symbiosis Institute of Technology, Pune

LOVELY PROFESSIONAL UNIVERSITY, PUNJAB

2023

DECLARATION

I, hereby declared that the presented work in the thesis entitled "**Assessment of Distribution System with Integration of Distributed Energy Resources and Electric Vehicles**" in fulfilment of degree of **Doctor of Philosophy (Ph.D.)** is outcome of research work carried out by me under the supervision **Dr. Suresh Kumar Sudabattula**, working as Associate Professor, in the **Power Systems/School of Electronics and Electrical Engineering** of Lovely Professional University, Punjab, India. In keeping with general practice of reporting scientific observations, due acknowledgements have been made whenever work described here has been based on findings of other investigator. This work has not been submitted in part or full to any other University or Institute for the award of any degree.

D. Nagaraju.

Name of the scholar: Dharavat Nagaraju

Registration No.: 11916763

Department/school: Power Systems/School of Electronics and Electrical Engineering

Lovely Professional University,

Punjab, India

CERTIFICATE

This is to certify that the work reported in the Ph.D. thesis entitled "**Assessment of Distribution System with Integration of Distributed Energy Resources and Electric Vehicles**" submitted in fulfillment of the requirement for the reward of degree of **Doctor of Philosophy (Ph.D.)** in the **Power Systems/School of Electronics and Electrical Engineering**, is a research work carried out by **Dharavat Nagaraju**, Registration No. **11916763**, is bonafide record of his/her original work carried out under my supervision and that no part of thesis has been submitted for any other degree, diploma or equivalent course.

(Signature of Supervisor)

Name of supervisor: Dr. Suresh Kumar Sudabattula

Designation: Associate Professor

Department/school: Power Systems/School of Electronics and Electrical Engineering

University: Lovely Professional University, Phagwara, Punjab (India)

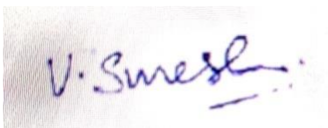

(Signature of Co-Supervisor)

Co-Supervisor: Dr. Velamuri Suresh

Designation: Assistant Professor

Department/School: Power Systems/Electronics and Telecommunication

University: Symbiosis Institute of Technology, Pune (India)

Place: Phagwara

Date: 06/06/2023

ABSTRACT

Distributed Energy Resources (DERs) usage in the distribution system (DS) is becoming more prevalent due to several factors, including rising demand for electricity, concern about environmental issues, uncertainty in fuel costs, trends toward deregulatory action, and rapid technological advancement. According to the findings of numerous studies, most of the electricity produced is lost in the DS in the form of I^2R losses. Consequently, minimising power losses (P_{Loss}) as much as possible and enhancing the voltage profile and stability of the DS have become essential concerns in the modern era. Since the beginning of the 21st century, a wide variety of power system engineers, researchers, and scientists have been focusing their efforts in this field to efficiently solve the issue of DERs allocation in the DS to get the maximum feasible benefits.

Electric Vehicles (EVs) are gradually becoming more popular than gasoline-powered automobiles as a solution to the environmental issues caused by greenhouse emissions and as a means to protect ourselves from the consumption of fossil fuels. The rapidly growing number of EVs has the possibility of raising the load demands, further increasing the feeder currents and degrading the voltage profiles of the DS. If DGs are placed in improper locations, this will lead to additional P_{Loss} and will cause a significant fall in voltage profile and voltage stability. Placing renewable distributed generators (RDGs) as a technique for revamping the voltage profile of the DS is a standard procedure for electrical engineers who work for utility companies. Establishing strategies for through this thesis, an efficient method for addressing the issue of DERs allocation in DS has been given. Optimally sizing and placing RDGs and Electric vehicle charging stations (EVCS) in the DS is essential to minimise the P_{Loss} and voltage profile enhancement.

In this research work an efficient technique for tackling distributed generators (DGs) allocation problems, EVCS location problems, and simultaneous RDGs and EVCS problems in the DS is discussed. The primary goals are to shrink the P_{Loss} and increase the voltage profile of the DS. In addition, the uncertainties in generation associated with RDGs powered by solar irradiation or wind speed can be properly predicted using appropriate probability distribution functions (PDFs). Beta PDF for modelling solar irradiation and weibull PDF for modelling wind speed and further the exact output power from the solar and wind based DGs are calculated. The loss sensitivity factor (LSF) and voltage stability Index (VSI) are utilised to determine the suitable placement of RDGs and EVCSs. In addition, the sizes at these

places are determined by the political optimisation algorithm (POA). Further, several operational constraints associated with the DS are considered while solving this problem. Also, the efficacy of POA is compared with other existing algorithms in the literature; it observed that POA performance is superior to other methods in all aspects.

The developed approach is evaluated on the standard IEEE 33, IEEE 69 bus systems and 28 Indian bus system. Further, EV charging and discharging patterns are examined to check the performance of DS. The static and dynamic load variations are considered to study the performance of the system. Different cases, such as single RDG, multiple RDGs, only EVs and the combination of RDGs plus EVs, are considered to check the method's effectiveness. Furthermore, different EV charging methods, such as conventional charging method (CCM), optimised charging method (OCM) and different modes such Grid 2Vehicle (G2V) plus vehicle 2 Grid (V2G) assessed. And the results are simulated, and from the results, it is observed G2V plus V2G method gives the best results. The obtained results verified that proper placement of RDGs and effective charging strategies for EVs reduce the P_{Loss} considerably.

PREFACE/ACKNOWLEDGEMENT

Without the encouragement and assistance of wonderful people throughout my time as a PhD student, I would never have been able to complete this work. While I was doing this research, I was accompanied by a humongous number of people, and I am extremely grateful to each and every one of them.

To my esteemed Supervisor, **Dr. Suresh Kumar Sudabattula**, Associate Professor at the School of Electronics and Electrical Engineering in Phagwara, Punjab (India), I would like to extend my deepest gratitude for his direction, motivation, constructive criticism, and support. In my pursuit of knowledge, he has been there for me, giving his wholehearted support at all times and providing me with helpful guidance, inspiration, and insights.

Dr. Velamuri Suresh, Assistant Professor, Symbiosis Institute of Technology, Pune (India) my co-supervisor, is acknowledged with sincerity and a great sense of gratitude for his useful guidance, motivating attitude, and on-going stimulation in the pursuit of the current study. I appreciate his patience and the time he took to go through the research work.

Where emotions are involved, words don’t seem adequate to express. A vocabulary finds no appreciation to express my heartfelt love and thanks to my cherishing parents, **Dharavat Gyamla** and **Dharavat Jeji**, who have been the fulcrum of true life to me as well as making me realize the importance of time.

I express my gratitude to **Dr. Shama Kakkar**, **Dr. Leander Corrie**, **Dr. Vaseem Akram**, and **Dr. Yasir Afaq** who has stood rock solid since we`ve been friends. They gave advice when sought and their role in keeping me well-grounded by advising me not to forget to take care of myself during research.

I’d want to thank everyone at Lovely Professional University for their help in getting me set up with the resources I needed to do my work on time. I’d also like to express my respect and gratitude to the School of Electronics and Electrical Engineering and the Division of Research & Development for their encouragement throughout my time as a PhD scholar. Finally, I’d like to thank the almighty God for helping me to reach such a significant milestone.

Date: 06/06/2023 Dharavat Nagaraju

TABLE OF CONTENT

LIST OF TABLES

LIST OF FIGURES

LIST OF ABBREVIATIONS

ALOA	Ant Lion Optimisation Algorithm
BFWA	Backward-forward Sweep Algorithm
BPSO	Binary Particle Swarm Optimization Algorithm
BEV	Battery Electric Vehicle
BC-ABOA	Binary Collective-Animal Behaviour Optimization Algorithm
BLPM	Bi-level Programming Model
BFPF	Backward Forward Power Flow
BOA	Bat Optimization Algorithm
CCM	Conventional Charging Method
CSA	Cuckoo Search Algorithm
CSA-PSO	Crow Search Algorithm-Particle Swarm Optimisation
CTLBO	Comprehensive Teaching Learning-Based Optimisation
CF-PSO	Constriction Factor-Particle Swarm Optimisation
DGs	Distributed Generators
DS	Distribution System
DER	Distributed Energy Resources
DA	Dragonfly Algorithm
EVs	Electric Vehicles
EDS	Electric Distribution System
EP	Evolutionary Programming
EGOA	Enhanced Grasshopper Optimization Algorithm
EDM	Empirical Discrete Metaheuristic

FAME	Faster Adaption and Manufacturing
Full-HEV	Full Hybrid Electric Vehicle
FA	Firefly Algorithm
FCEV	Fuel Cell Electric Vehicle
FES	Fuzzy Expert System
FPA	Flower Pollination Algorithm
FBSM	Forward Back Word Sweep Method
GW	Gigawatts
G2V	Grid 2 Vehicle
GA	Genetic Algorithms
GWO	Grey Wolf Optimizer
GOA	Grasshopper Optimisation Algorithm
GAMS	General Algebraic Modelling System
GRASP	Greedy Random Adaptative Search Procedure
GOA	Grasshopper Optimization Algorithm
GABC	Gbest-guided Artificial Bee Colony
HBB-BC	Hybrid Big Bang- Big Crunch
HGWO	Hybrid Grey Wolf Optimizer
HM	Heuristic Method
HQCFT	Heuristic Quadratic Curve Fitting Technique
HOA	Hybrid Optimization Algorithm
HHOA	Harris Hawk Optimization Algorithm
HAPSO	Hybrid Analytical-Particle Swarm Optimization

IA	Improved Analytical
ICA	Imperialist Competitive Algorithm
IPSO	Improved Particle Swarm Optimization
IMDEA	Intersect Mutation Differential Evolution
JOA	Jaya Optimization Algorithm
kW	Kilo Watt
kVAr	Kilo Volt Ampere of Reactive Power
LV	Low Voltage
LSF	Loss Sensitivity Factor
LHS	Latin Hypercube Sampling
LSF	Loss Sensitivity Factor
LSF-BFOA	Loss Sensitivity Factor -Bacterial Foraging Optimisation Algorithm
MW	Mega Watt
M-HEV	Mild Hybrid Electric Vehicle
MILP	Mixed-integer Linear Problem
MMOPM	Maximum and Minimum Optimization Planning Model
MCS	Monte Carlo Simulation
MPSO	Modified-Particle Swarm Optimisation
MCS	Monte Carlo Simulation
MPDIPA	Modified Primal-dual Interior Point Algorithm
NSGA	Non-Dominated Sorting Genetic Algorithm
NDC	National Determined Contribution

OCM	Optimized Charging Method
OCSTA	Optimal Charging Starting Time Algorithm
OPF	Optimal Power Flow
OT	Optimization Technique
PAR	Peak-to-Average Ratio
P_R	Power Ratio
P_{Loss}	Power Loss
PF	Power Factor
P-HEV	Plug-in Hybrid Electric Vehicle
PSO	Particle Swarm Optimization
POA	Political Optimisation Algorithm
QOTLBO	Quasi-Oppositional Teaching Learning-Based Optimisation
RDGs	Renewable Distributed Generators
RDER	Renewable Distributed Energy Resource
RES	Renewable Energy Sources
SCs	Shunt Capacitors
SoC	State of Charge
SSA	Salp Swarm Algorithm
SCA	Sine Cosine Algorithm
SFSA	Stochastic Fractal Search Algorithm
SHADEOA	Success History Based Adaptive Differential Evolution Algorithm
TSA	Tabu Search Algorithm

UPF	Unity Power Factor
VRE	Variable Renewable Energy
V2G	Vehicle 2 Grid
VSI	Voltage Stability Index
WOA	Whale Optimisation Algorithm

CHAPTER 1

INTRODUCTION

1.1 Introduction:

The Paris Agreement, signed in 2015 by parties to the United Nations Framework Convention on Climate Change (UNFCCC), was a significant agreement to combat global warming. To meet the aims of this agreement, several countries worldwide foresee a fully carbon-free and sustainable energy grid by 2050[1]. The use of renewable energy sources (RES) is rapidly increasing to meet expanding global electricity demand. Wind and solar RES presently provide the most worldwide renewables, and they are predicted to continue their phenomenal rise to overtake mainstream power plants in the power generation sector. This rise is primarily due to the environmental benefits of renewable energy over conventional power plants, such as reduced CO_2 pollution and global warming, the economic benefits of RESs and the creation of employment opportunities [2]. The coal-fired power plants are far from the load centres, resulting in significant losses in transmission and distribution (T&D). Distributed Generators (DGs) are small, economical, and decentralized power production systems that rely primarily on renewables such as solar and wind energy and are situated near load centres. Using RES-based DGs to generate electricity has several advantages, including reduced power loss (P_{Loss}), zero-carbon output, lower operational expenses and enhanced voltage profile.

Further, electric vehicles (EVs) utilization in the current scenario increased drastically throughout the world. This creates problems in the existing system, particularly during peak demand. But, from an environmental perspective, it is vital to use EVs in the transportation sector. Furthermore, proper assessment is needed in a distribution system (DS), such as integrating DGs and EVs. The concept of an alternative sources DS and its control has grown as one of the most important research areas in the electricity sector [3].

1.2 Renewable Energy Development:

Asia continued its dominance over other regions in terms of new solar photo voltaic (PV) installations for the ninth year in a row, accounting for 52% of the world’s total capacity increase in 2021. In addition, the bulk of photovoltaic farms is located in Asia. Asia (mainly China) was the leading regional consumer of wind power for the thirteenth year in a row, accounting for around 61.4% of newly installed wind power capacity (an increase from nearly 60% in 2020).

Approximately 48.6% of the world's offshore capacity was located in Asia, primarily in China. As of 2019, it is predicted that there are 47 million people connected to a total of 19,000 mini-grids worldwide. Asia was home to sixty percent of all mini-grids already in operation and over two thousand mini-grids still in development. South Asia had the third largest market internationally in 2021, with 869,833 off-grid PV goods sold [4].

With a renewable electricity capacity addition of 15.4 gigawatts (GW) in 2021, India was positioned third on the global stage, behind only China (136 GW) and the Americas (43 GW). India's overall amount of hydropower plants increased to 45.3 GW due to the addition of 843 MW in 2021. Regarding new solar photovoltaic capacity, India was the 3rd biggest market in the world and the 2nd biggest market in Asia (13 GW of added in 2021). In total installations, it achieved position number 4th (60.4 GW), moving ahead of Germany (59.2 GW) for the first time. After China, the United States of America, and Germany, India came in third place worldwide in terms of the total installed capacity of wind power (40.1 GW) [5]. India has expanded its countrywide solar generation initiative, offering incentives to local and foreign firms for setting up battery manufacturing units by INR 18,100 crore (USD 24.3 billion). The amount of money put into renewable energy in India climbed by 70 percent, to USD 11.3 billion [5].

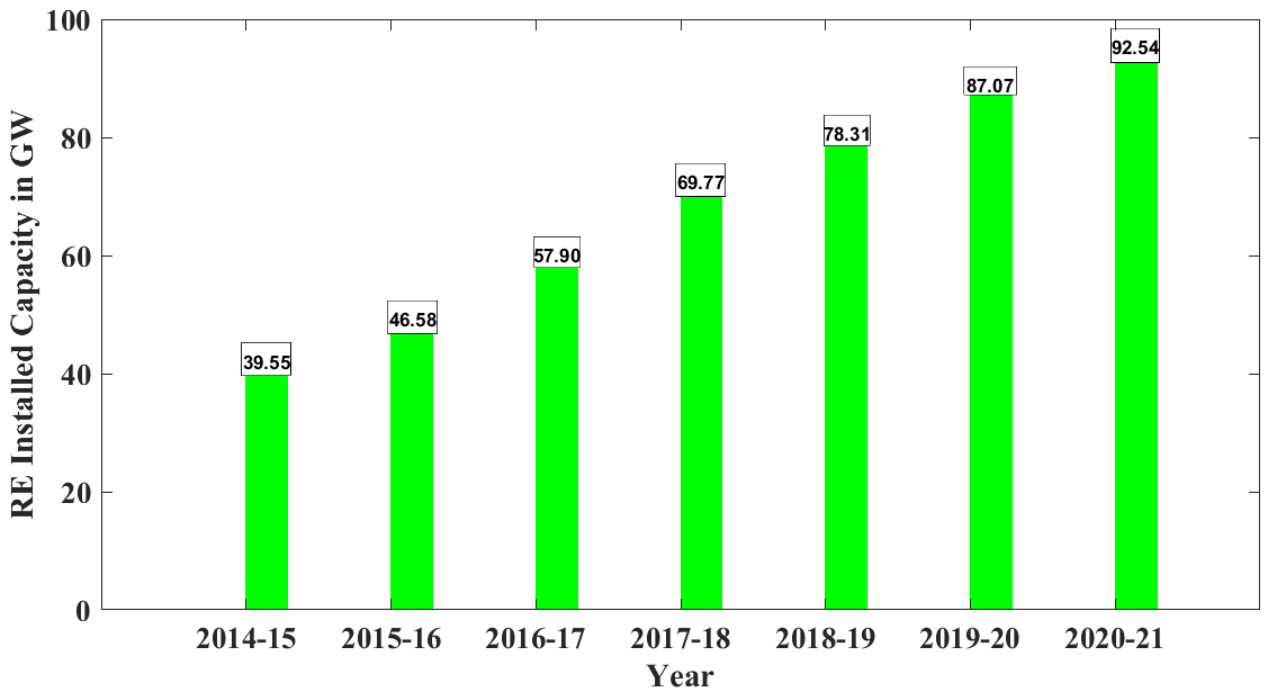

Fig. 1.1. Renewable energy installed capacity for the period of 2014-21

To decrease the amount of carbon pollution that its GDP produces by 33 to 35% by the year 2030 compared to the level it was at in 2005. To accomplish about 40% of cumulative electric power installed capacity from Non-fossil fuel-based energy resources by the year 2030 with the assistance of the transfer of technology and low-cost international financing. By the Paris Agreement, these commitments represent India's NDC for 2021-2030. The government of India is well on its way to accomplishing these goals. [6] The installed capacity of RE in India expanded by two and a half times in the middle of April 2014 and January 2021, the same depicted in Fig. 1.1, while within the same time period, the installed capacity of solar energy climbed by 15 times; In the middle of April 2020 and January 2021, India added 5.47 GW to its cumulative installed capacity for renewable energy sources, bringing the total to 92.54 GW, excluding extensive hydroelectric facilities. % of RE installed capacity is shown in Fig. 1.2. India now holds the fourth-highest capacity in the world for renewable energy sources, the fourth-highest capacity for wind power, and the fifth-highest capacity for solar power [6].

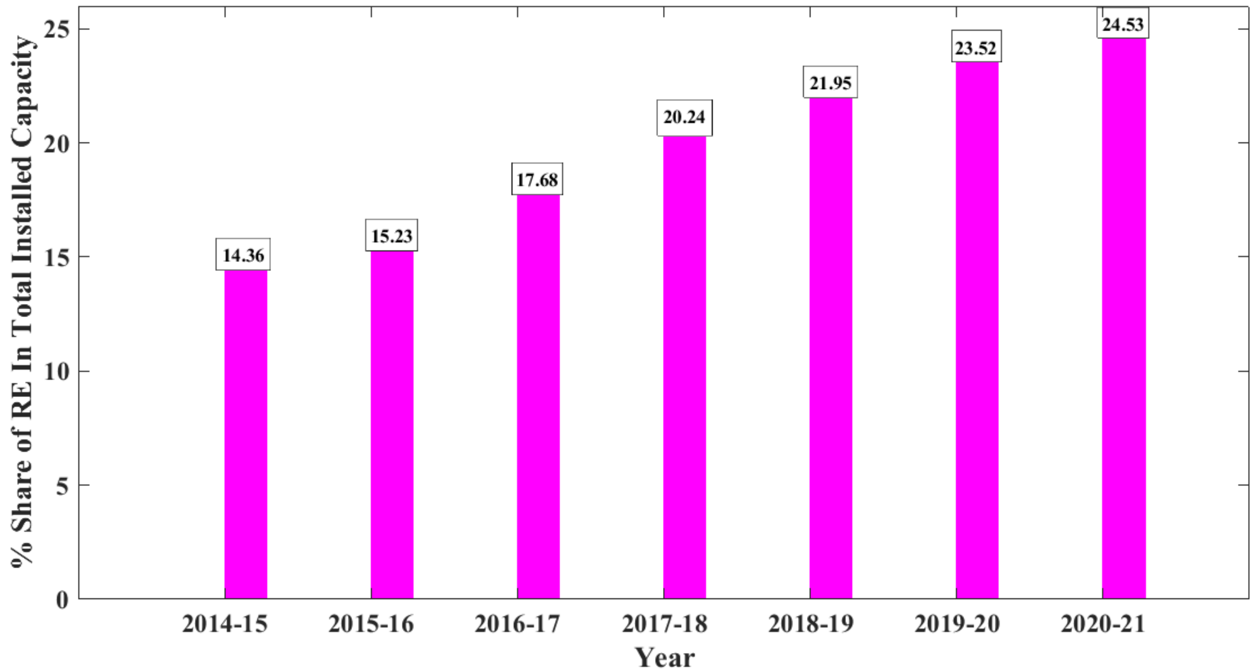

Fig. 1.2. Percentage share of Renewable installed capacity for the period of 2014-21

Some “smart cities” have adopted renewables in Asia, which has largely happened in India. [7] Diu Smart City made history in India in 2018 by being the first city to run entirely on renewable energy. The use of solar photovoltaic panels for on-site renewable energy generation in India’s urban centres is on the rise. The digitalization of urban transportation (as part of India’s FAME-II in 2019-2020) has been combined with the nation’s 2015 smart cities project to expand solar power production capabilities in urban areas. In 2020, just 13 cities across India had set goals for or implemented legislation related to renewable energy (from a global total of over 1,300 cities). However, this accounts for 18% of India’s urban population or 67.6 million people. There is less emphasis on net-zero goals in urban areas across India. Kolkata (2015), Chennai (2019), and Delhi (2020) are India's only net-zero-energy-by-2050 goal cities [7].

India faces three significant challenges: (1) how to increase the share of the population with access to affordable, clean electricity; (2) how to combine revamping shares of sustainable energy in a safe and trustworthy manner; and (3) how to decrease emissions to meet innovative and promising and environmental objectives without compromising economic growth. The amount of RE used varies significantly from state to state in India. Some of India's states are so abundant in renewable resources that they already have a more significant percentage of Variable RE (VRE) than the rest of the world combined. Gujarat, Tamil Nadu, Andhra Pradesh, Karnataka, Punjab, Telangana, Maharashtra, Rajasthan, Madhya Pradesh, and Kerala are some of India's most RE-rich states, each with a share of wind and solar that is much greater than the national average of 8.2%. In the finance year 2020/21, solar and wind will account for 29 percent of energy generation in Karnataka, 20% in Rajasthan, 18% in Tamil Nadu, and 14% in Gujarat [8].

Consequently, several states are already encountering difficulties with system integration. Further, massive changes are planned for the Indian electrical grid in the next decade. According to government plans, there will be a significant rise in renewable generating capacity from the current 175 GW in 2022 to 450 GW in 2030. The early power infrastructure in the country consisted of decentralized, locally owned generators. These were eventually linked together to construct grids across multiple states. The Indian government divided the country's states into five regions in the 1980s. Currently, the country's five regional grids, the Northern, Western, Eastern, Southern, and Northeastern, are all synchronously interconnected. It was in 2014 when India's system surpassed China's as the largest synchronous grid in operation. National Green Energy Corridor has been a strong advocate for developing renewable energy transmission networks since 2011. In order to reduce carbon from the power sector and keep up with the rising energy demand, it is crucial to integrate increasing shares of VRE, such as wind and solar PV, in power systems. Recent years have seen a meteoric rise in solar and wind installations due to plummeting prices and encouraging legislation [8].

In India, as per Central Electricity Authority (CEA) sector-wise installed capacity, in January 2022, installed capacity in the central sector = 98326.93 million units (MU), the private sector = 191434.46 MU, state sector = 105313. 68 MU, total installed capacity = 395075.07 MW. In April, the central sector = 99004.93 MU, private sector = 197148.33 MU, state sector = 104856.98 MU, total installed capacity = 401010.24 MW. In July 2022, the central sector = 99004.93 MU, private sector = 200158.70 MU, state sector = 104969.33 MU, total installed capacity = 404132.96 MW. On September 2022, the central sector = 99004.93 MU, private sector = 203831.84 MU, state sector = 104959.80 MU, total installed capacity = 407796.57 MW. The same is depicted in Fig. 1.3.

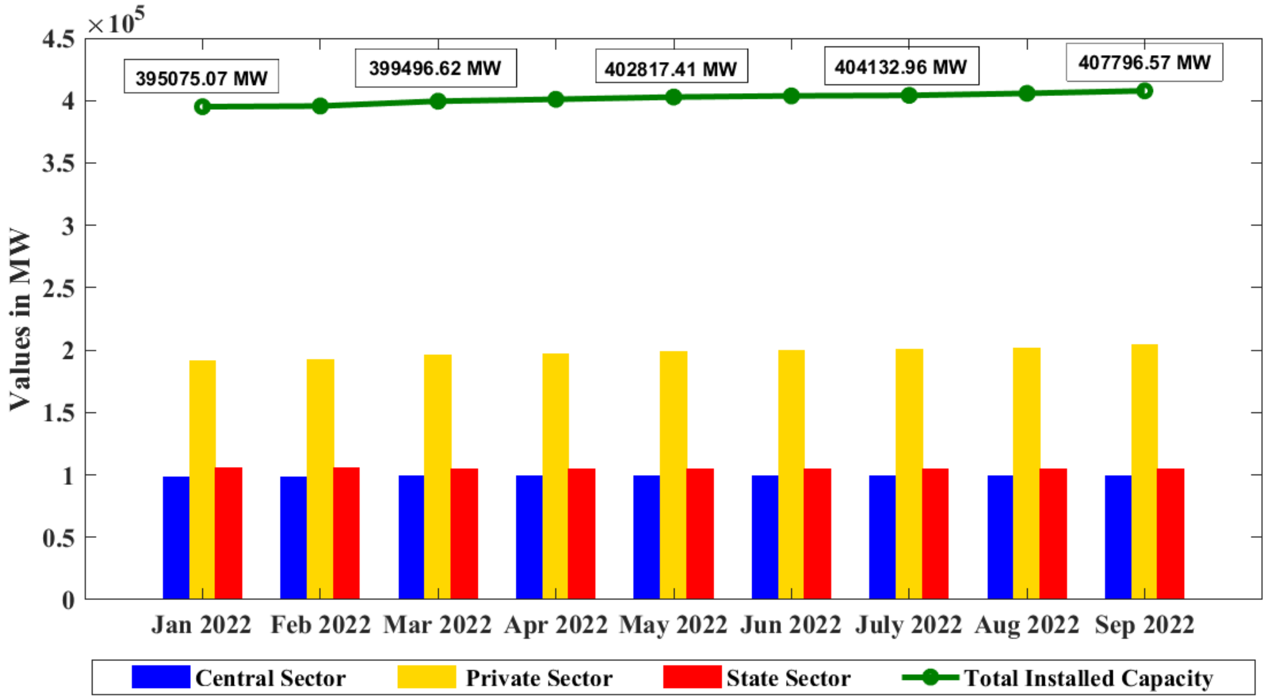

Fig. 1.3. In India sector wise installed capacity of RES from Jan 2022 To Sep 2022

1.3 Renewable Energy Global Investments:

Despite the setback imposed by Covid-19, investment in renewable energy sources for new power generation remained strong in 2020. In 2020, renewable energy accounted for more than 45 percent of overall power sector spending (including infrastructural development in networks). As the economy continues to improve, renewable energy investment is anticipated to rise further in 2021. Even though capital expenses are expected to decrease further in 2020, they are expected to climb by about 7% from 2019. In 2020, for instance, the worldwide average cost of installing utility-scale solar PV systems fell by 10%, while the cost of installing onshore wind systems fell by 5%. Spending on wind and solar PV installations in 2022 will yield four times as much as in 2010 due to technological advancements and cost reductions. The record number of wind turbines installed in 2020 significantly affected the 45 percent rise in renewable adoption that year. To reach 114 GW, wind capacity increased by almost double what it was in 2019, while solar PV grew by about a quarter to approximately 135 GW. While China installed an incredible 70 GW of new wind generating capacity, the United States came in second with the installation of more than

15 GW of wind generation. Though there were exceptions, many emerging markets and developing economics (EMDEs) experienced a negative shock to renewable investment in 2020. Vietnam, for instance, did a remarkable job of navigating the crisis while maintaining its ability to attract capital to renewables. While eliminating feed-in tariffs (FITs) for solar PV projects led to a decline in utility-scale investment, distributed PV drove sustained rapid growth in 2020, with more than 9 GW of rooftop solar placed [9]. Table 1 represents 2017 to 2021 global investment in green energy. In section 1.4 discussed DS impact on power system.

Table 1.1 Global Investments in Clean Energy 2017-2021

Globally Investment in Clean Energy			
Year	**Power Generation Investment In Billion Dollars**	**Renewable Generation Investment In Billion Dollars**	**% of amount Invested on Total Clean Energy**
2017	481	310	34
2018	480	318	34.3
2019	505	336	35.2
2020	513	359	41.7
2021	530	367	40.7

1.4 Distribution System (DS):

The electrical power system would not function properly without the presence of an electrical distribution system (DS). A type of distribution network is required to carry electrical energy from either an AC or DC source to the location where it will be consumed. Power distribution can be fast and simple, from where it is generated to where it is needed. More advanced electrical DS are used to distribute electrical power from the power station to factories, residential, and industrial sites. Main substations and customer substations are the two primary categories of DS that can be found nowadays. The primary substation, which acts as a load center, and the customer substation, which interfaces with the low voltage (LV) system, is considered substations. The term "consumer substation" is commonly used to describe a distribution room the customer typically supplies. The distribution room has space for several high-voltage switchgear panels and the transformer that enables low-voltage connections to the customer's incoming switchboard.

To achieve the desired level of supply reliability, a variety of network designs are feasible options. Depending on the geographic region, the DS can consist of overhead lines or underground cables. In most urban areas, electrical connections are made through cables, whereas overhead lines are the norm in rural areas. Equipment for protection, control, and monitoring is supplied to facilitate the efficient distribution network operation. Different types of DS are shown in Fig. 1.4. DGs role in DS discussed in section 1.5.

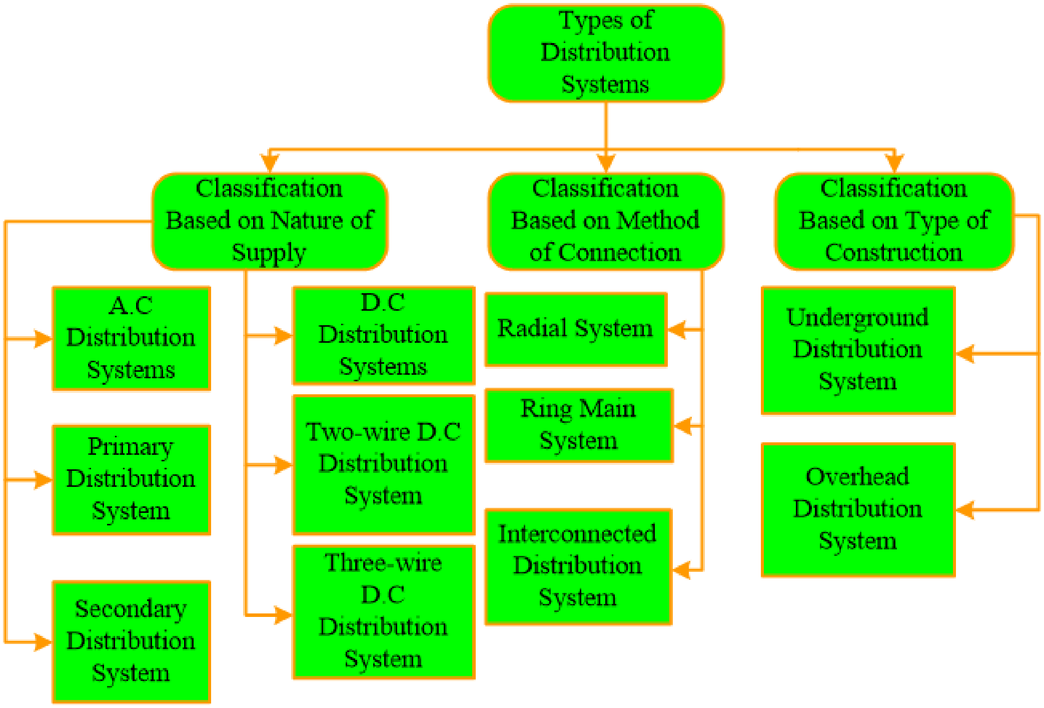

Fig. 1.4. Different types of DS

1.5 Distributed Generators (DGs):

The primary goal of utility companies is to offer electricity to their clients consistently, reasonably, and cost-effectively. Conventional power generation sources have been steadily reduced due to the continuously growing demand for electricity, which is increasing at an enormous speed. In today's liberalized electricity market, conventional electricity generating sources, which are run by a centralized authority, are not suitable due to the ecological and financial concerns they raise. From this point of view, DGs could be an answer to these problems, at least to some extent.

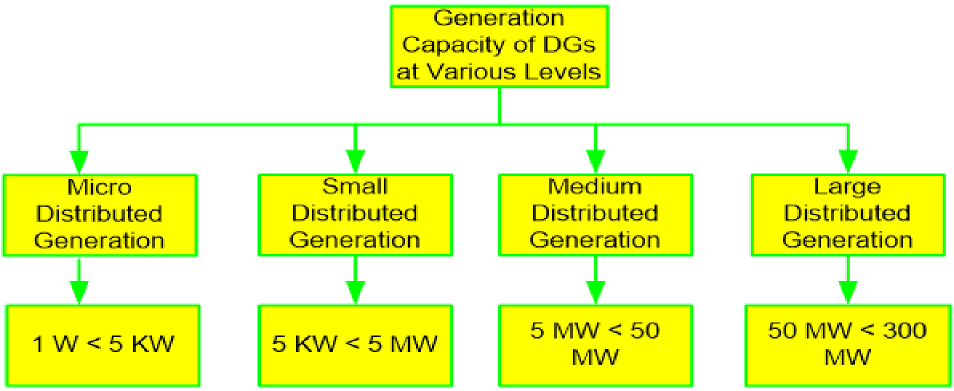

Fig. 1.5. Generation ranges of DGs [10]

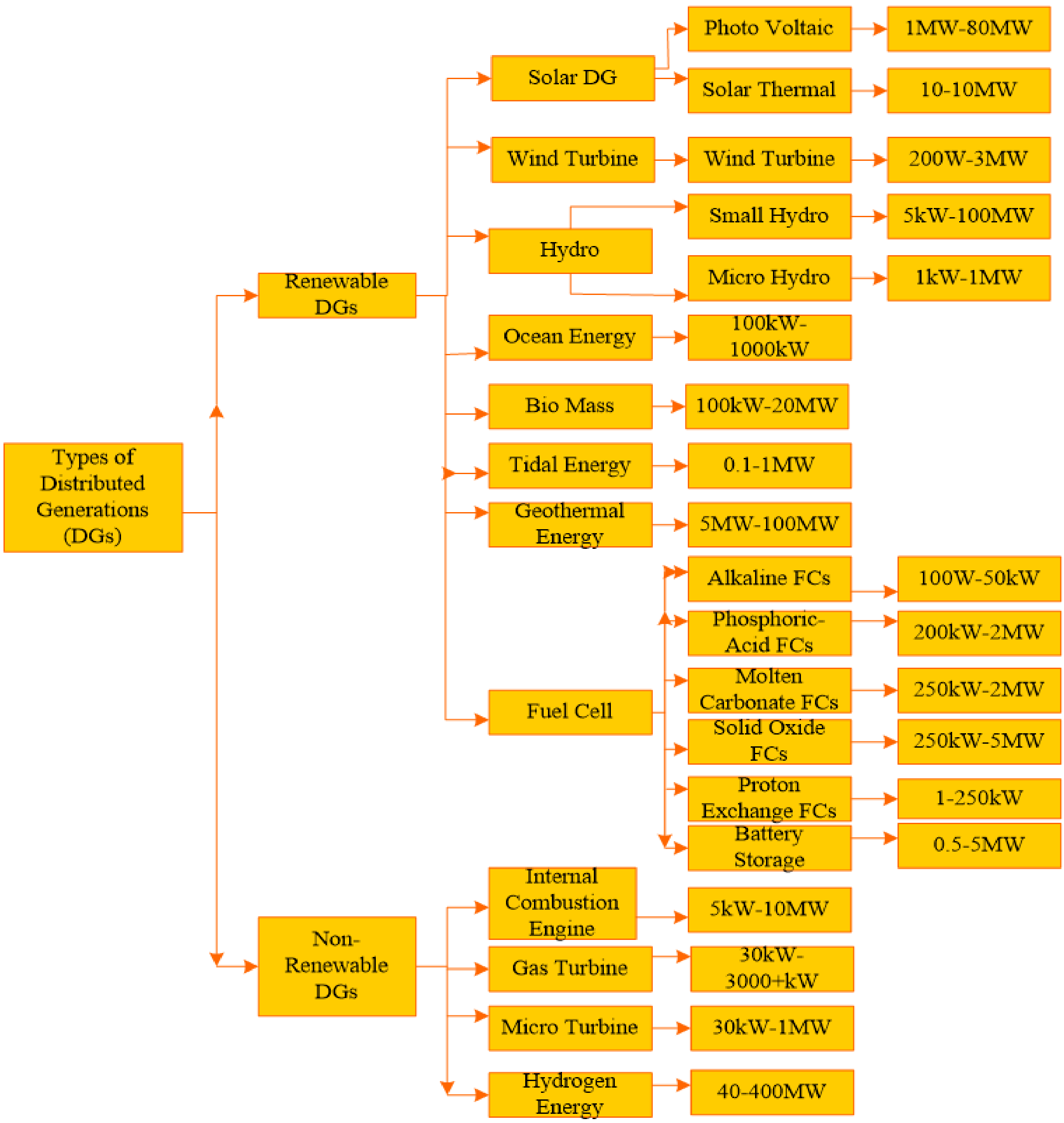

Fig. 1.6. Types of DGs and electricity generating ranges [10]

DGs are progressively becoming an essential component of the electric distribution system (EDS) as a result of their lower space requirements for installation, smaller unit sizes, and ability to be supplied by both renewable and non-renewable sources of energy.

The DGs have relatively low power outputs, which can range anywhere from a few kW to close to 300 MW, the same represented in Fig. 1.5 and different types of renewable and non-renewable DGs are represented with their generating capacities in Fig.1.6. In addition, DGs are sources of generating power that are connected directly to the customer's end of the supply chain. When DG units are located in the most convenient locations, system losses are drastically reduced, resulting in improvements in the voltage profile, system efficiency, stability, voltage security, and power quality. Additionally, DGs can dramatically reduce harmonics as well as voltage sags and swells, which are all undesirable phenomena. In addition to deferred expenditures in the transmission and distribution networks. As a result, the installation of DG in distribution networks is advantageous not only for end users but also for the supplying companies. In addition, the development of flexible DGs necessitates a smaller footprint, shorter construction time, and a smaller initial expenditure. As a direct result, DG has developed into a topic that many scientists are interested in studying [10].

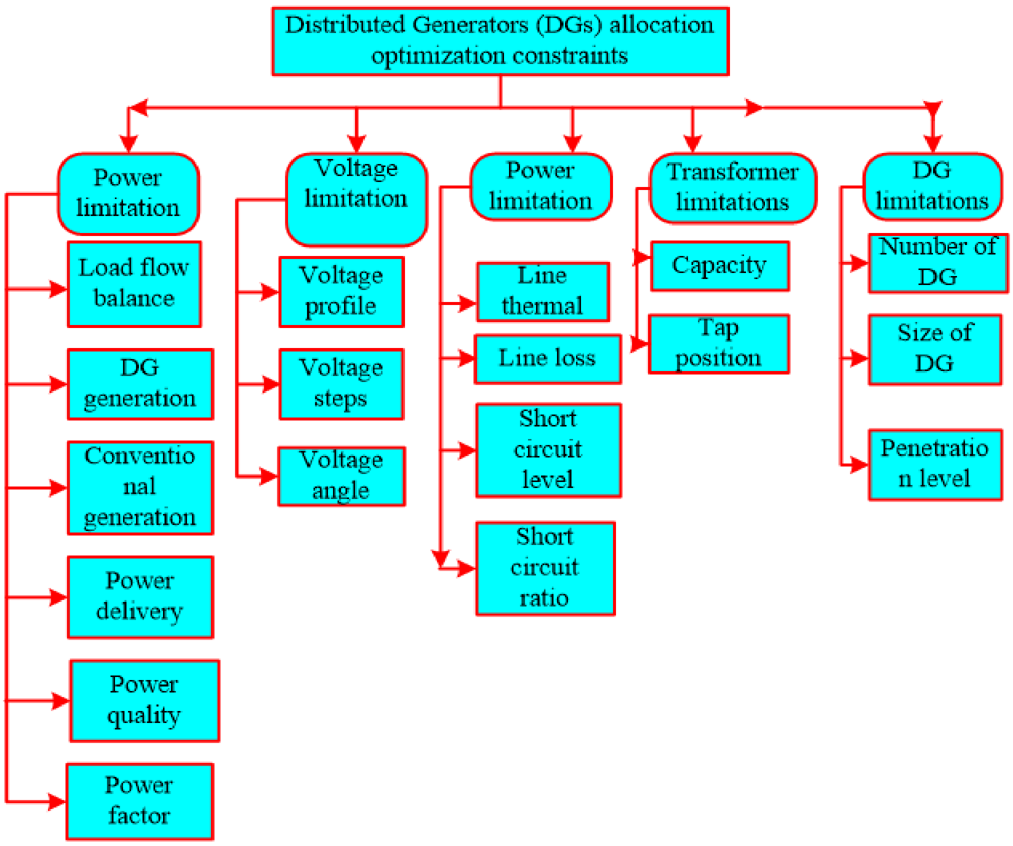

Fig. 1.7 DGs Constraints

If the DGs are not put in the most desirable areas, it has several drawbacks in addition to these advantages. There is a possibility that DG will cause stability issues. There is a possibility that bidirectional power flow will cause security challenges. In addition to the case of landing issues, there is also the possibility of frequency issues. Therefore, it is necessary to consider the significant difficulties and facts listed below regarding the allocation and sizing of DGs. Different types of DG constraints are represented in Fig. 1.7.

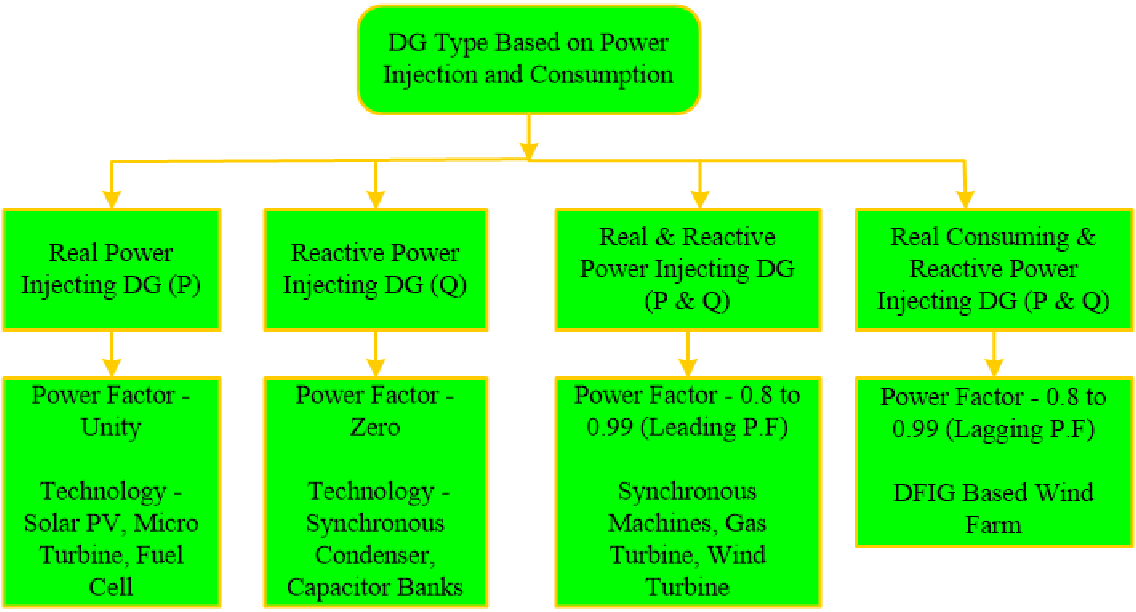

Fig.1.8 Different types of DGs based on electricity injecting and consumption [10]

When it comes to achieving maximum efficiency in the DS, the types of DGs that are used are an essential component. The kind of DG that will be put in to meet the load's requirements will determine. Only that, the nature of the electricity injected from DG units is the same as represented in Fig. 1.8. To optimize the overall effectiveness and efficiency of the system from a technical perspective, the parameters of DG, including their size and position, need to be appropriately determined. Assess the number of DGs to be installed in the power network and their classification (size) to ensure the system's most cost-effective functioning. Since DGs of an excessive size affect power flow in both directions. Analyze the system security components necessary for performing continuous duty and ensure that the applicable indexes (voltage profile index, power loss index, penetration level index, and short-circuit level index) are kept within the allowed ranges at all times. As a result, the placement of the DG becomes extremely important for ensuring a reliable operation and satisfying the requirements posed by the customers. Consequently, each of these factors needs to be carefully studied to get the most effective placement and sizing of the DG.

Fig. 1.9 The appropriate location of DG depends on seven different variables [10]

The location and size of a Solar and wind DGs inside an electrical system are decided by an optimization method that considers the system's objectives and other relevant criteria. For optimal placement of solar and wind DGs or any different DG types, factors such as Power Factor (PF), configuration system, limitations, and DG type may play a role the same represented in Fig.1.9 Both the distribution and transmission systems can benefit from these considerations.

It is vital to address DG's correct sizing and location in DS to make the most of the benefits that DG may provide. Consequently, it leads to a decrease in system losses, costs, and investments made by distribution firms or power utilities, as well as an increment in the voltage profile, system efficiency, and voltage stability, among other things. Prior researchers used the following techniques because they were found to achieve their objectives effectively. The primary strategies and approaches currently being utilized for obtaining the appropriate size and placement of DG can be divided into the following categories shown in Fig. 1.10. Importance of EVs in DS discussed briefly in section 1.6

Fig. 1.10. Different methodologies for determining the optimal size of DGs [10]

1.6 Electric Vehicles (EVs):

The EV market is one of the most vibrant in the clean energy sector. In 2021, 6.6 million EVs were sold, more than doubling the previous year's total. The global sales of EVs peaked in 2012 at only 120,00 units. Weekly sales in 2021 are expected to be higher than that. In 2021, about 10% of all automobile sales were electric, 4 times the overall share in 2019. This boosted the comprehensive number of EVs on the world's highways to approximately 16.5 million, which is approximately three times as many as in 2018. In the 1st quarter of 2022, 2 million EVs were sold worldwide, a 75% augmentation compared to the same period in 2021. Many factors are contributing to the EV market's growth. The primary support comes from continuing policy initiatives. By 2021, government investment in EV incentives and subsidies had nearly doubled to approximately USD 30 billion. An increasing number of nations have either committed to completely eliminating the use of internal combustion engines or set aims for the percentage of vehicles that will be electrified by 2050. While several manufacturers are planning to revamp their vehicles, they are going above and beyond what policy requires. Last but not least, the number of new EV models accessible to consumers in 2021 was five times higher than in 2015, making them a more appealing option. Roughly 450 different EV models are currently sold worldwide. In contrast, EV sales are still falling in other emerging and developing countries. This is because the many presently available cars are priced so high that they are expensive for customers purchasing in the marketplace. EV sales account for less than 0.5% of the total market in India, Brazil and Indonesia, respectively. In spite of this, EV sales more than double in several regions in 2021, particularly in India, which may open the door for more rapid market penetration by 2030 if resources and regulations that support it are in place [11].

Hybrid electric vehicles (HEVs) and all-electric vehicles (AEVs) are the two primary classifications that can be used for electric EVs. AEVs only have electric motors that are powered by other electrical components in their vehicles. Additional subtypes of AEVs include Battery Electric Vehicles (BEVs) and Fuel Cell Electric Vehicles (FCEVs) (FCEVs). An FCEV does not need a charging system located outside the vehicle. On the other hand, a BEV's storage unit can only be charged by utilising the external electricity supplied by the grid. One kind of hybrid electric vehicle (HEV) is called a plug-in hybrid electric vehicle (PHEV), and it has the capability of getting its battery charged from the power grid. Fig 1.11 provides a classification of the various types of EVs. The electrical infrastructure connects EVs to the grid. It's categorized by power type, charging circuit size, physical communication needs, and electricity flow direction, as shown in Fig 1.13. The supply grid, the EV charging points, and the EVs are all components of the EV charging governing structure, which can be categorized according to flexibility, collaboration, and the control framework itself. See Fig 1.14 for an illustration of this [12].

EVs are primarily utilized for transportation, but their influence can be seen in various contexts. As a consequence of this, the transformation in the automobile industry brought about by EVs has a significant impact not only on the environment but also on the economy and the power in substantial portions of electrical systems. The effect of EVs on the economy, climate, and electricity system is depicted in Fig 1.12. When charging happens during peak times, the system is overloaded, which can lead to malfunctioning or broken network infrastructure, disabling protection relays, and higher overall installation costs. The EVs' location, penetration level, and the amount of time they spend charging can all impact the grid's voltage stability. Load demand rises because EV charging locations, penetration rates, and plug-in and unplug times are all subject to the EVs' vagaries.

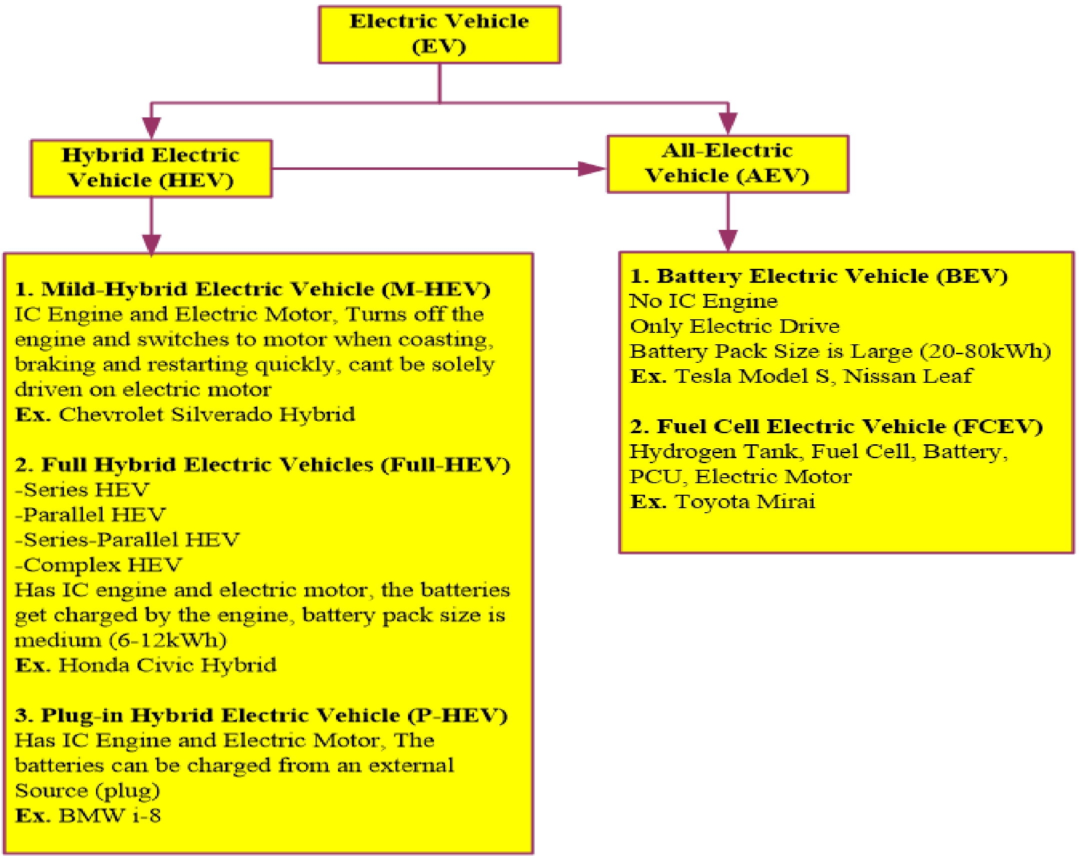

Fig. 1.11 various types of EVs [12]

The public's understanding of EVs' positive impacts on the economy and the ecosystem is increasing. This pattern will probably continue as more people are exposed to information about technology. Because the DS has a lower voltage profile and experiences a P_{Loss}, the placement of EVCS in the DS to accommodate the increasing demands for EV charging has certain drawbacks in the implementation of fast-charging stations. These drawbacks include the fact that the demand for EV charging has increased. These unfavorable results can be avoided, however, by positioning the EVCS strategically and incorporating it into the DS that is already in place. The DS ought to be able to satisfy the electricity requirements of the charging station. PHEVs offer a number of advantages; unfortunately, the widespread adoption of these vehicles and the absence of regulated charging will lead to an increase in peak demand. The appropriate planning of EVCS is required in order to fulfill the requirements of enhancing the voltage profile of the DS while EVCS is present. Therefore, the correct placement of EVCS installation within the DS significantly impacts the outcome.

The sudden adoption of EVCS over the current grid system results in significant issues with the power systems. These difficulties include electrical harmonics, a poor power factor, unpredictable voltage, and voltage instability. Because of these concerns, the capacity of the distribution equipment, such as conductors, electrical wires, and converters, is reduced, and the equipment also experiences a significant distribution loss, which brings down the system's overall efficiency. When EVs are being charged, the distribution branches of the network carry a significant quantity of current. This has a considerable impact on the electrical grid's power production and transmission systems. The influence on the distribution system depends on a broad range of variables, such as the methodology for charging, the demographic density of automobiles at their particular charging stations, and so on. This influence can be positive or negative depending on the parameters. Overall schematic diagram integrated solar, wind based DGs and EVs into the DS given in Fig 1.15.

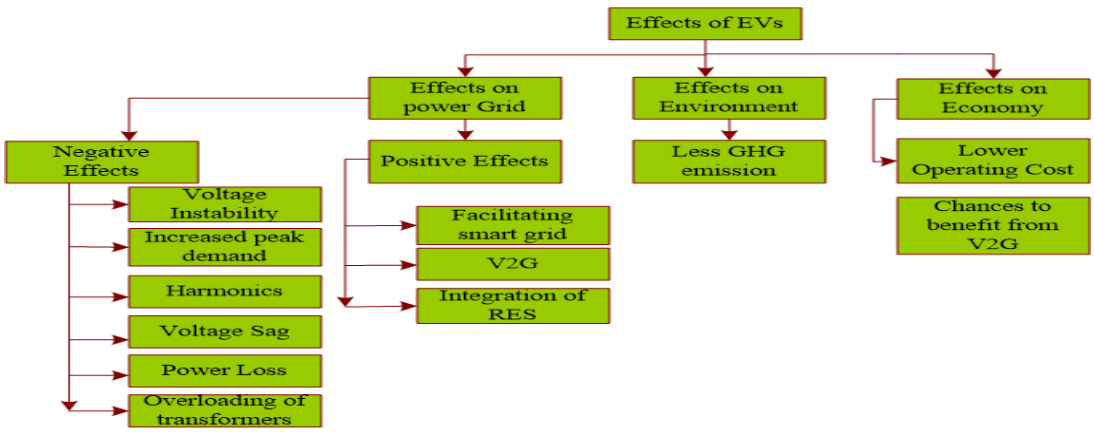

Fig. 1.12 Effects of EVs

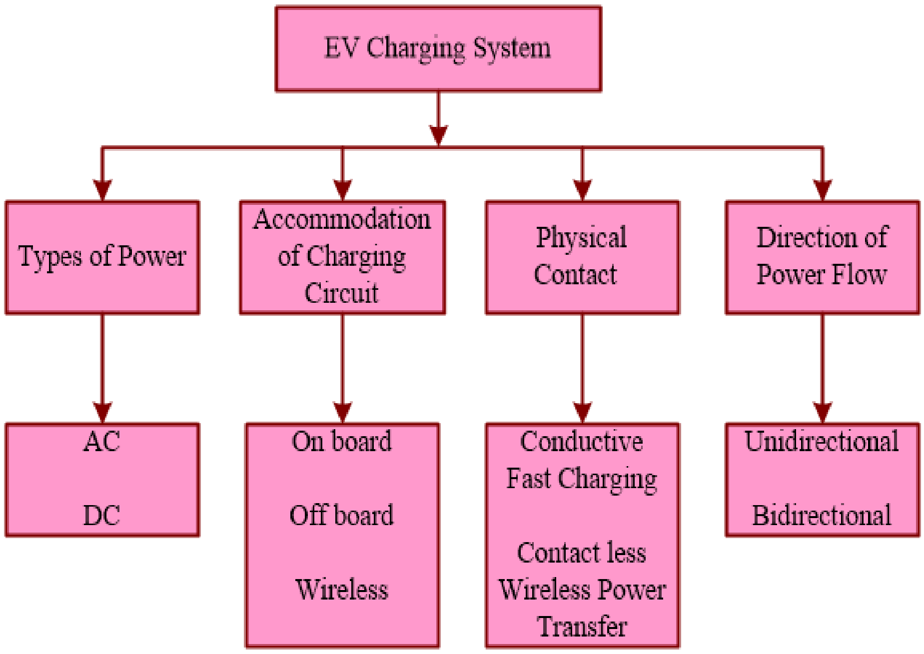

Fig. 1.13 different types of EV charging systems [12]

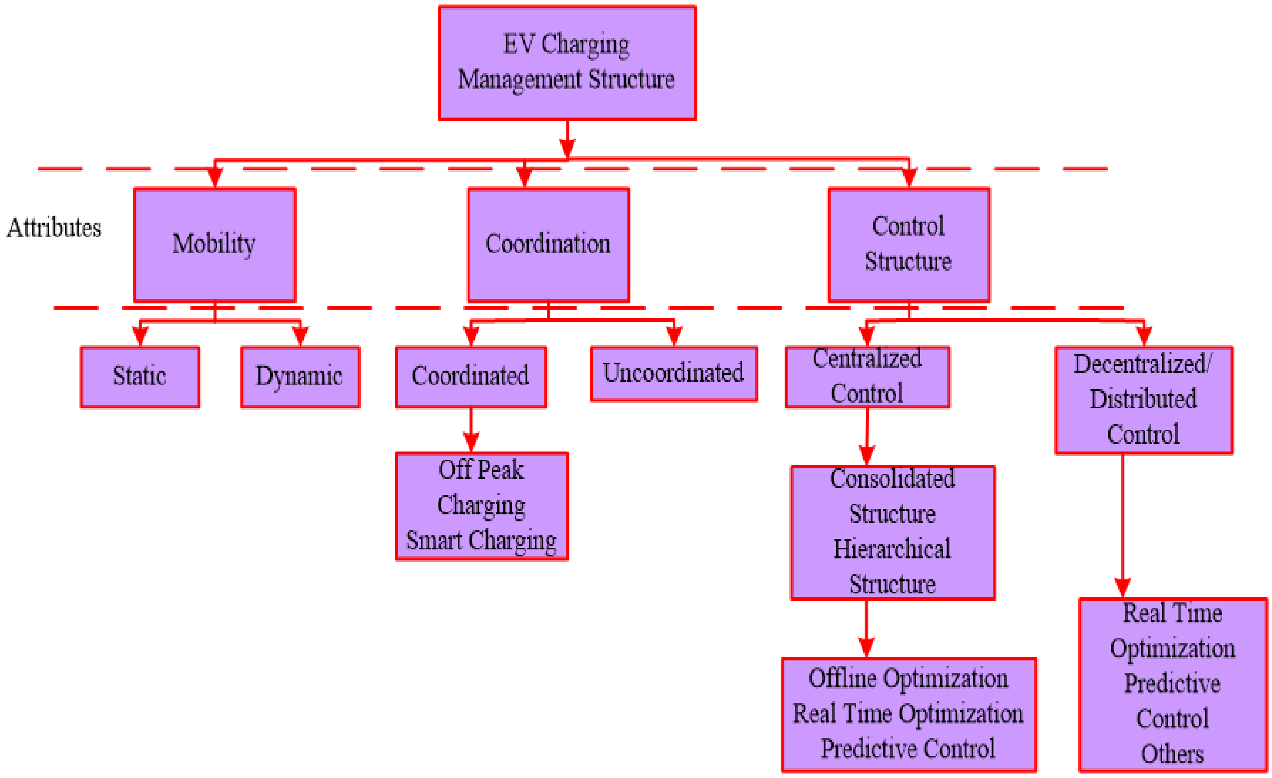

Fig. 1.14 EV charging management structure [12]

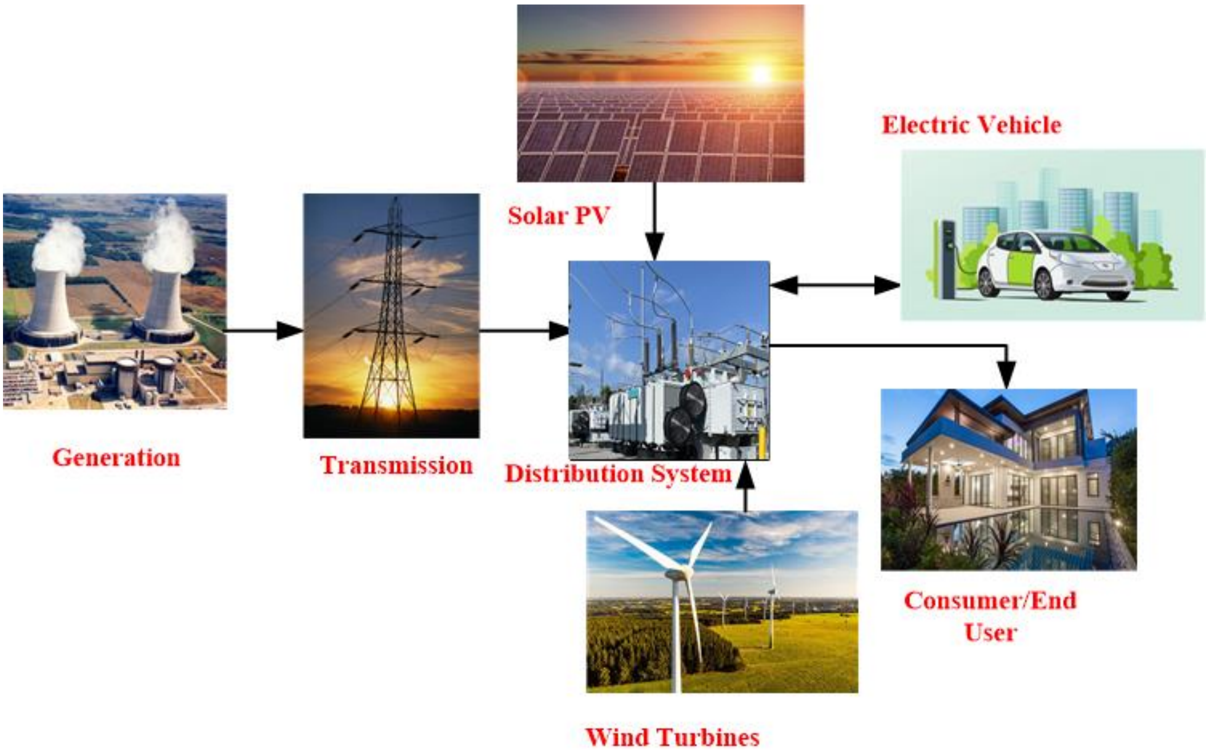

Fig. 1.15 Overall schematic diagram of DGs and EVs into the DS

CHAPTER 2

Literature Review, Research Objective and Methodology

2.1 Introduction:

This chapter briefly discusses 2012 to 2022, with several authors' points of view on minimizing P_{Loss} and enhancing voltage profile using different strategies. [13-24], allocation of DGs into DS. Allocation of renewables DGs into DS [25-36]. [37-47], simultaneous allocation of DGs and shunt capacitors (SCs) into DS. [48-58], allocation of EVCS into DS. Integration of renewable DGs and EVCS into DS [59-70]. The same depicted in Table 2.1 allocations of DGs, renewable based DGs, allocation of EVCS and allocation of renewable DGs and EVCS into DS.

2.2 Literature Review:

Table 2.1 allocations of DGs, renewable based DGs, allocation of EVCS and allocation of renewable DGs and EVCS into DS

References	**Author**	**Year**	**Objective**	**Optimization Techniques (OTs)**	**Test Systems**
Allocation of DGs					
[13]	Gopiya Naik et al.	2012	P_{Loss} minimization and voltage profile enhancement	FBSM	IEEE 33
[14]	Abdi & Afshar	2013	Reduction of active & reactive losses, voltage profile increment	IPSO & MCS	33-bus
[15]	Sedighizadeh et al.	2014	Decrement of Power loss, enhancements of voltage profile	HBB-BC	32 and 25 buses
[16]	Gopiya Naik et al.	2015	Shrinking real & reactive loses	Analytical method	IEEE 33 and 69 buses
[17]	T. T. Nguyen et al.	2016	Minimizing active P_{Loss} & augmenting voltage	CSA	33, 69 & 119 Buses

			stability		
[18]	Sanjay et al.	2017	Shrink the power loss	HGWO	IEEE 33, IEEE 69 & 85 RDS
[19]	T. P. Nguyen & Vo	2018	Real power loss decrement & voltage profile revamping	SFSA	IEEE 33, 69 & 118 buses
[20]	Li et al.	2019	Alleviating the losses	LHS method	36-Bus
[21]	Coelho et al.	2020	Power loss reduction & inflate voltage profile	EDM	IEEE 34 & 123-bus
[22]	Naguib et al.	2021	Minimizing system losses, augmenting reliability	FA	IEEE 33
[23]	Werkie & Kefale	2022	To shrink power loss & argumentation of voltage profile	IPSO	IEEE 33
[24]	Machava et al.	2022	Shrinking overall power losses	GA	IEEE 13, 34 & 123 buses
Allocation of Renewable-Based DGs					
[25]	Jamil & Kirmani	2012	Power loss decreasing & voltage profile revamping	FES	IEEE 33
[26]	Khatod et al.	2013	Decreased real power losses	EP method	69 Bus
[27]	Montoya-Bueno et al.	2014	Reducing losses & maintenance cost	MILP	10 kV real Azores island DN
[28]	Kayal & Chanda	2015	Decreasing power loss, enhancing voltage stability	PSO	28 Indian system
[29]	Kalkhambkar et al.	2016	Energy loss and cost alleviating	GWO	34 Bus
[30]	Ali et al.	2017	Minimizing overall power loss & increasing voltage profile	ALOA	IEEE 33 & 69

[31]	Naeem et al.	2018	Real power loss minimization	PSO	IEEE 33
[32]	Sambaiah & Jayabarathi	2019	Alleviating the voltage deviation & power loss	SSA	33 & 69 Buses
[33]	Farh et al.	2020	Decreasing overall cost & power loss	CSA-PSO	IEEE 30
[34]	Rathore & Patidar	2021	Decrease the energy losses	PSO, BFWA	IEEE 33
[35]	Sun et al.	2022	Minimizing voltage drop & operating cost	MMOPM	IEEE 33
[36]	Purlu & Turkay	2022	Alleviating the annual losses & voltage drop	GA & PSO	IEEE 33
Simultaneous allocation of DGs and SCs to DS					
[37]	Baghipour & Hosseini	2012	Power loss reduction, voltage & reliability increment	BPSO	10 & 33 buses
[38]	Gopiya Naik et al.	2013	Shrinking P_{Loss}, enhancing voltage profile	HM, HQCFT	IEEE 33 & 12 Buses
[39]	Devi & Geethanjali	2014	Minimizing power loss, augmenting voltage profile	PSO, LSF	12, 34 & 69 Buses
[40]	Khan et al.	2015	Decreasing total power loss, inflating voltage profile	BC-ABOA	IEEE 12, 33 & 69 Buses
[41]	Khodabakhshian & Andishgar	2016	Shrinking power loss, improving voltage	IMDEA	IEEE 33, 69 buses
[42]	Dixit et al.	2017	Decreasing real power loss	GABC	33 and 85 buses
[43]	Zhang et al.	2018	Minimizing the voltage fluctuation	GA, BLPM	IEEE 33
[44]	Bayat & Bagheri	2019	Decreases power loss	PSO, HAPSO, IA,	33, 69 & 119 Buses

				QOTLBO, LSF-BFOA, CTLBO	
[45]	Balu & Mukherjee	2020	Minimizing P_{Loss} & voltage drops. Improves voltage stability and profile	CF-PSO, MPSO	IEEE 33 & 136 Brazil RDS
[46]	Yuvaraj et al.	2021	Power loss decrement, voltage stability inflating	BOA	IEEE 33
[47]	Sayed et al.	2022	Power loss shrinking, voltage profile augmenting	SHADEOA	33 & 59 buses
Allocation of EVCS					
[48]	Liu et al.	2012	Revamping voltage profile, shrinking system losses	MPDIPA	IEEE 123
[49]	Su et al.	2013	Minimizing losses	GA	20-Bus
[50]	Niazazari et al.	2014	Inflate voltage profile	GAMS	33_Bus
[51]	Banol A. et al.	2015	Decreasing operation costs and losses	TSA	20-Bus
[52]	N. B.Arias et al.	2016	Reducing overall cost and losses	GRASP	449-Bus
[53]	A. Arias et al.	2017	Shrinking real & reactive losses and cost	MCS	19, 35 Buses
[54]	Gong et al.	2018	Reducing voltage fluctuation & losses,	PSO	IEEE 33
[55]	Suresh et al.	2019	Increasing efficiency & voltage profile, decreasing losses	FPA	IEEE 69
[56]	Amin et al.	2020	Decreasing power loss	BPSO	IEEE 33
[57]	Usman et al.	2021	Minimizing system losses, inflate voltage profile	OCSTA	IEEE 31

[58]	Kumar Reddy & Selvajyothi	2022	Decreasing initial cost and losses	PSO	19 & 25 Buses
Allocation of RDGs and EVCS					
[59]	Hafez & Bhattacharya	2012	Reducing bus losses & vehicle charging cost	OPF	59, 65, and 69 buses
[60]	Mohammadi et al.	2013	Energy loss minimization & voltage profile enhancement	BFPF, GA	IEEE 33
[61]	Fazelpour et al.	2014	Shrinking Power loss & cost, voltage increment	GA	30-bus
[62]	Abdelsamad et al.	2015	Decreasing energy losses	MCS	IEEE 123 RPDS
[63]	Shojaabadi et al.	2016	Minimizing voltage fluctuation and losses	MCS, NSGA-II	33-Bus
[64]	Arias et al.	2017	Reducing total maintenance cost	GRASP, TS & HOA	449-Bus
[65]	Liu et al.	2018	Increasing income & reducing losses	GA	33 Bus
[66]	Cheng & Li	2019	Improving voltage stability, reducing system losses	GA	IEEE 33
[67]	Gampa et al.	2020	Increasing voltage profile, minimizing losses	GOA, GA & PSO	51 & 69 Buses
[68]	Janamala et al.	2021	Maximizing voltage stability, shrinking losses	FSA	36 bus RRF
[69]	Shokouhandeh et al.	2022	Decreasing maintenance cost	ICA	33-Bus
[70]	Babu et al.	2022	Shrinking losses, enhancing voltage profile	HHOA	IEEE 25

2.3 Research Gap from the literature:

The authors implemented the DG allocation problem and studied various test systems. In most of the works, it is observed that the objective function considered is to minimize the P_{Loss} alone.

Most researchers didn’t consider generation uncertainties associated with renewable DG sources (solar & wind), and EV scheduling patterns are not addressed.

From the above-mentioned literature it is observed, most of the authors and researchers used Standard IEEE test systems; most researchers did not use real power test systems for assessment.

The authors considered a single load level to assess the performance of DS. These methods don't yield appropriately installed capacities of DGs and SCs with dynamic load level changes.

In the literature, most authors determined DG size for a static or fixed demand. But, in practical aspects, load varies dynamically according to the time. Further, the output power generation of renewable sources is not constant and depends upon environmental changes. So, it is vital to consider the variable load demand and calculate the exact output power from renewable resources.

The authors solved the DG allocation problem effectively in the presence of EVs. But, a suitable strategy to charge the EVs during peak demand is still a problem. In this work, an effective methodology is proposed to place DGs in the presence of EVs

The authors considered EV integration as an additional load. But, its charging and discharging patterns and their impact on the system are not appropriately addressed.

2.4 Research Objectives:

Nowadays, the usage of EVs and RESs is improved more because of global benefits. But, the penetration process of these sources shows problems in the power system. Finally, inserting these sources incorrectly with incorrect size increases voltage disturbances and P_{Loss}.

1. Mathematical modelling of different DGs (Solar and Wind) and their uncertainties are considered and study the performance.
2. Placement of solar DGs and EVs are connected to the DS and analyze the performance. (IEEE and Real Test Systems)
3. Placement of Wind DGs and EVs are connected to the DS and analyze the performance. (IEEE and Real Test Systems)
4. Integration of both solar, wind DGs and EVs integrated into DS and assessed the performance of DS.

The objective functions of the problems mentioned above are P_{Loss}, voltage profile & voltage stability of the system.

2.5 Research Methodology:

Develop proper DS load flow and use sensitivity index to identify the desired locations for placement of DGs and EVCS. Further, develop different types of DGs mathematical modelling considering generation uncertainties and dynamic load variations. Next, suitable weibull and beta probability distribution functions (PDF) are considered for modelling solar irradiance and wind speed. Finally, Mathematical modelling of plug-in EVs uncertainties is considered.

MATLAB software is used and writes the suitable programs. After implementation, consider relevant test systems and study the performance of DS. So, explore the efficacy of the developed approach results are validated with existing literature.

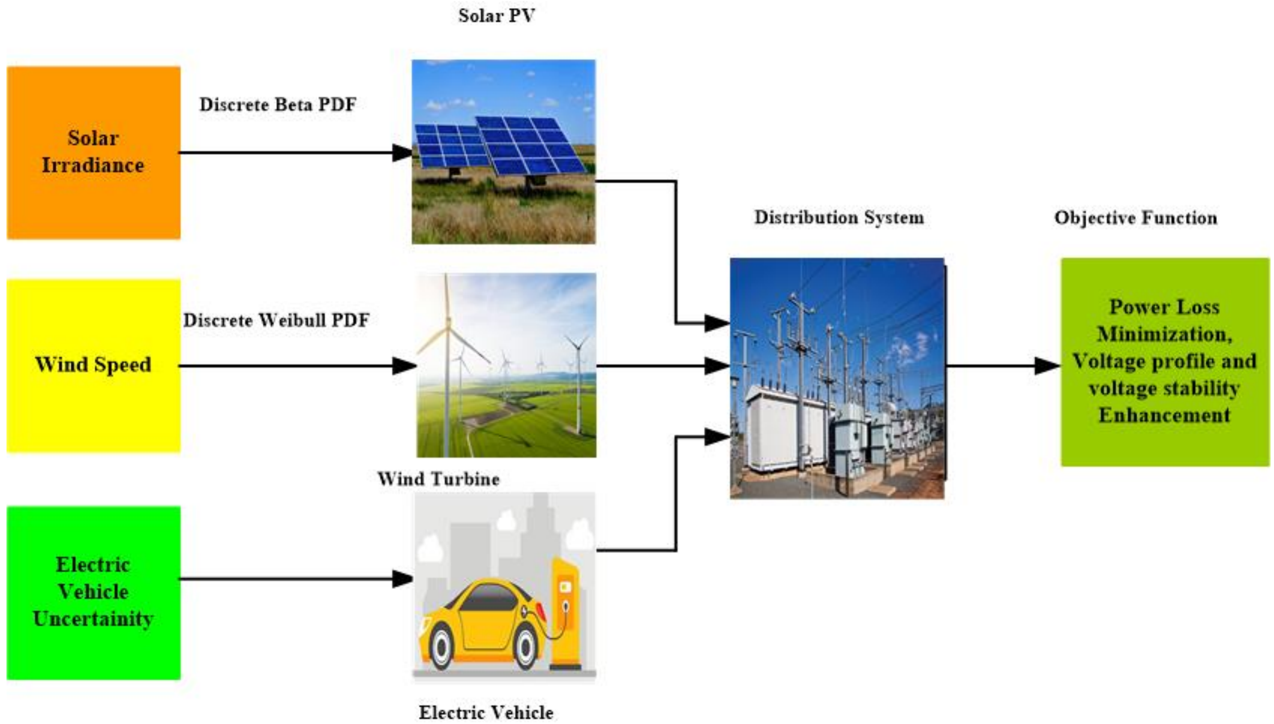

Fig 2.1 Schematic diagram of research methodology

2.6 Organization of Thesis:

Chapter 3: This chapter discusses uncertainties related to solar irradiance and wind speed with their respective PDFs. Different EV charging methods are elaborated.

Chapter 4: deals with integrating solar DGs and EVs into the DS. A combination of LSF and POA methods was used to determine the location and size of solar DGs and EVCSs. Various test systems, such as IEEE 33 and 28 Indian buses, simulate outcomes. Compared results with other techniques.

Chapter 5: This chapter discusses the integration of wind-based DGs and EVs into DS. A combined LSF and POA method was considered to find an apt location and size for wind DGs, and EVCS injected kW and kVAr to the DS. The standard IEEE 69 test system and 28 Indian bus system are simulated results.

Chapter 6: This chapter integrates solar and wind DGs with EVs into DS. Here, the Voltage stability index (VSI) and POA method are used to find the site and size of the DGs and EVCS. Solar, wind and EVs-based results were simulated with 28 Indian real test system.

Chapter 7: In this chapter, the final part covers the future scope and conclusion.

CHAPTER 3

Mathematical Modelling of Distributed Energy Resources and Electric Vehicles

3.1 Introduction:

This work describes the optimum allocation of solar, wind DGs and EVCS. Further, the generation uncertainties are considered, and the exact output power from these sources is found. Finally, the EVs charging and discharging patterns importance are considered.

3.2 Mathematical modelling of solar irradiance:

[28, 71and 72] Solar panel's exact output power is calculated with the beta probability distribution function (PDF). Beta PDF is more suitable for statistical analysis to model solar irradiance. Tables 3.1 and 3.2 represent solar PV specifications and the mean standard deviation of the summer season on a typical day [28]. Fig. 3.1 shows the expected output power from the solar module. Equation 3.1 to 3.10 represents the mathematical modelling of solar irradiance.

$$f_s^m(s) = \frac{\Gamma(\alpha^m+\beta^m)}{\Gamma(\alpha^m).\Gamma(\beta^m)}.(s^m)^{\alpha^m-1}.(1-s^m)^{\beta^m-1} \ For\ \alpha^m > 0;\ \beta^m > 0 \tag{3.1}$$

m, Γ = Gamma function

With mean(μ), Standard deviation (σ) determined$f_s^m(s)$, $s = \frac{kW}{m^2}$

$$\beta^m = (1-\mu_s^m).\left(\frac{\mu_s^m(1+\mu_s^m)}{(\sigma_s^m)^2} - 1\right) \tag{3.2}$$

$$\alpha^m = \frac{\mu_s^m * \beta^m}{(1-\mu_s^m)} \tag{3.3}$$

α^m, β^m= Shape parameters

$$P^{PVA}(s) = N^{PVM} * V^y * I^y * FF \tag{3.4}$$

Where

$$FF = \frac{V^{MPP} * I^{MPP}}{V_{oc} * I_{sc}} \tag{3.5}$$

$$I^y = s[I_{sc} + K^i(T^{cy} - 25)] \tag{3.6}$$

$$V^y = V_{oc} - K^v . T^{cy} \tag{3.7}$$

$$T^{cy} = T^A + s(\frac{N^{OT}-20}{0.8}) \tag{3.8}$$

FF = fill factor, the sum of all PV modules $=N^{PVM}$, I_{sc}= short circuit current, V_{oc}= open-circuit voltage, T^{cy}=cell temperature, T^A= ambient temperature,K^i, K^v= current & voltage temperature coefficients, N^{OT}= nominal operating temperature.

$$P(s) = P^{PVA}(s) * f_s^m(s) \tag{3.9}$$

$$\text{Total Expected Output Power} = \int_0^1 P^{PVA}(s) * f_s^m(s) \tag{3.10}$$

Table 3.1 Solar PV Specifications

Description	**Specifications**	**Ratings**
Solar PV	Solar panel	220W
	Ambient Temperature(T_a)	30.76 ^{o}c
	Nominal cell operating temperature (N_{ot})	43^{o}c
	Open Circuit Voltage	36.96V
	Short Circuit Current	8.38A
	Max. Powerpoint voltage ($V_{m\ ppt}$)	28.36V
	Max. Powerpoint Current ($I_{m\ ppt}$)	7.76A
	Coefficient of voltage temperature (K_v)	0.1278 V/C
	Coefficient of current temperature (K_i)	0.00545 A/C

Table 3.2 Mean, standard deviation of the summer season on a typical day

Hour	**Mean**	**StandDev**	**Expected total output power (W)**
1	0	0	NA
2	0	0	NA
3	0	0	NA
4	0	0	NA
5	0.0032	0.0045	NA
6	0.1278	0.0406	24.9491

7	0.2538	0.0714	48.8601
8	0.3824	0.1189	72.6721
9	0.4908	0.1388	92.3087
10	0.568	0.1659	106.0076
11	0.6164	0.1445	114.5426
12	0.599	0.1175	111.5308
13	0.5614	0.0995	104.9347
14	0.4672	0.0788	88.1518
15	0.3548	0.055	67.6923
16	0.2228	0.041	43.0653
17	0.103	0.0276	20.5279
18	0	0	NA
19	0	0	NA
20	0	0	NA
21	0	0	NA
22	0	0	NA
23	0	0	NA
24	0	0	NA

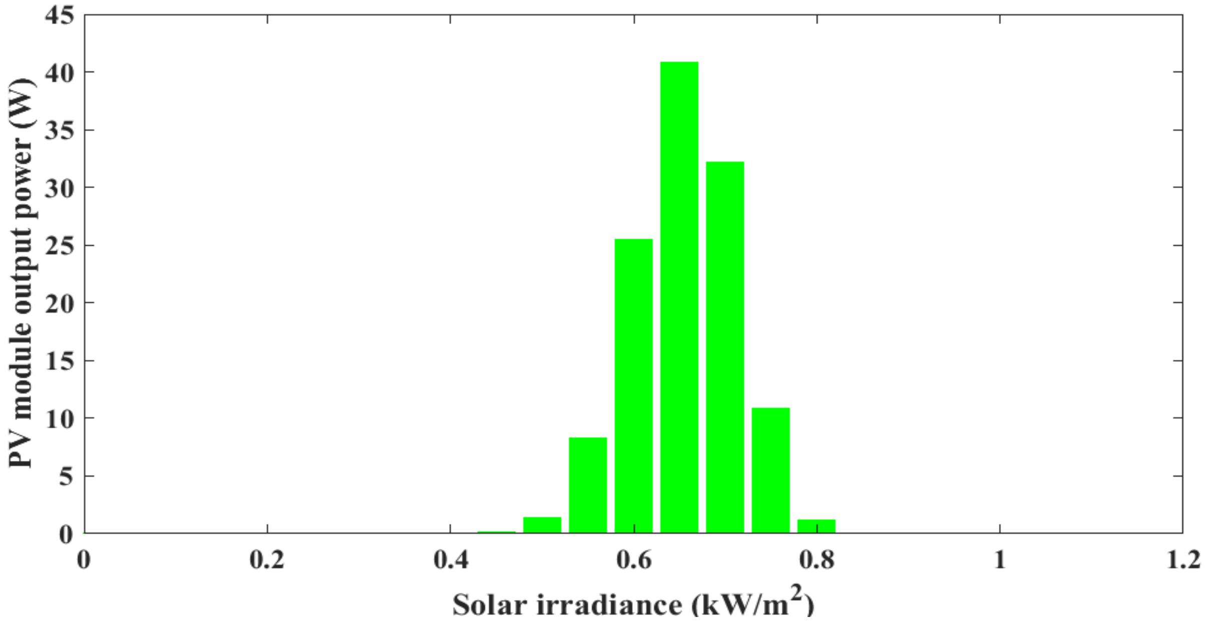

Fig. 3.1 Expected Output Power from Solar Module

3.3. Mathematical modelling of wind speed

The wind speed significantly impacts the output power of wind-based DGs. Therefore, the uncertainty related to wind speed is adequately simulated before placing these sources in DS. Weibull PDF has been utilized. Tables 3.3 and 3.4 represent the wind turbine specification and the mean, standard deviation of the summer season on a typical day [28]. Fig 3.2 shows the wind turbine expected output power for 1 hour. Equation 3.11 to 3.18 represents mathematical modelling of wind speed.

$$f_v(V) = \frac{k}{c}.(\frac{v}{c})^{k-1}.e^{-(\frac{v}{c})^k} \; for\; c > 1;\; k > 0 \qquad (3.11)$$

Where,

k = shape factor, c = scale factor

$$k = (\frac{\sigma}{\mu})^{-1.086} \qquad (3.12)$$

$$c = \frac{\mu}{\Gamma(1+\frac{1}{k})} \qquad (3.13)$$

$$P_{WT}(V) = \begin{Bmatrix} 0 & for\;\; 0 \le v < v_{cut-in}\; and\; v > v_{cut-out} \\ (a.v^3 + b.P_r & for\; v_{cut-in} \le v \le v_r \\ P_r & for\; v_r \le v \le v_{cut-out} \end{Bmatrix} \qquad (3.14)$$

Where

$$a = \frac{P_r}{(v_r^3 - v_{cut-in}^3)} \qquad (3.15)$$

$$b = \frac{v_{cut-in}^3}{(v_r^3 - v_{cut-in}^3} \qquad (3.16)$$

$$P_{WE} = P_{WT}(V) * f_v(V) \qquad (3.17)$$

$$\text{Expected total output power} = \int_0^1 P_{WT}(V) * f_v(V) dv \qquad (3.18)$$

Table 3.3 Specifications of Wind Turbine

Description	Specifications	Ratings
Wind Turbine	Wind Turbine rating	3000kW
	Cut-in Speed	3.5m/s
	Cut-out Speed	25m/s
	Hub height	66m
	Rated Speed	15m/s

Table 3.4 Mean, standard deviation of the summer season on a typical day

Hour	Mean	StandDev	Expected total output power (kW)
1	9.9	0.7937	220.7474
2	9.3667	0.8021	191.2799
3	9.1667	0.8505	180.8715
4	9	0.8185	171.6584
5	8.7	0.755	153.1758
6	8.6	1.0583	153.6114
7	9	1.1533	174.5944
8	9.0333	1.1504	176.2964
9	9.3333	0.9504	189.7201
10	9.6	1.1533	207.9257
11	10.1333	1.0066	238.9737
12	10.2667	0.8622	246.9246
13	7.9667	0.3786	146.3168
14	8	0.4583	119.3015
15	8	0.5	114.0872
16	7.7333	0.4509	136.6521
17	6.9667	0.2309	172.4661
18	5.9667	0.3786	69.5131
19	4.8333	0.3215	57.3336
20	4.4333	0.3215	16.3767
21	4.3333	0.4163	24.242

22	4.1	0.2646	33.2545
23	4.0667	0.2082	44.3591
24	4	0.1732	66.1166

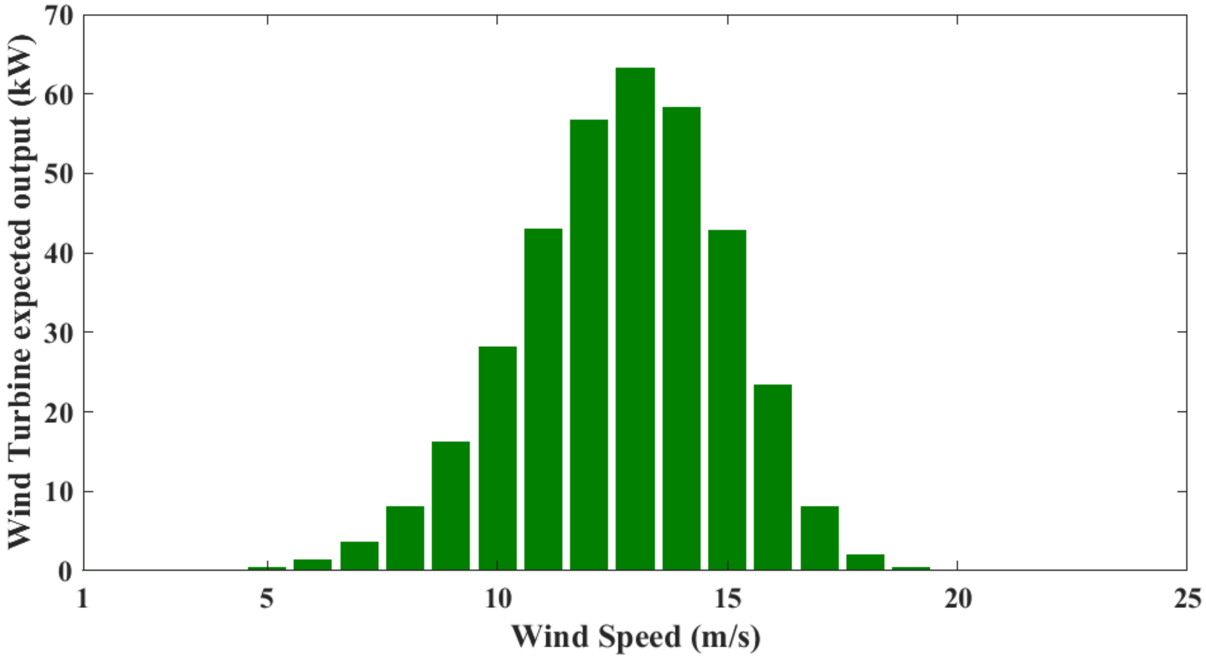

Fig 3.2 Wind turbine expected output power for 1 hour

3.4. Mathematical modelling of EV uncertainty

[81] Users determine when to charge (DoC), depending on the electricity SoC, trip distance and charge power. The DoC is influenced by the following trip's distance among these variables. Table 3.5 represents the specifications of EVs. Equation 3.19 to 3.22 represents the mathematical modelling of EV uncertainty. The primary SoC of mth EV at the nth hour is given below equation 3.19.

$$SoC_n^m = \left(1 - \frac{\tau t}{t_r}\right).100\% \quad (3.19)$$

Where τ = no. of trips, t = EV travel distance, t_r = EV travel range

Battery Storage Constraint:

$$SoC_{min} \leq SoC_n^{EV} \leq SoC_{max} \quad (3.20)$$

$$P_{ch,n,t} \leq P_{ch,n}^{max} \quad (3.21)$$

$$P_{disch,n,t} \leq P_{disch,n}^{max} \tag{3.22}$$

3.5 Method for Scheduling of RDGs & EVs

3.5.1 Conventional and optimized charging methods for EVs

After arriving home in the conventional charging method (CCM), the EVs are instantly connected to a charging point. They are unconcerned with the demands of the system. The traditional charging approach may not be advantageous because it results in significant energy loss, a system voltage decrease, and system maloperation caused to congestion. The suggested technique should help charge EVs (V 2 G) while off-hours and transfer electricity to the grid (G2V) during peak hours. EV charging and discharging are prioritized based on demand. This strategy is referred to as the optimized charging method. In this strategy, EV consumers care about system load. EVs are not allowed to be charged during peak load. Following the load demand curve, EVs are charged during low-load hours through an optimized charging method (OCM). A consistent voltage profile and low P_{Loss} are obtained using an OCM. Using this approach, the utility and EV consumers will communicate about the system's demand and devise new strategies for enhancing the system's efficiency. Scheduling is based on the system's peak-to-average ratio (PAR) of demand. Fig 3.3 shows flow chart steps for scheduling EVs.

The fundamental aim of EV scheduling is to reduce PAR, as shown:

$$PAR = \frac{P_{d,peak}}{P_{d,mean}} \tag{3.23}$$

Where $P_{d,mean}$ = average system demand, $P_{d,peak}$ = peak system demand

This work provides a suitable scheduling technique to reduce the PAR.

Charge or discharge is also determined by the power ratio (PR) magnitude, which is represented as follows:

$$P_R = \frac{P_D(n)}{P_{d,mean}} \tag{3.24}$$

It is essential to keep two conditions in mind: the number of EVs assigned should not be negative (-), and the number of EVs granted at the next step must be more significant than the number in the first step.

$$\sum_{t=1}^{N} EV_{pit} \leq EV_T \tag{3.25}$$

Table 3.5 Specification of EVs

Description	**Specifications**	**Ratings**
EVs	EV Capacity or Battery	16 kWh
	No.of EVs	60
	SoC_{min}	0.2
	SoC_{max}	0.9
	Avg. power consumption per km	0.175 kWh/km
	Avg. distance travelled by each EV	30km

3.5.2 Scheduling procedures to follow.

- The OCM first looks at the type of vehicle, how many vehicles need to be charged, how much each vehicle needs to be charged, and how long the system will run before the next trip.
- The system for each hour, the PAR and P_R It is calculated both either with or without taking EVs into account.
- V2G mode is started if the power ratio (P_R) is smaller than the average power demand$P_{d,mean}$.
- Otherwise, if the P_R of the specific interval of time is larger than the overall power demand $P_{d,mean}$. The vehicle can send electricity back to the grid while taking into account the existing SoC.
- These details will be sent to the POA method every hour to identify the optimal size of renewable DGs.

Once the EVs have reached SoC and are available for the next journey, the procedure is completed.

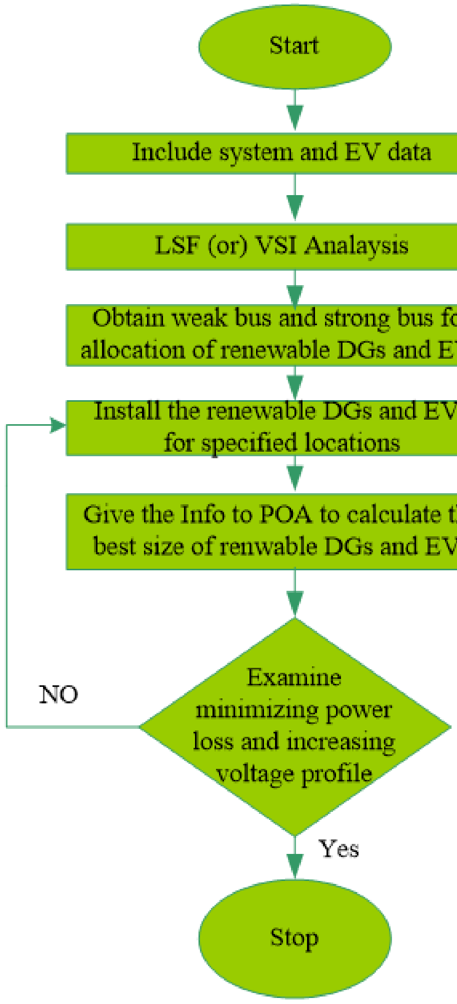

Fig 3.3 Flow chart steps for Scheduling EVs

3.6 Summary of the chapter:

This chapter discusses solar irradiance and wind speed uncertainties with their respective PDFs. Solar, wind and EV specifications are given in the tables. EV scheduling patterns and charging methods such as CCM and OCM are discussed.

CHAPTER 4

Integration of Solar Distributed Generators and Electric Vehicles into the Distribution System

4.1 Introduction:

It is essential to properly allocate the Distributed Generators (DGs) and Electric Vehicle charging stations (EVCS) to satisfy the rising active power demand of a distribution system (DS). To attain the objectives of this chapter, minimal P_{Loss}, increased voltage profile, and a more uniform voltage stability index (VSI) across the system, multiple DGs and EVCSs are allocated simultaneously in the DS. A combination strategy is given to address the allocation and sizing of solar DGs and EVCS, taking into account the loss sensitivity factor (LSF) and the political optimizer algorithm (POA). Considering various possible outcomes, a study is conducted on standard IEEE 33 and 28 Indian bus systems. Further, different EV charging methods are considered to study the performance. The analysis is continued for 24 hours to demonstrate the suggested combination method's efficacy. Finally, the developed method was compared with other metaheuristic algorithms to validate the results. Figure 4.1 represents schematic diagram of integration of solar DGs and EVs into DS.

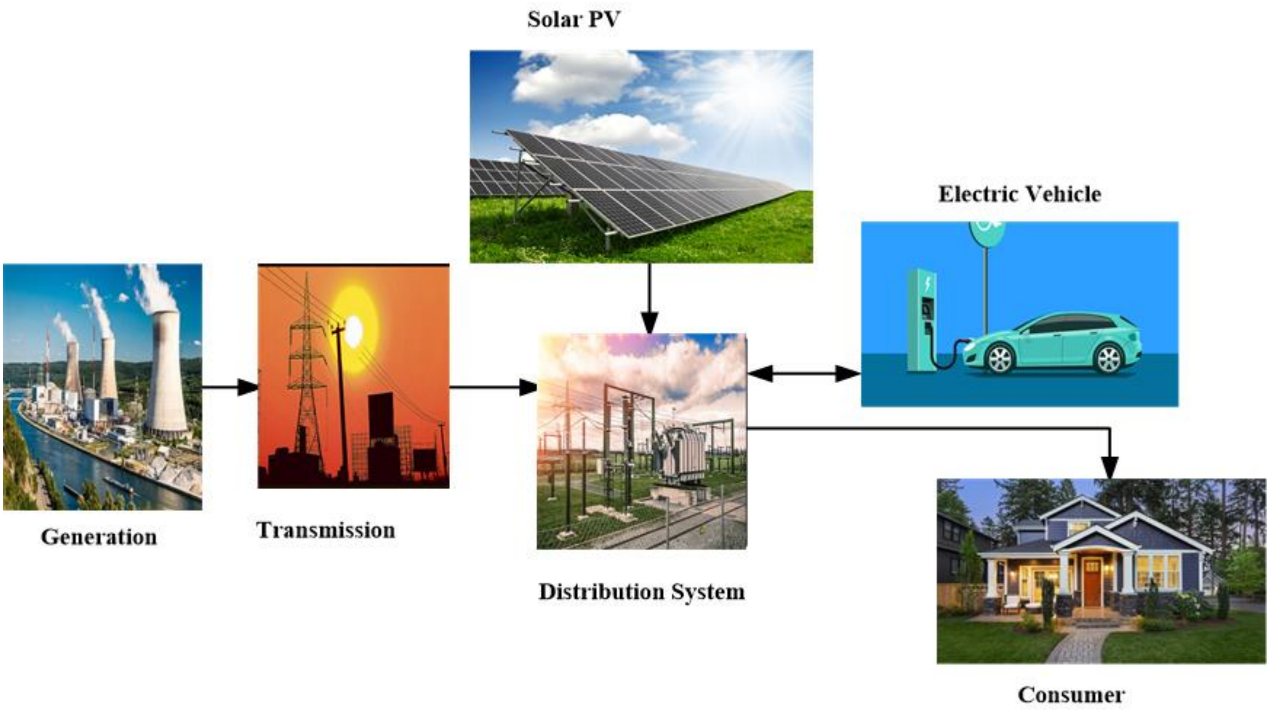

Fig 4.1 Schematic diagram of integration of solar DGs and EVs into DS

4.2 Objective:

The objective function is minimizing P_{Loss} and voltage profile enhancement with satisfying all the constraints. The real P_{Loss} and voltage magnitude equation are represented as follows.

The objective P_{Loss} reduction is

$$min \sum_{n=1}^{24} P_{Loss}(n) \tag{4.1}$$

Where

$$P_{Loss}(n) = \sum_{n=1}^{24} I_n^2 R_n \tag{4.2}$$

The following are the main constraints related to the objective function

Power balance constraints:

$$\sum_{n=1}^{24} P^{S_{DG}}(n) = \sum_{n=1}^{24}[P^{Demand}(n) \pm P^{EV}(n) + P_{Loss}(n)] \tag{4.3}$$

Where, $P^G(n)$= n^{th} hour power generator, $P^{Demand}(n)$= n^{th} hour power demand, $P^{EV}(n)$= During an n^{th} hour, EV supplied/consumed power.

Bus Voltage Profile Constraints:

DS's voltage profile must always be within the specified ranges.

$$V_{m,min} \leq |V_{m,n}| \leq V_{m,max} \tag{4.4}$$

Where, $V_{m,n}$ = m^{th} bus voltage at the n^{th} hour.

DG Capacity Range:

$$P_{m,min}^{DG} \leq P_m^{DG} \leq P_{m,max}^{DG} \tag{4.5}$$

Where

$$(P_{m,min}^{DG} = 0.1 \sum_{m=2}^{n} P_m^{DG}, P_{m,max}^{DG} = 0.8 \sum_{m=2}^{n} P_m^{DG})$$

The constraint related to the EVs are given in Chapter 3, equation 3.19 to Equation 3.22

4.3 Combined method for optimal location and sizing of solar DGs

The combined approach considers the LSF method for finding locations of solar DGs and EVCS and passes the obtained sites to the meta-heuristic optimization technique (POA). POA determines the appropriate sizes of solar DGs.

4.3.1. LSF method for obtaining the suitable location of DGs and EVs

[73 – 75], the LSF method is mainly utilized to find the possible places for the allocation of solar DGs and EVCS. The P_{Loss} Equation is given below. From that equation, calculate real P_{Loss} sensitivities. The buses with minimum and maximum loss sensitivities should be considered the best locations for placing solar DGs and EVCS.

$$P_{Line\ loss} = \left(\frac{P_{m+1,eff}^{2} + Q_{m+1,eff}^{2}}{|V_{m+1}|^{2}}\right). R_{m,m+1} \quad (4.6)$$

Sensitivity analysis of actual & reactive P_{Loss} is determined by the partial derivative of real P_{Loss} while injecting real and reactive power.

$$APLSF = \frac{\partial P_{line\ loss}}{\partial P_{m+1,eff}} = \frac{2P_{m+1,eff}.R_{m,m+1}}{|V_{m+1}|^{2}} \quad (4.7)$$

$$RAPLSF = \frac{\partial P_{line\ loss}}{\partial Q_{m+1,eff}} = \frac{2Q_{m+1,eff}.R_{m,m+1}}{|V_{m+1}|^{2}} \quad (4.8)$$

4.4. Political Optimization Algorithm (POA)

Askari developed the latest meta-heuristic technique, a political optimizer (PO). This method is influenced by several phases of politics. POA is mainly a human behaviour-based approach. This method successfully solves issues involving applied mathematics, and it excels in terms of convergence speed, quality of research, and the number of fast iterations. The mathematical modelling of PO covers all main stages of politics. “PO consists of five stages 1. Party formation, 2. Constituency allocation, 3. Election campaign, 4. Party switching, 5. Parliamentary affairs” [76 - 78]. Fig 4.2 and 4.3 depicts the mechanism and flow chart of POA. POA standard deviation and time taken to achieve the best solution is low; POA performed well compared to other algorithms

All citizens categorized into n political parties

$$P = \{P_1 ,\ P_2 , P_3 , \dots\dots\ P_n\} \quad (4.9)$$

Every party include n members, as given eq below

$$P_i = \{P_i^1 ,\ P_i^2 , P_i^3 , \dots\dots\ P_i^n\} \quad (4.10)$$

Every member of the party considers dimension d, the following eq

$$P_i^j = [\, P_{i,1}^j\,, P_{i,2}^j, P_{i,3}^j, \dots \dots .\,. P_{i,d}^j]^T \tag{4.11}$$

n number of electoral districts demonstrated below

$$C = \{C_1, C_2, C_3 \dots \dots C_n\} \tag{4.12}$$

Every constituency n member is considered

$$C_j = \{P_1^j\,,\; P_2^j\,, P_3^j\,, \dots \dots .\; P_n^j\} \tag{4.13}$$

Head of the party determined with good fitness

$$q = \underset{1\le j\le n}{argmin}\, \mathrm{f}(P_i^j), \forall i \epsilon \{1, \dots \dots, n\} \tag{4.14}$$

$$P_i^* = P_i^q$$

Champion of every individual constituency called member parliament demonstrated below

$$P^* = \{P_1^*\,,\; P_2^*\,, P_3^*\,, \dots .\,. P_n^*\} \tag{4.15}$$

$$C^* = \{c_1^*, c_2^*\,, c_3^*\,, \dots \dots .\, c_n^*\} \tag{4.16}$$

$$P_{i,k}^j(t+1) = \begin{cases} if\ P_{i,k}^j(t-1) \le P_{i,k}^j(t) \le m^*\ or\ P_{i,k}^j(t-1) \ge P_{i,k}^j(t) \ge m^*, \\ \quad m^* + r\left(m^* - P_{i,k}^j(t)\right); \\ if\ P_{i,k}^j(t-1) \le m^* \le P_{i,k}^j(t)\ or\ P_{i,k}^j(t-1) \ge m^* \ge P_{i,k}^j(t), \\ \quad m^* + (2r-1)\left|m^* - P_{i,k}^j(t)\right|; \\ if\ m^* \le P_{i,k}^j(t-1) \le P_{i,k}^j(t)\ or\ m^* \ge P_{i,k}^j(t-1) \ge P_{i,k}^j(t), \\ \quad m^* + (2r-1)\left|m^* - P_{i,k}^j(t-1)\right|; \end{cases} \tag{4.17}$$

$$P_{i,k}^j(t+1) = \begin{cases} if\ P_{i,k}^j(t-1) \le P_{i,k}^j(t) \le m^*\ or\ P_{i,k}^j(t-1) \ge P_{i,k}^j(t) \ge m^*, \\ \quad m^* + (2r-1)\left|m^* - P_{i,k}^j(t)\right|; \\ if\ P_{i,k}^j(t-1) \le m^* \le P_{i,k}^j(t)\ or\ P_{i,k}^j(t-1) \ge m^* \ge P_{i,k}^j(t), \\ \quad P_{i,k}^j(t-1) + r\left(P_{i,k}^j(t) - P_{i,k}^j(t-1)\right); \\ if\ m^* \le P_{i,k}^j(t-1) \le P_{i,k}^j(t)\ or\ m^* \ge P_{i,k}^j(t-1) \ge P_{i,k}^j(t), \\ \quad m^* + (2r-1)\left|m^* - P_{i,k}^j(t-1)\right|; \end{cases} \tag{4.18}$$

λ Utilized as an adaptive parameter, it is reduced from 1 to 0 throughout the iterative process. Every member is nominated as per probabilityλ.

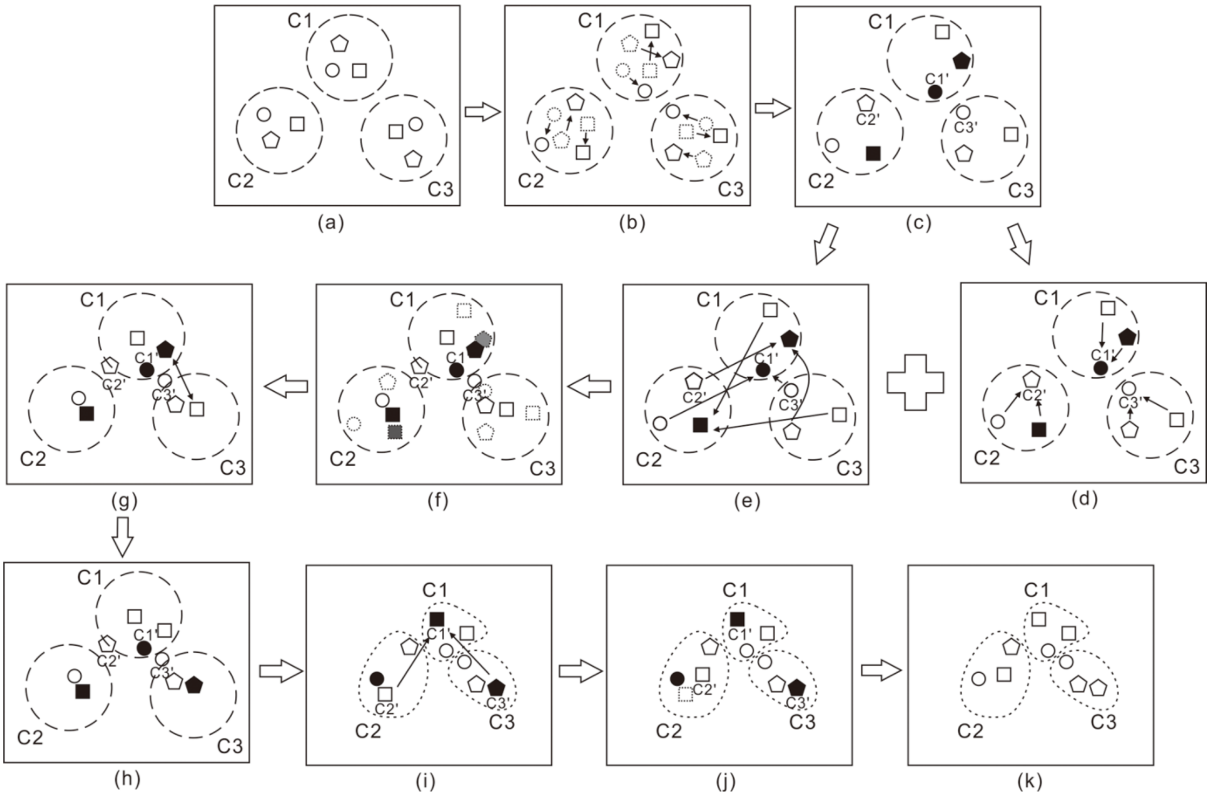

Fig 4.2 POA mechanism [78]

$$q = \underset{1 \le j \le n}{argmax} f(P_i^j) \tag{4.19}$$

Champion of constituency determined with the following eq.

$$q = \underset{1 \le j \le n}{argmax} f(P_i^j) \tag{4.20}$$

$$c_j^* = p_q^j$$

4.4.1 Steps for calculating best sizes of DGs using POA:

Step 1: Read the DS data (Line and Bus data)

Step 2: Run the base case load flow

Step3: Find suitable locations for solar DGs and EVCS with the LSF method

Step 4: Suitable locations of solar DGs and EVCS determined using LSF should be given as input to POA

Step 5: As per eq. 4.9 all citizens are categorized into 'n' political parties; each party include 'n' member by using eq. 4.10.

Step 6: Chief of the party determined with good fitness in eq. 4.14, champion of every individual constituency called a member of parliament by using eq. 4.15

Step 7: Compared present values with the previous position values

Step 8: At the beginning of algorithm loops, fitness values and positions are created temporarily.

Step 9: Eq. 4.17, 4.18 represents the 2^{nd} phase election campaign, using this eq's all political parties' member values and positions updated

Step 10: Eq. 4.19 represents the election campaign after the phase; every individual member of the switching phase runs

Step 11: Champions of constituency calculated with eq. 4.20.

Step 12: In this step, the algorithm shows all the champions of parliamentary locations, called the parliamentary affairs phase

Step 13: This final step is upgrading all fitness values (P_{Loss}) and positions, such as best DG sizes.

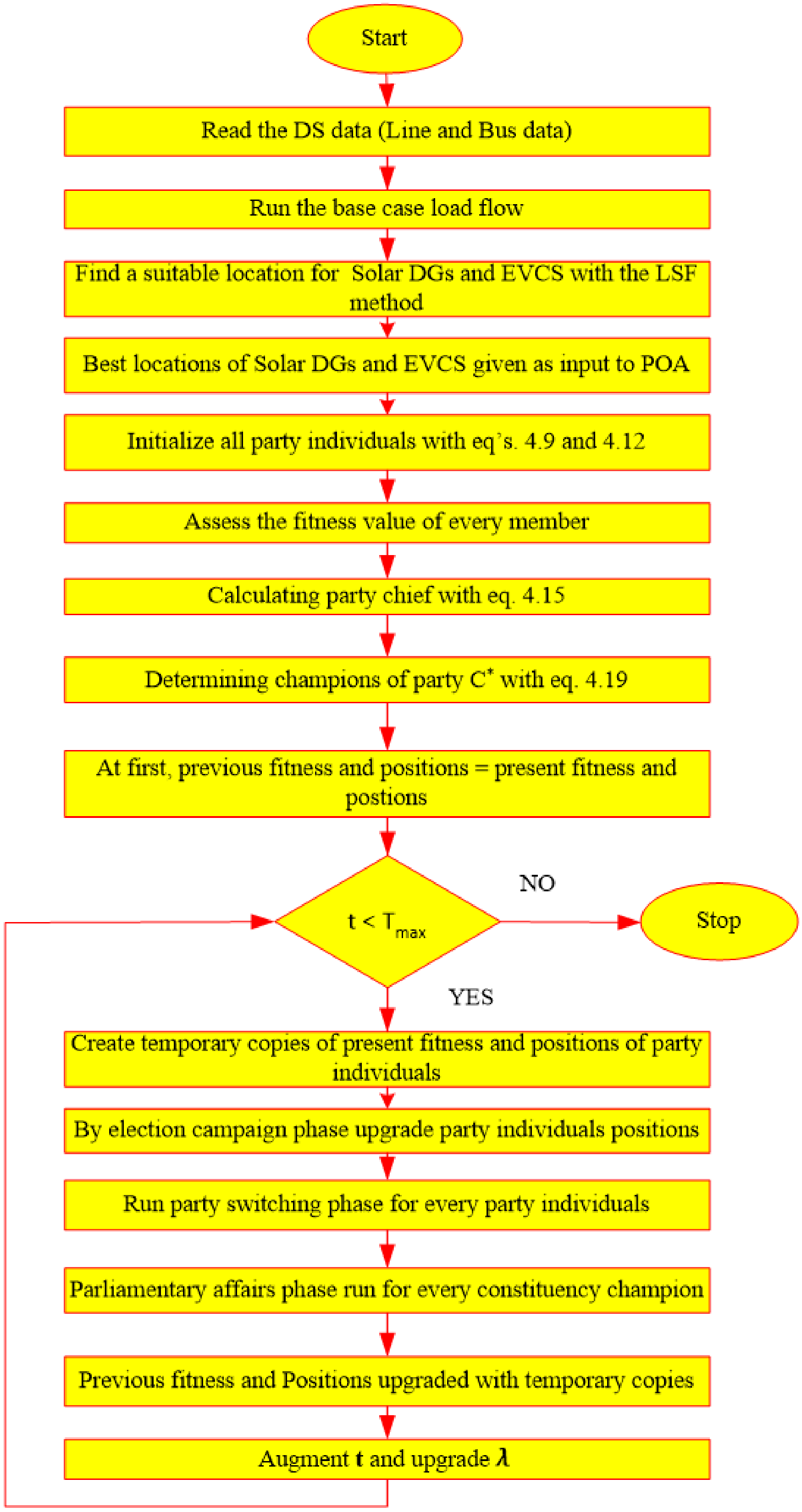

Fig 4.3 Flow Chart of POA

4.5 Results and Discussion:

Before implementing the combined approach for dynamic loading conditions, a general static method of solar DG allocation is simulated, and the outcomes are compared with existing methodologies in state of the art. [73, 79] The analysis is implemented on the IEEE 33 bus system in MATLAB (R2017a) and the single-line diagram of the same test system is represented in Fig 4.4. This section presents the outcomes obtained using the proposed combined method. The various cases are considered to show the proposed method's efficacy, which is represented in Table 4.1.

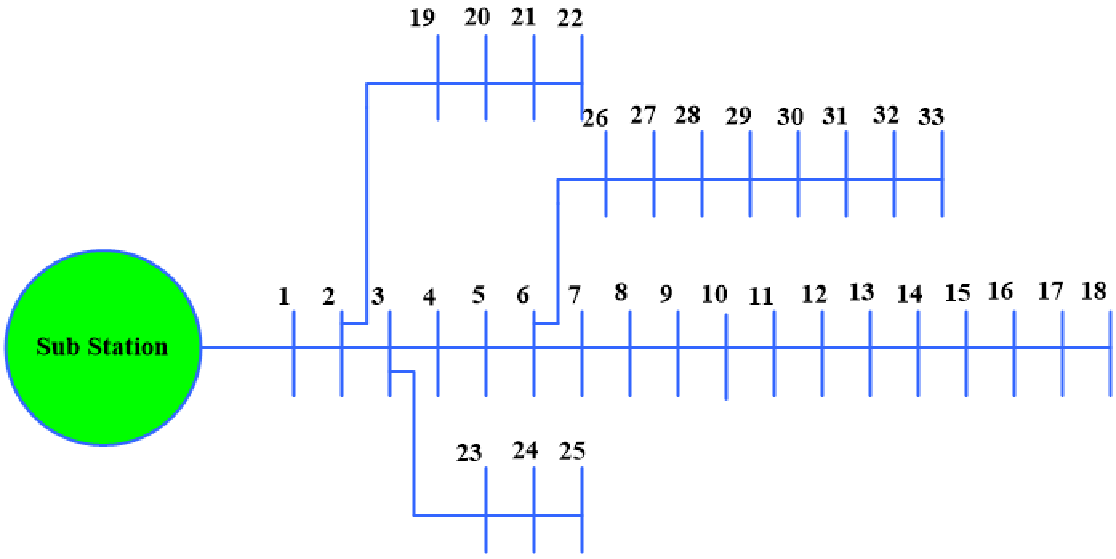

Fig 4.4 Single line diagram of IEEE 33 bus

Table 4.1 Comparison of results for Base Case, Case 1, Case 2, and Case 3 using POA

Different Cases	**OT's**	**Bus No**	**Solar DG Size in kW**	**P_{Loss} (kW) With Solar DGs Placement**	**V_{min} (p.u.)**	**VSI_{min} (p.u.)**	**Time (Sec)**
Base Case	NA	NA	NA	202.6666	0.9166	0.7045	14.155
Case 1	DA	30	1535.931	116.0409	0.9362	0.7621	15.669
	GOA	30	1535.92	117.613	0.9675	0.8747	18.401
	WOA	30	1535.931	116.6409	0.9362	0.7621	17.327
	POA	**30**	**1535.92**	**115.6295**	**0.9675**	**0.8747**	**15.501**
Case 2	DA	14	807.7806	86.7442	0.9677	0.8687	18.062

		30	1174.61				
	GOA	14 30	807.7843 1174.747	86.9598	0.9677	0.8756	18.690
	WOA	14 30	779.9395 1205.793	86.5912	0.9683	0.8708	16.920
	POA	**14** **30**	**807.7966** **1174.832**	**86.0429**	**0.9676**	**0.8753**	**16.834**
Case 3	DA	14 24 30	753.3605 1102.13 1070.822	71.4573	0.9679	0.8694	20.183
	GOA	14 24 30	754.091 1099.5 1071.406	71.756	0.9679	0.8763	20.821
	WOA	14 24 30	675.3904 1215.805 1106.958	71.9866	0.9685	0.8715	18.557
	POA	**14** **24** **30**	**753.2918** **1100.695** **1071.494**	**71.056**	**0.9679**	**0.8762**	**18.321**

Base Case: without DGs:

This case study doesn't consider the allocation of solar DGs. From the base case load flow, the following results are obtained. P_{Loss}=202.6666 kW, V_{min} = 0.9166 p.u, VS_{Imin} = 0.7045 p.u.

Case 1: **Single solar DG placement:**

From the LSF method, bus 30 is identified for placing a single solar DG. This information is passed to POA, and the single solar DG size is determined as 1535.92 kW. The results are given in Table 4.1 and compared with different algorithms. The combined approach helps to reduce the P_{Loss} by 42.94 %, which is better than other OTs. Further, the VSI_{min} and V_{min} are improved compared to the base case. Fig 4.5 shows the comparison of POA convergence characteristics with other metaheuristic methods.

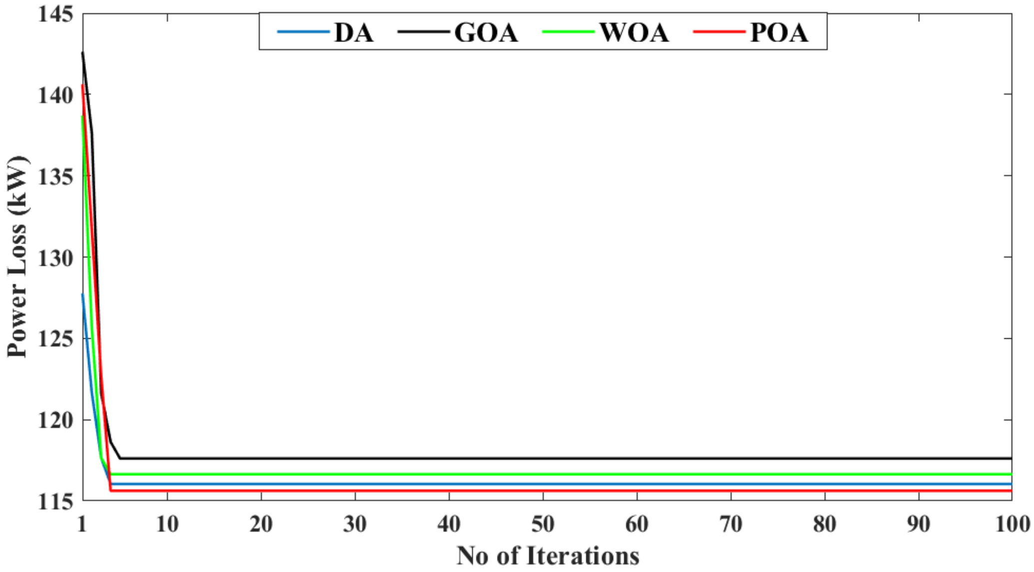

Fig.4.5. Convergence characteristics of single solar DG allocation

Case 2: Two solar DGs placement:

Using the LSF technique, bus numbers 14 and 30 are determined for allocating two solar DGs. The solar DG sizes are DG_1 = 807.7966 kW and DG_2 = 1174.832 kW using the POA. In Table 4.1, the results are compared with other OTs. A reduction of 57.54 % P_{Loss} is observed with the allocation of two solar DGs. Fig 4.6 shows the convergence characteristics of two solar DGs.

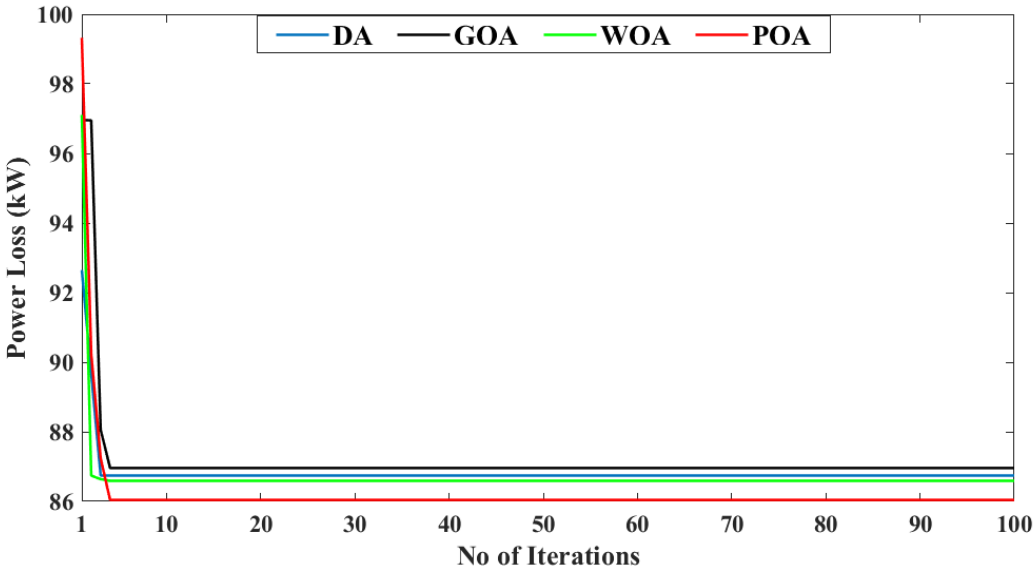

Fig.4.6 Convergence characteristics of two solar DGs allocation

Case 3: Three Solar DGs placement:

The suitable locations determined using LSF to allocate solar DGs are 14, 24 and 30. Multi-solar DGs inject kW power into the system. This three solar DGs case is more efficient than the allocation of single, two DGs, as shown in Table 4.1. An overall reduction of 64.93% P_{Loss} is observed in this case which can be treated as the best way to P_{Loss} minimization and voltage profile improvement. To prove the efficacy of POA, the results are compared with other simulated OTs in Fig 4.7. It is proven that POA is superior to other compared methods and helpful in proceeding with dynamic case studies. The proposed method is compared with the existing algorithms in the literature, and the same is given in Table 4.2

Further, in Table 4.3, the various metrics such as mean, median and standard deviation are compared with other OTs, and it is found that POA outperforms in all aspects effectively. Finally, a comparison between all case studies in terms of voltage profile, VSI and P_{Loss} are made in Figs 4.8, 4.9 and 4.10. It is evident from the Figure that was using a combined approach of LSF and POA, the overall system performance is improved drastically.

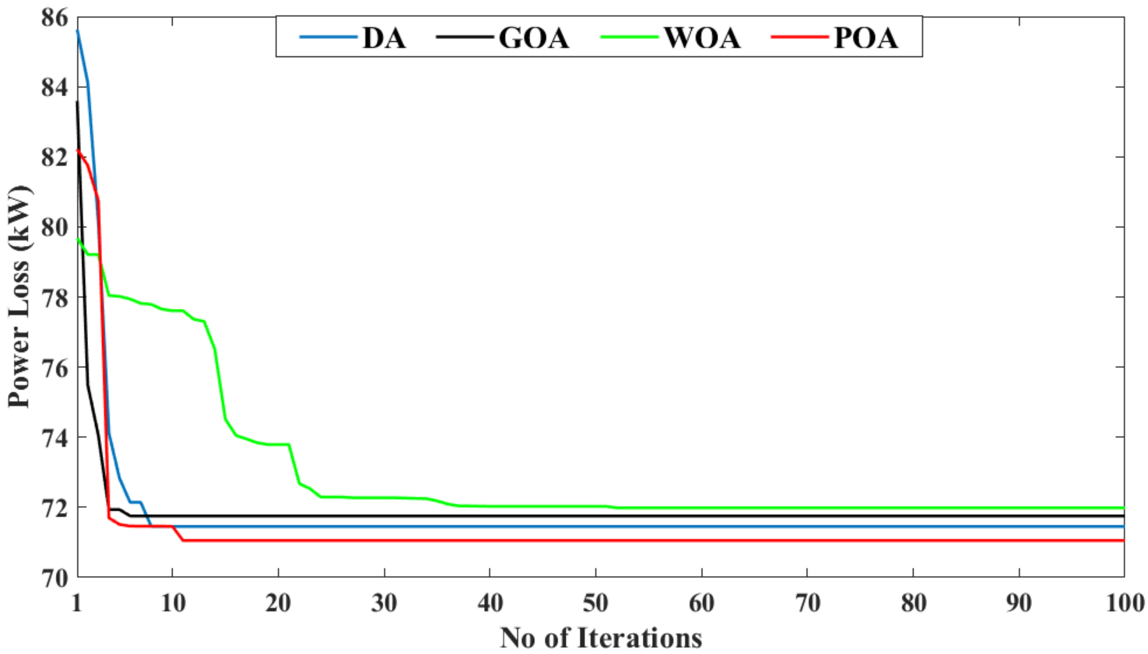

Fig.4.7 Convergence characteristics of three DGs allocation

Table 4.2 POA performance comparison with other existing algorithms

Optimization Method	**SFSA[19]**	**SSA[32]**	**SCA [80]**	**EGOA [81]**	**POA method**
Size and Location of DGs	964.7 (13) 1133.7(24) 1301.8(30)	753.6(13) 1100.4(23) 1070.6(29)	803.2998(13) 1166.7845(24) 1044.7203(30)	674.81(17) 171.04(18) 1032.31(31)	753.2918 (14) 1100.695 (24) 1071.494 (30)
Base Case P_{Loss} (kW)	210.99	202.66	211.0058	202.67	202.6666
Multi solar DGs P_{Loss} (kW)	77.410	71.45	72.8570	87.31	71.056
% of Minimized P_{Loss} (kW)	63.31	64.74	65.47	56.92	64.93

Table 4.3 Comparison of various metrics for OTs

OTs	**Mean**	**Median**	**Standard Deviation**	**Time(s)**
DA	11.7691	11.6908	0.2341	23.872
GOA	11.6295	11.6295	0.0598	20.698
WOA	13.60938	13.4604	1.1388	17.075
POA	**11.6137**	**11.6031**	**0.0561**	**17.043**

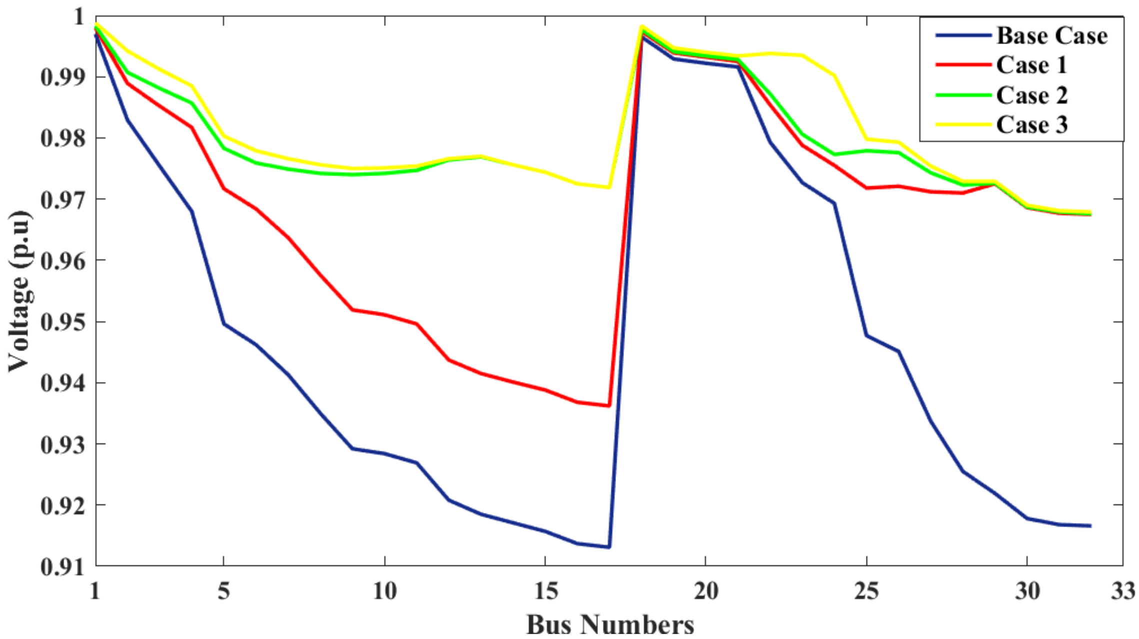

Fig. 4.8 33 bus voltage profile characteristics for various cases

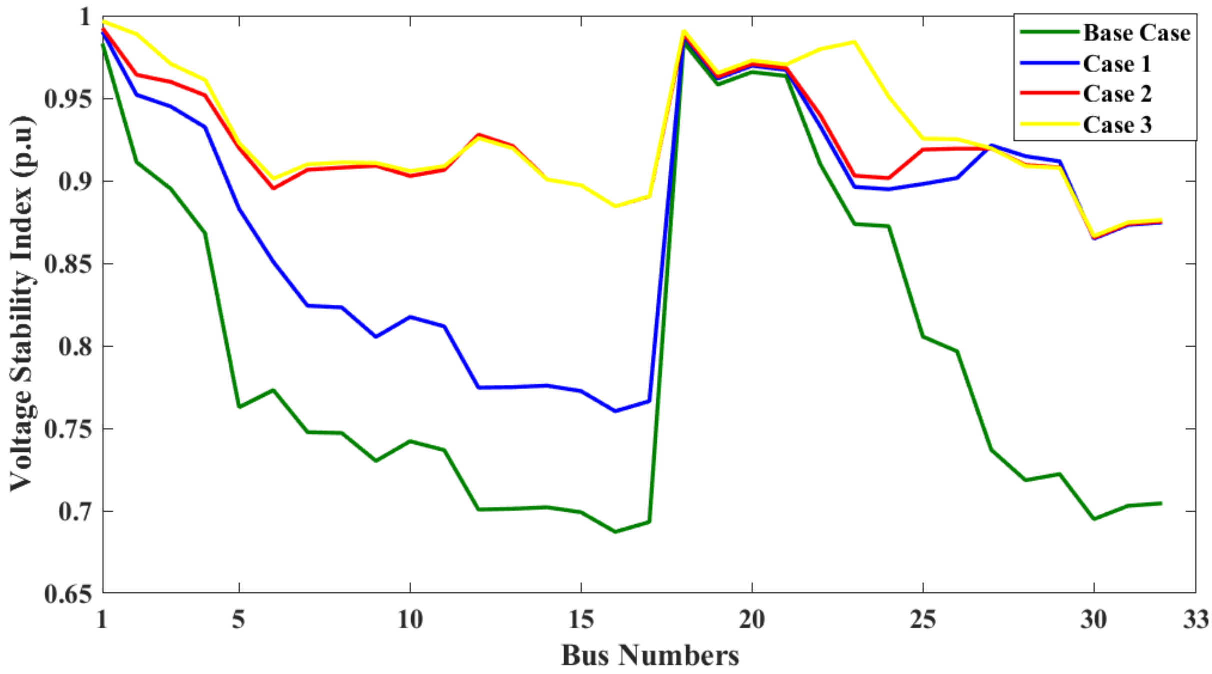

Fig. 4.9 Voltage stability index of 33 bus systems for different cases

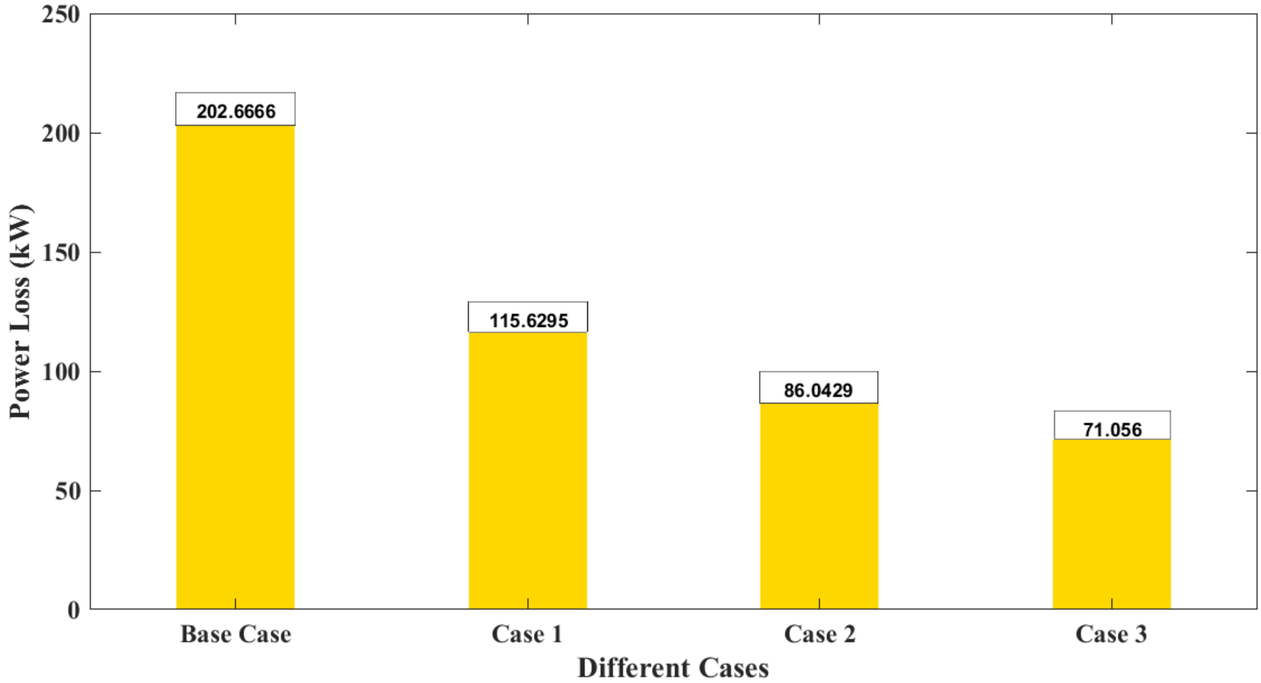

Fig.4.10. P_{Loss} reduction for different cases

4.6 Dynamic Analysis of IEEE 33 Test System:

Case 4: Dynamic analysis of IEEE 33 bus system with solar-based DGs

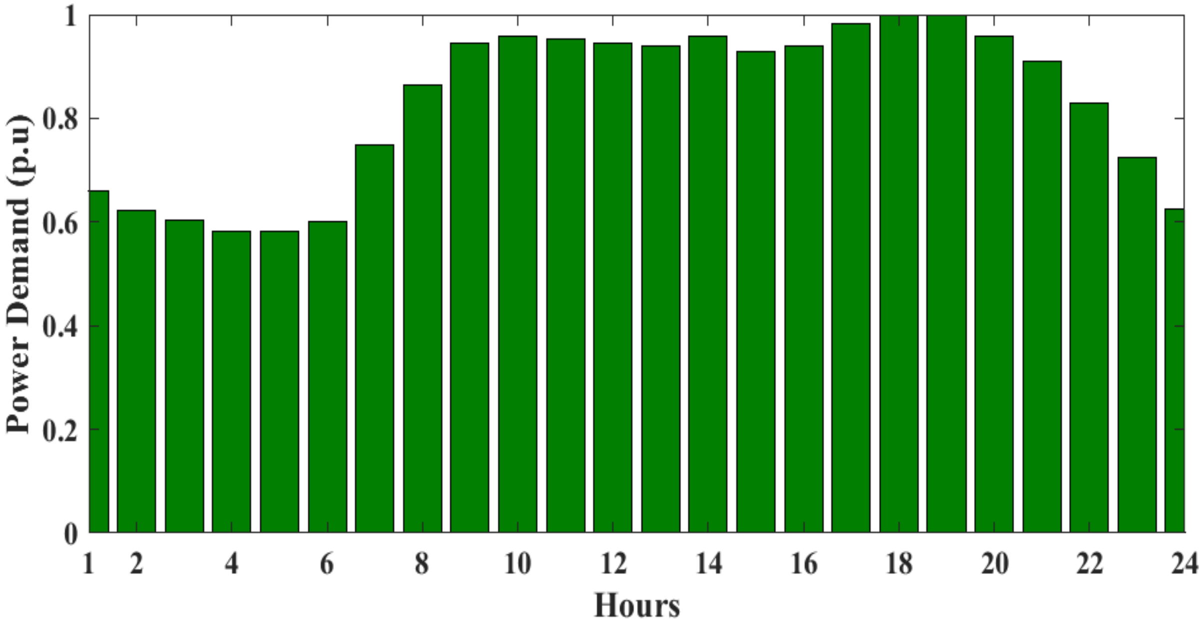

Fig.4.11. The power demand curve for a typical day

As the load continuously changes from hour to hour, analysing the dynamic changes in the system's voltage profile and P_{Loss} is essential. The typical load curve for 24 hours is given in Fig 4.11. The analysis presented in case 3 is extended for a typical 24-hour simulation using the LSF and POA combined approach. The load flow incorporating dynamic changes in system demand is simulated, and the suitable locations of solar DGs and EVCS for all the hours are identified using the LSF technique. In any system, generally, the DGs will be immovable assets. Therefore, the specified location should be unique for all dynamic changes in system demand. The best locations identified for all the dynamic load changes are 14, 24 and 30, respectively. The optimal solar DG sizes for the dynamic cases are presented in Table 4.4, Table 4.5, P_{Loss}, V_{min} and VSI_{min} obtained using the POA. It is evident that V_{min} and VSI_{min} are within permissible limits for all 24 hours. Compared to the base case P_{Loss} 3-solar DGs were minimized more, as shown in Fig 4.12. V_{min} and VSI_{min} various case comparison characteristics are shown in Figures 4.13 and 4.14. The

Table 4.4 Variation of P_{Loss}, V_{min} and VSI_{min} for 24 hours

Hours	**Base Case P_{Loss} (kW)**	**3 Solar DGs P_{Loss} in (kW)**	**Vmin (p.u)**	**VSImin (p.u)**
1	84.1544	30.57938	0.9727	0.8934
2	73.8534	26.92558	0.9797	0.9195

3	69.6966	25.44493	0.9825	0.93
4	64.5108	23.59614	0.9829	0.9318
5	64.5108	23.59369	0.9829	0.9318
6	68.7376	25.10265	0.98	0.9207
7	109.7536	39.58196	0.9806	0.9141
8	148.1548	52.89892	0.9708	0.8858
9	179.8568	63.73791	0.9718	0.8869
10	184.3782	65.27355	0.9759	0.8942
11	183.1387	64.85281	0.9706	0.8849
12	179.8568	63.73798	0.9718	0.8869
13	177.013	62.77088	0.9694	0.8804
14	184.3782	65.27366	0.9759	0.8942
15	172.9955	61.40268	0.9704	0.8841
16	177.013	62.77079	0.9694	0.8804
17	194.8954	68.8376	0.9714	0.8875
18	202.6666	71.0560	0.9723	0.8821
19	202.6666	71.0560	0.9723	0.8821
20	184.3782	65.27445	0.9759	0.8942
21	165.8967	58.98042	0.969	0.879
22	135.6764	48.59356	0.979	0.9128
23	102.1834	36.92998	0.9768	0.9085
24	74.8505	27.2792	0.9809	0.924

Table.4.5. Hourly variation of solar DG sizes with POA

Hours	**DG_1 (kW)**	**DG_2 (kW)**	**DG_3 (kW)**
1	506.9745	553.5879	674.4651
2	499.5958	560.213	577.8148
3	454.7839	503.1594	579.4696
4	484.2353	511.4542	559.2546

5	484.2353	511.4542	559.2546
6	482.012	520.1042	521.6075
7	594.0906	639.9615	765.857
8	757.4179	772.5085	822.3429
9	763.4068	807.96	928.067
10	752.167	842.1351	966.8828
11	757.3233	765.9752	947.3609
12	763.4068	807.96	928.067
13	735.6201	811.2937	869.6256
14	752.167	842.1351	966.8828
15	730.914	806.8769	854.0021
16	735.6201	811.2937	869.6256
17	786.0859	864.9384	978.3929
18	797.4713	892.5939	974.4764
19	797.4713	892.5939	974.4764
20	752.167	842.1351	966.8828
21	747.6536	729.6743	887.546
22	642.2859	721.8435	808.5834
23	564.018	647.5285	655.2067
24	553.751	553.751	553.751

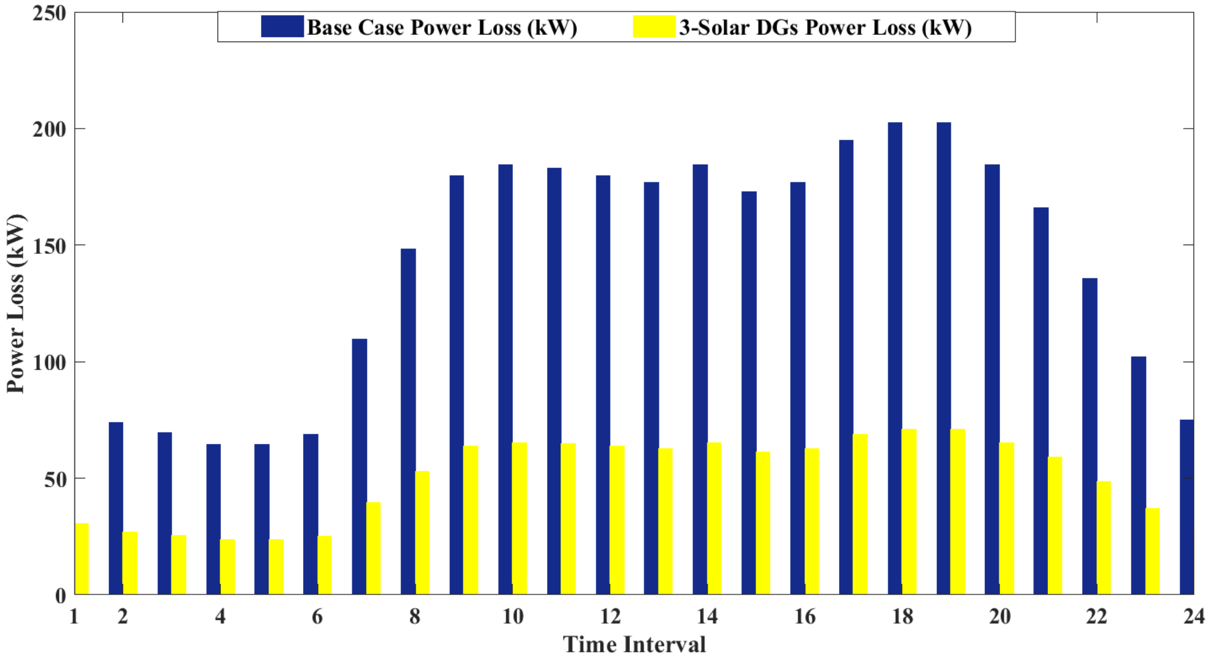

Fig 4.12 P_{Loss} comparison (Dynamic variations of load)

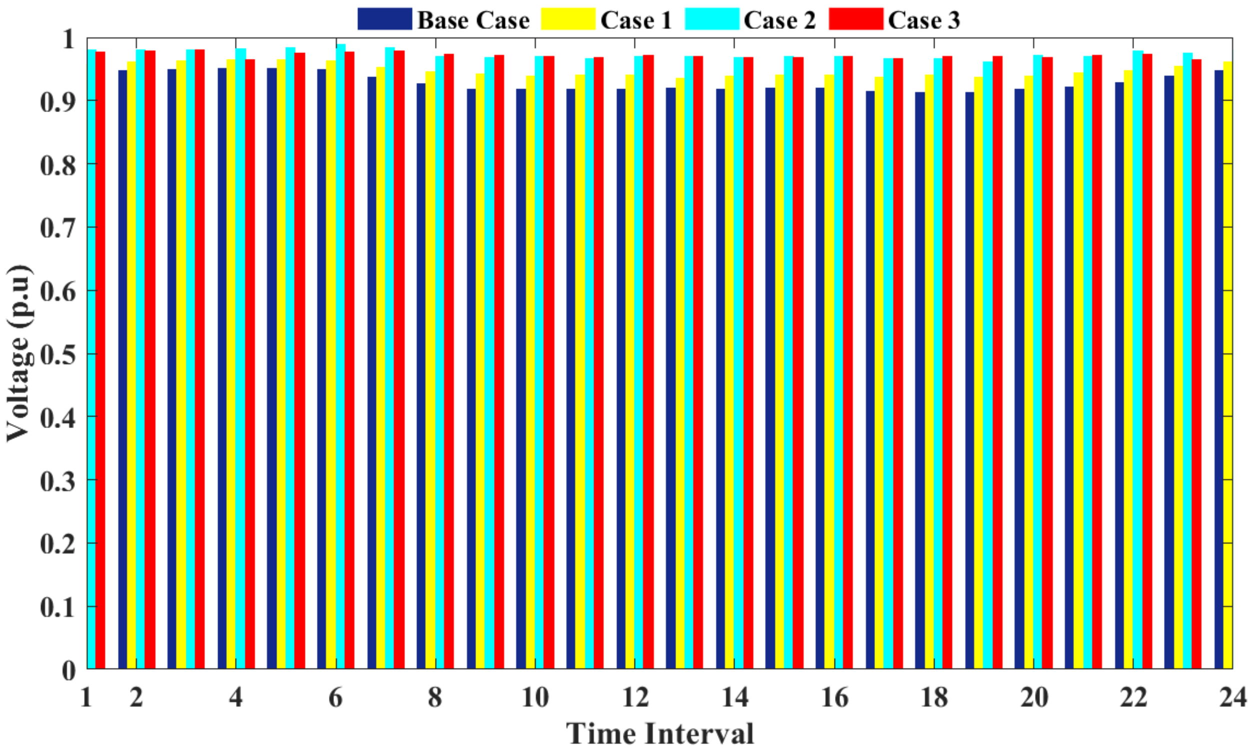

Fig 4.13 Comparison voltage profile for different cases (Dynamic Variations of load)

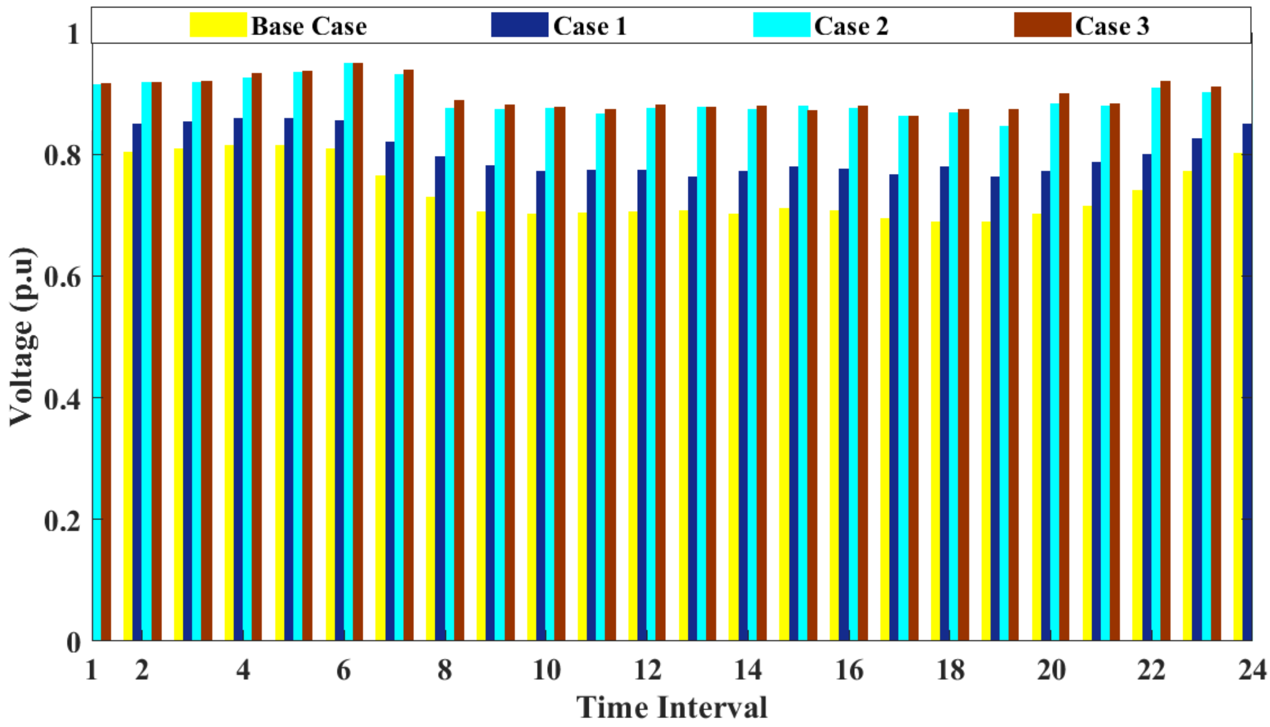

Fig 4.14 Comparison of voltage stability index for different cases (Dynamic Variations of load)

4.7 Different EV Charging Approaches:

In this case, the analysis with EVs and DGs is performed. The ratings of the considered EV are represented in Table 3.5. The EV will start their trip at 8.00 AM and end at 17.00 PM. The EVs should be charged before their next trip. The EVs are charged using two methods: the conventional charging method (CCM) and the optimized charging method (OCM).

4.7.1 Conventional Charging Method (CCM):

In this method, the EVs are charged immediately after their scheduled trip without considering the system demand, which increases the system's P_{Loss}.

4.7.2 Optimized EV charging method (OEV):

In this method, the EVs will be charged during off-peak hours determined by the OEV method. In Table 4.6, the comparison of P_{Loss} without EVs with EVs and DGs is given. It is observed that the OEV method, along with POA based DG allocation, gives better results than the conventional method.

IEEE 33 test system base case P_{Loss} = 3385.216 kW for 24hrs. Using the CCM (G2V) strategy, if we connect three solar DGs and EVs to the system, P_{Loss} = 1241.547kW means 63.32% of P_{Loss} is reduced. OCM performs better than the CCM method P_{Loss} = 1240.071kW.

Compared to the base case, the CCM (G2V) and OCM (G2V) combination of G2V plus V2G technique reduce more P_{Loss}. The same is shown in Fig 4.15 and tabulated data in Table 4.6.

Table 4.6 Different EV charging methods

Different Cases	**P_{Loss} (kW)**
Base Case	3385.216
With EVs & Conventional Charging Method (G2V)	1241.547
With EVs & Optimized Charging Method (G2V)	1240.071
With EVs & (G2V + V2G) Method	1239.001

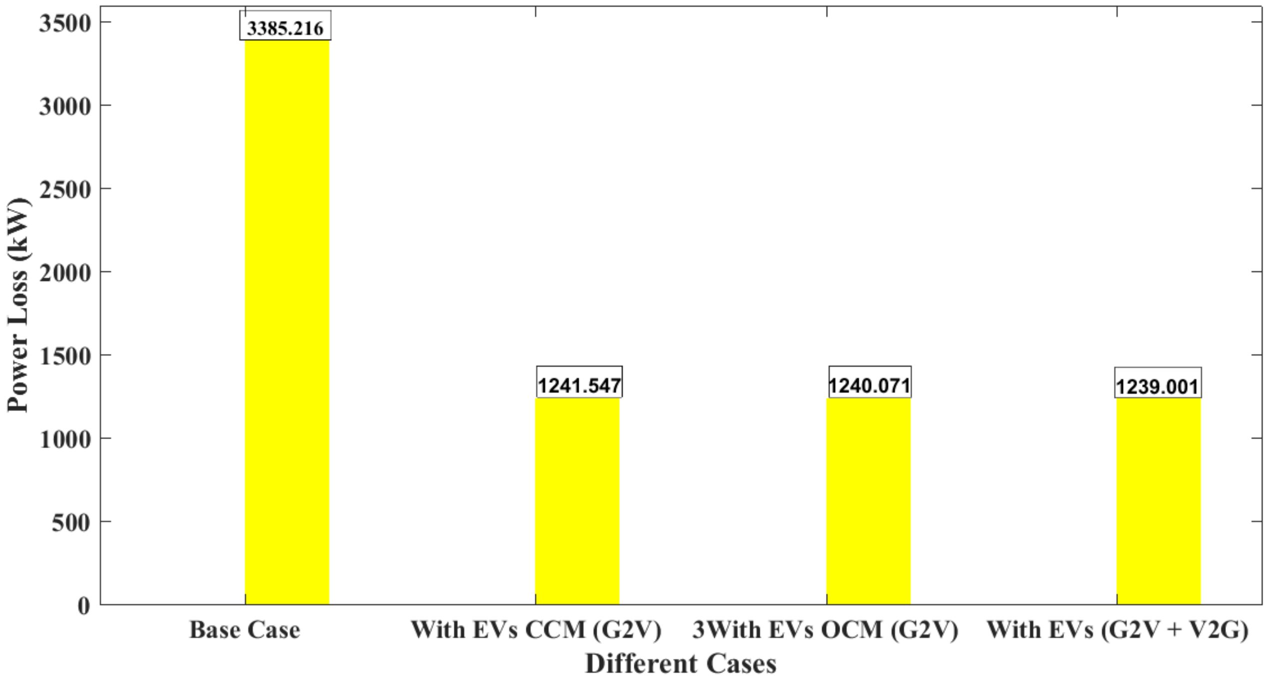

Fig. 4.15 33 bus P_{Loss} comparison of different EV charging methods

4.8 Dynamic analysis of solar DGs and EVs on 28 Indian bus system:

In this case, simulated results on 28 Indian bus system [82 - 83]. Without considering solar-based DGs and EVs, the P_{Loss} of 28 Indian bus system is 1147.1245 kW for a typical day. Without considering EVs, three solar-based DGs P_{Loss} = 951.084 kW for 24hr dynamic load variation considered. Considering different EV charging methods, CCM and OCM P_{Loss} reduced but compared to these two methods G2V plus V2G method decreased more P_{Loss}. Table 4.7 and Fig 4.16 the same is represented.

Table 4.7 Solar DGs and EVs are connected to the DS and analyzed the performance.

Hours	**Base case P_{Loss} (kW)**	**P_{Loss} with Solar DGs and EVs (kW)**	**P_{Loss} with Solar DGs and EVs (Conventional Method) (kW)**	**P_{Loss} with Solar DGs and EVs (Optimised Method) (kW)**	**P_{Loss} with Solar DGs and EVs (G2V +V2G) (kW)**
1	28.4096	28.4096	28.4096	28.4096	28.4096
2	24.9163	24.9163	24.9163	24.9163	24.9163
3	23.5076	23.5076	23.5076	23.5076	23.5076
4	21.751	21.751	21.751	25.273	25.273
5	21.751	21.751	21.751	25.273	25.273
6	23.1827	19.3841	19.3841	22.4215	19.3841
7	37.1053	28.0265	28.0265	28.0265	28.0265
8	50.1845	34.9842	34.9842	34.9842	34.9842
9	61.0107	40.2336	40.2336	40.2336	40.2336
10	62.5568	39.2832	39.2832	39.2832	39.2832
11	62.1329	37.7864	37.7864	37.7864	37.7864
12	61.0107	37.3954	37.3954	37.3954	37.3954

13	60.0386	37.6079	37.6079	37.6079	37.6079
14	62.5568	42.1009	42.1009	42.1009	42.1009
15	58.6655	42.6768	42.6768	42.6768	42.6768
16	60.0386	48.9409	48.9409	48.9409	48.9409
17	66.1549	60.1776	60.1776	60.1776	60.1776
18	68.8189	68.8189	75.2974	68.8189	63.0291
19	68.8189	68.8189	75.2974	68.8189	63.0291
20	62.5568	62.5568	68.7003	62.5568	62.5568
21	56.2403	56.2403	56.2403	56.2403	56.2403
22	45.9301	45.9301	45.9301	45.9301	45.9301
23	34.5317	34.5317	34.5317	34.5317	34.5317
24	25.2543	25.2543	25.2543	25.2543	25.2543
Total P_{Loss} - (kW)	**1147.1245**	**951.084**	**970.1845**	**961.1654**	**946.5484**

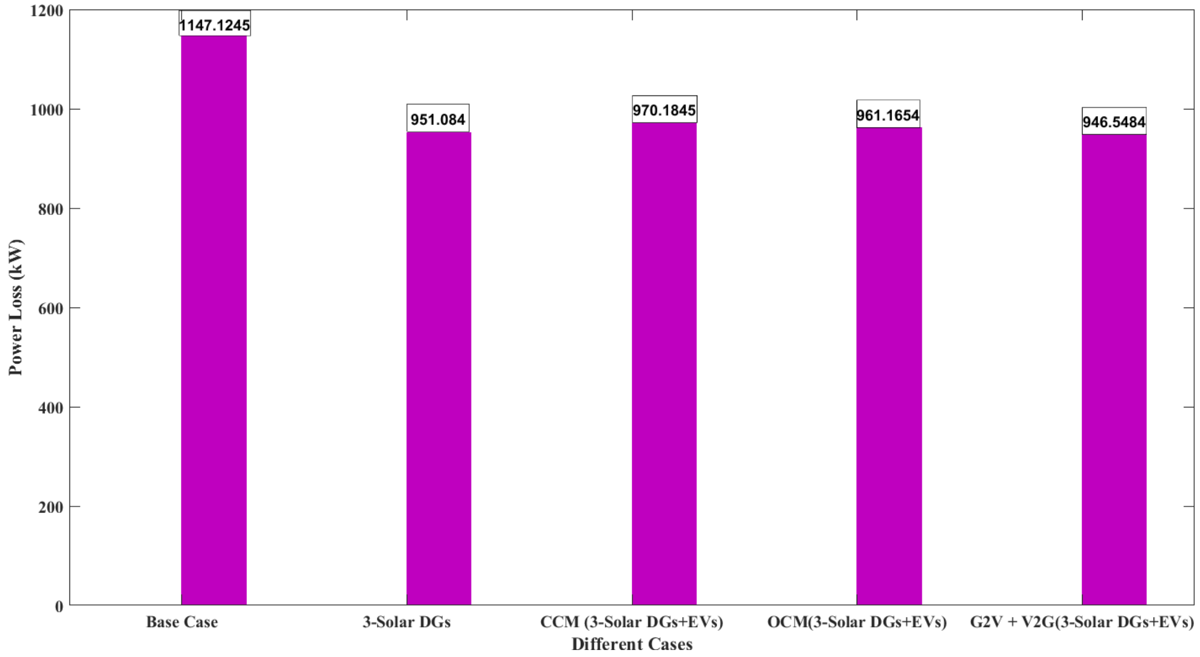

Fig. 4.16 28 real test system P_{Loss} Comparison for Different cases for dynamic variation

4.9 Summary and conclusion of the chapter:

This chapter uses a combined approach of LSF and POA methods to evaluate the allocation and sizing of solar DGs and EVCS in a DS. This method alleviates P_{Loss} and significantly inflates the VSI & voltage profile of the DS. LSF technique determines the suitable locations of solar DGs, and EVCS pass the values to POA to choose desired sizes. The analysis is performed on an IEEE 33 and 28 Indian real bus system considering various cases, and the outcomes are compared with other Meta heuristic methods. From the simulated three different case studies, it can be inferred that the chosen DS requires DGs and EVs in 3 locations for effective operation. In the identified 3 locations, POA will give the suitable size of solar-based DGs. From the appropriate size and location of DGs and EVCS, P_{Loss} is minimized by 63.39%. The VSI and voltage profile are abruptly improved with the combined approach. The evaluations are further extended for a 24-hour study, and the results demonstrate that P_{Loss} is minimized significantly throughout the period. The VSI and voltage profile are improved for the entire simulation period. This shows that the proposed combined approach is effective in static and dynamic load conditions.

CHAPTER 5

Integration of Wind Distributed Generators and Electric Vehicles to the Distribution System

5.1 Introduction:

In this chapter, a combined approach based on LSF and POA is proposed to solve the problem of wind-based distributed generators (DGs) and Electric Vehicles (EVs) allocation in the distribution system (DS). Further, the objective of this method is to minimize P_{Loss} and enhance the voltage profile of the DS. Also, the developed method is tested on IEEE 69 and practical 28 bus Indian DS. Different operational cases are used to compare the proposed POA method with DA, GOA, and WOA techniques. Different cases, such as single DG, multiple DGs, and the combination of DGs plus EVs, are considered to check the method's effectiveness. The static and dynamic load variations are considered to study the performance. EV charging and discharging patterns are considered to check the performance of DS. Finally, the results related to grid vehicle (G2V), vehicle to grid (V2G), conventional charging and optimized charging are projected. The obtained results verified that proper placement of DGs and effective charging strategies for EVs reduce the P_{Loss} to a considerable extent. In figure 5.1 given schematic diagram of wind DGs and EVs into DS.

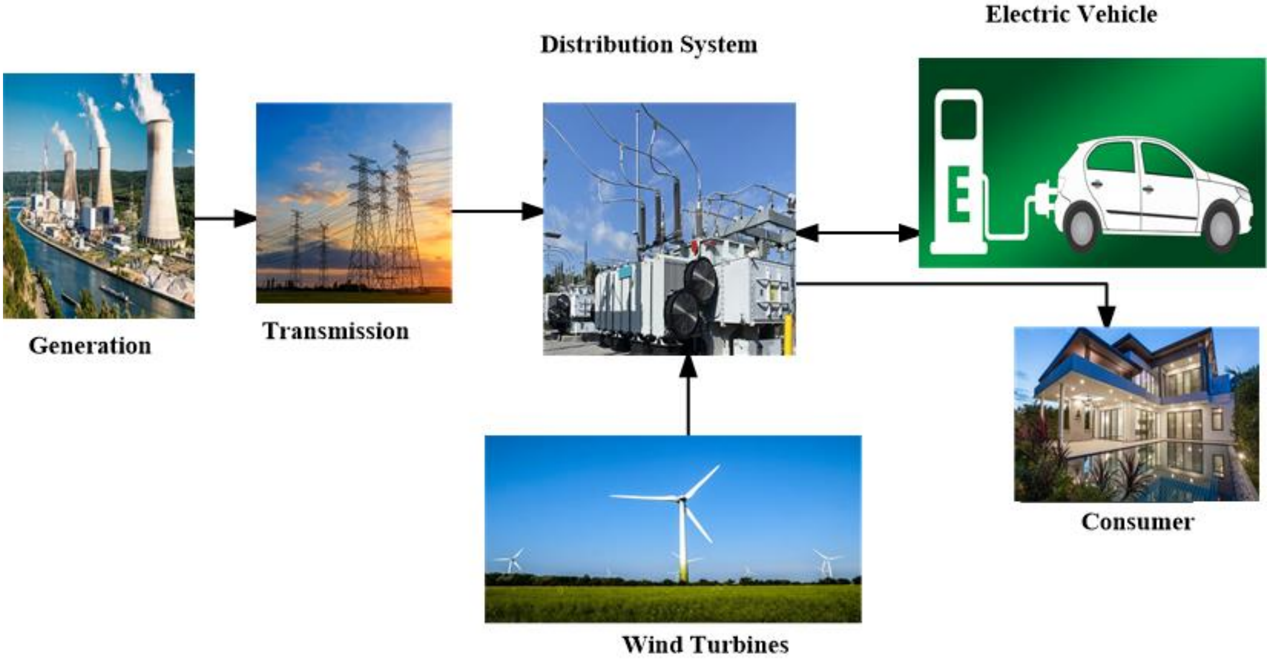

Fig 5.1 Schematic diagram of wind DGs and EVs into DS

5.2 Mathematical Problem Formulation:

The primary objective is to minimize the P_{Loss} of the DS and the improving voltage profile of all buses with the optimal integration of wind DGs and EVs. The active, reactive P_{Loss} and voltage injection at specific bus equations are given below

$$P_{k+1} = P_k - P_{Lk+1} - R_{k,k+1}.\frac{P_k^2+Q_k^2}{|V_k|^2} \tag{5.1}$$

$$Q_{k+1} = Q_k - Q_{Lk+1} - X_{k,k+1}.\frac{P_k^2+Q_k^2}{|V_k|^2} \tag{5.2}$$

$$|V_{k+1}|^2 = |V_k|^2 - 2\left(R_{k,k+1}.P_k + X_{k,k+1}.Q_k\right) + (R_{k,k+1}^2 + X_{k,k+1}^2).\frac{P_k^2+Q_k^2}{|V_k|^2} \tag{5.3}$$

Where at node k → P_k= Real power, Q_k= Reactive power

At node k+1 → P_{Lk+1}= Real power load, Q_{Lk+1}= Reactive power load

The line section between nodes k and k+1 → $R_{k,k+1}$= Resistance, $X_{k,k+1}$= Reactance

k^{th} node voltage magnitude = $|V_k|$

Equation (1) & (2) represents power balance

Eq's (3) fulfills sending and receiving end of voltage magnitude

Eq. 4 represents active P^{Loss}

$$min \sum_{k=1}^{24} P_{Loss}(k) \tag{5.4}$$

Where

$$P_{Loss}(k) = \sum_{k=1}^{24} I^2.R_k \tag{5.5}$$

Adding all line losses = total P_{Loss} represented by below eq.

$$Total\ P_{Loss} = \sum_{k=0}^{n-1} P_{Loss}\,(k.k+1) \tag{5.6}$$

$$P_{Loss(k,k+1)}^{WDG} = R_{k,k+1}.\left(\frac{P_{WDG,k,k+1}^2 + Q_{WDG,k,k+1}^2}{|V_k|^2}\right) \tag{5.7}$$

$$P_{TotalLoss(k,k+1)}^{WDG} = \sum_{k=1}^{nbk} P_{Loss(k,k+1)}^{WDG} \tag{5.8}$$

$$y_1 = \Delta P_{TotalLoss}^{WDG} = \frac{P_{TotalLoss}^{WDG}}{P_{TotalLoss}} \quad \text{or } y_1 = minimize(P_{Loss}) \tag{5.9}$$

$$y_2 = \text{maximize}(\text{VSI}) = \text{minimize}(\frac{1}{\text{VSI}}) \tag{5.10}$$

$$\text{Objective Function} = \text{y}_1 \times \text{w}_1 \times \text{y}_2 \times \text{w}_2 \tag{5.11}$$

5.2.1 Constraints

Power balance Constraints

$$\sum_{n=1}^{24} P^{W_{DG}}(n) = \sum_{n=1}^{24}[P^{Demand}(n) \pm P^{EV}(n) + P_{Loss}(n)] \tag{5.12}$$

Voltage Constraints

$$V_{k,min} \leq |V_k| \leq V_{k,max} \tag{5.13}$$

DG Size Constraints

$$P_{k,min}^{DG} \leq P_k^{DG} \leq P_{k,max}^{DG} \tag{5.14}$$

Where,

$$(P_{k,min}^{DG} = 0.1 \sum_{k=2}^{n} P_m^{DG}, P_{k,max}^{DG} = 0.8 \sum_{k=2}^{n} P_k^{DG})$$

Different constraints integrated with EVs are

EVs Battery storage Constraints:

EVs k[th] hour state of charge is

$$SoC_{min,k} \leq SoC_k^{EV} \leq SoC_{max,k} \tag{5.15}$$

Charging /Discharging EV Constraints:

EV power charging/discharging must be within below equation limits

$$P_{ch,k} \leq P_{ch,k}^{max} \tag{5.16}$$

$$P_{disch,k} \leq P_{disch,k}^{max} \tag{5.17}$$

Where, $P_{ch,k}$, $P_{disch,k}$ = EV battery k[th] hour charging & discharging power

5.3. Integrated solutions for optimal installation and sizing of wind DGs and EVCS

LSF method considered to find location of wind based DGs and EVCS. In chapter 4, section 4.3 and 4.3.1 discussed LSF method. To find size of wind DGs implemented POA method and the same step by step procedure given in Fig 5.2.

5.3.1 Steps for calculating the optimal sizes of DGs with POA:

Step 1: Read the DS data (Line and Bus data)

Step 2: Run the base case load flow

Step3: Find suitable locations for wind DGs and EVCS with the LSF method

Step 4: Best sites of wind DGs and EVCS determined using LSF should be given as input to POA

Step 5: As per eq. 4.9 all citizens are categorized into 'n' political parties; each party include 'n' member by using eq. 4.10.

Step 6: Chief of the party determined with good fitness in eq. 4.14, champion of every individual constituency called a member of parliament by using eq. 4.15

Step 7: Compared present values with the previous position values

Step 8: At the beginning of algorithm loops, fitness values and positions are created temporarily.

Step 9: Eq. 4.17, 4.18 represents the 2^{nd} phase election campaign, using this eq's all political parties' member values and positions updated

Step 10: Eq. 4.19 represents the election campaign after the phase, every individual member of the switching phase runs

Step 11: Champions of constituency calculated with eq. 4.20.

Step 12: In this step, the algorithm shows all the champions of parliamentary locations, called the parliamentary affairs phase

Step 13: This final step is upgrading the fitness value (P_{Loss}) and positions such as best wind-based DG sizes.

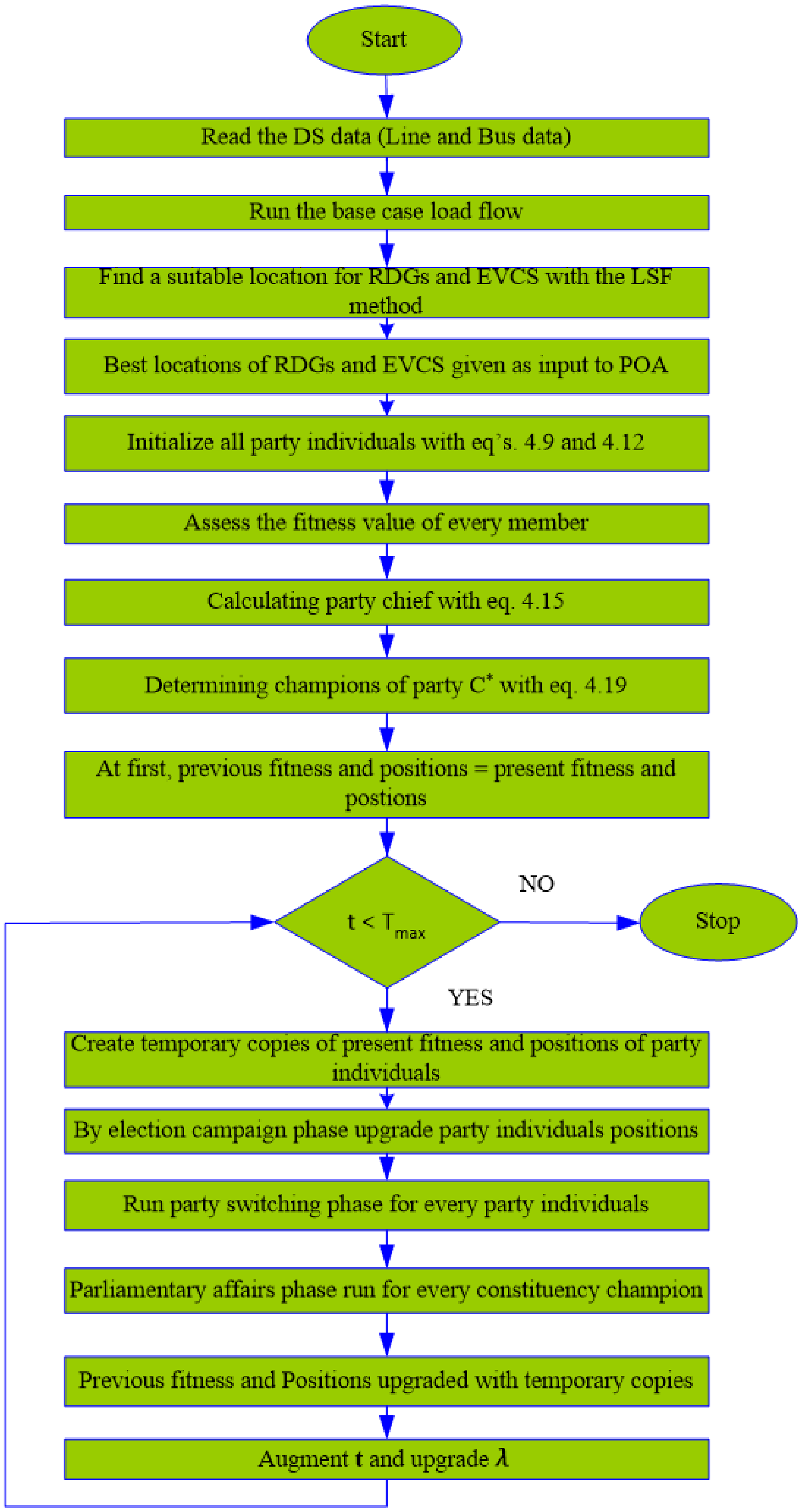

Fig 5.2 flow chart of POA to find wind DGs sizes

5.4 Results and Discussion:

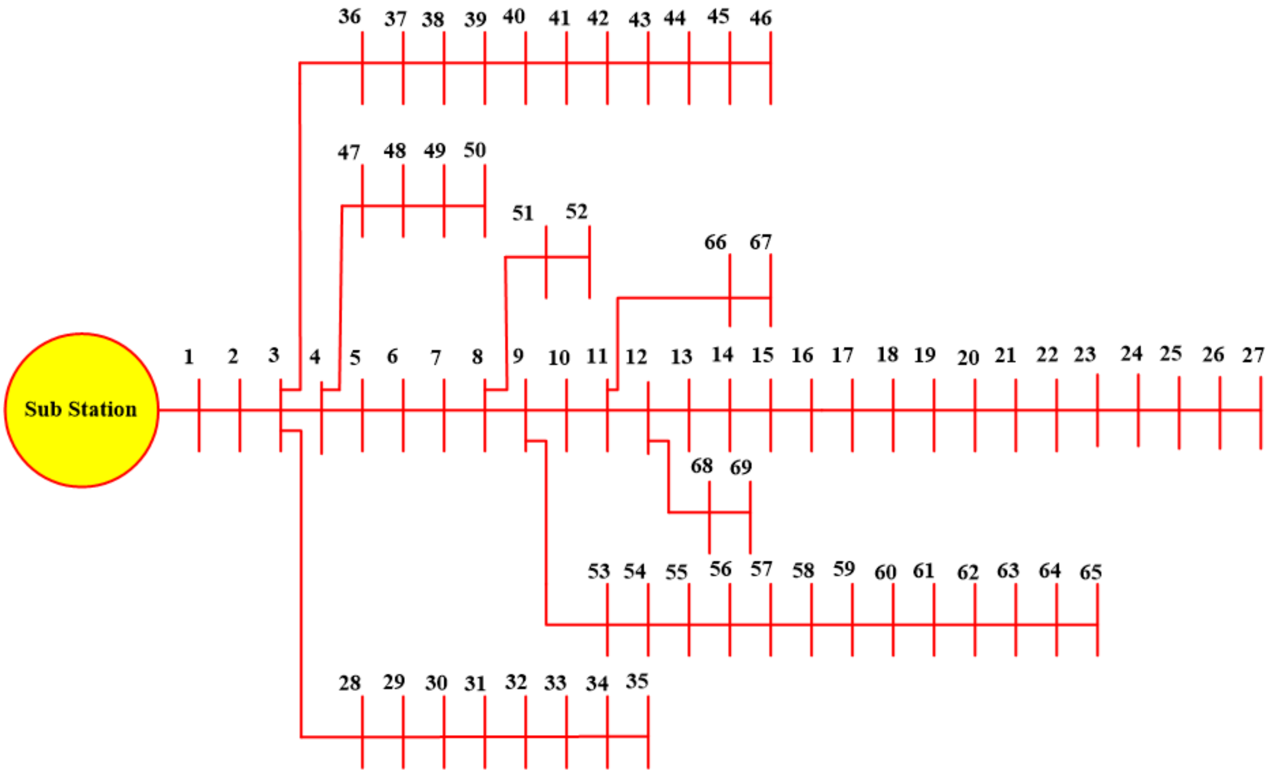

Fig 5.3 Single line diagram of IEEE 69 bus

We analyzed different case studies to optimize wind-based DGs and EVs in the DS. The simulation was performed on an IEEE 69 test system. IEEE 69 test system included 69 buses & 68 branches. The system configurations are as follows: Voltage: 11.4 kV, real and reactive power demands are 28.35 MW & 20.70 MVAr [73, 79 and 84]. Fig 5.3 represents the single-line diagram of the IEEE 69 bus. The impact of the simultaneous placement of wind DGs in DS and the effect of EV charging on DS are analyzed with different operating conditions. The best location of wind-based DGs and EVCS was found initially with the LSF method. The information was passed to POA. The combination of LSF and POA is presented to minimize P_{Loss} and augment the voltage profile, and the stability of DS is discussed in detail in this section. The total active P_{Loss} was calculated, and kW and kVAr sizes were found with POA. 69 test system different cases result tabulated in Table 5.1.

Base Case:

The placement of wind DGs is not considered in this case study. The following findings are obtained by analyzing the base case load flow factors. P_{Loss} = 225.0014 kW, V_{min} = 0.9678p.u, VSI_{min} = 0.8773p.u, time = 15.149s.

Case 1: With a single wind-based DG

In this case, it considered the single wind-based DG and the results are tabulated in table 5.1. As per the LSF method, 61 bus number is best for allocating single wind DG; it injects kW and kVAr power into the system. The message was passed to the POA. POA finds suitable sizes to place DGs. DG_1 size = 1828.478kW/1300.729kVAr, P_{Loss} = 23.1688kW, V_{min} = 0.9838p.u, VSI_{min} = 0.9368p.u, % of minimized P_{Loss} = 90.15. Fig 5.4 represents the convergence curve of single wind DG; this figure shows that POA reduces more P_{Loss} than other OTs. The single wind-based DG performs better than the base case.

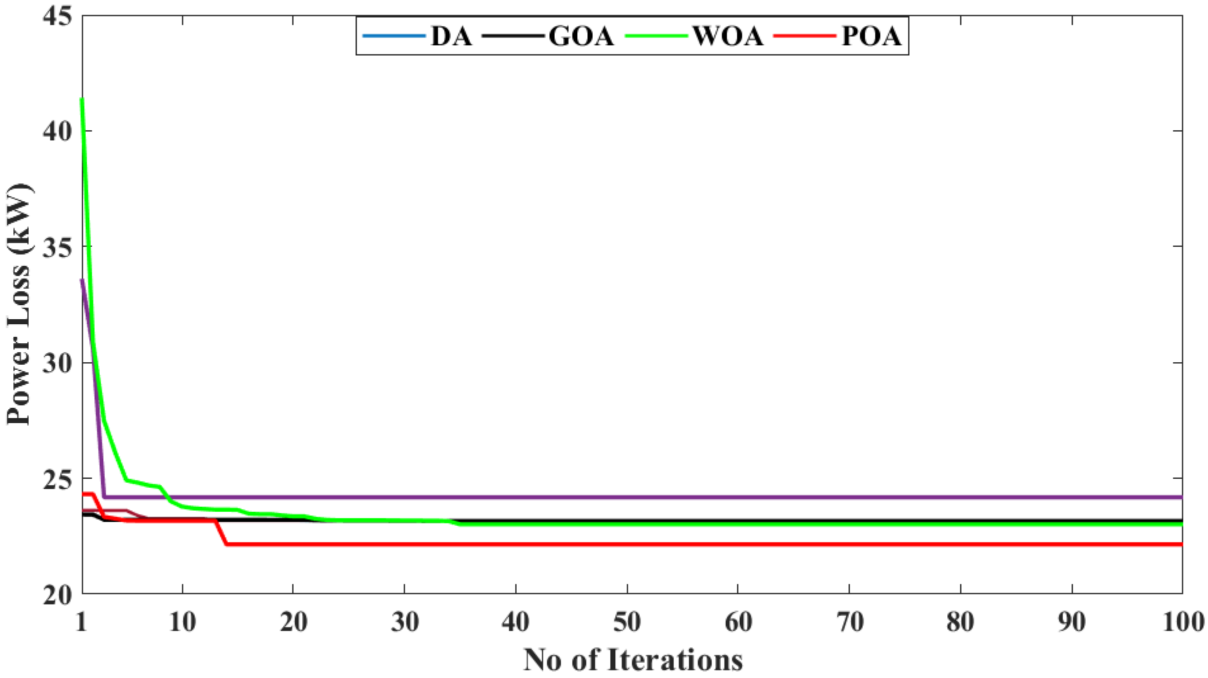

Fig 5.4 Convergence Curve of Single wind DG

Case 2: With Two wind-based DGs

This case consists of combining two wind-based DG results illustrated in table 5.1. According to the LSF technique, 11, 61 nodes are apt for locating two wind-based DGs injecting kW and kVAr into the system. It is observed that a combination of two wind DGs performs better in every aspect; it minimizes losses more compared to other cases. Augment voltage stability index and enhance voltage profile. With POA was found DG sizes DG_1 size = 883.2982kW/609.0988kVAr, DG_2 size = 1670.704kW/1194.508kVAr, P_{Loss} = 10.1082kW, V_{min} = 0.9965p.u, V_{max} = 0.9862p.u, % reducing P_{Loss} = 95.5. Fig 5.5 depicts the convergence curve of two wind-based DGs, and it's very clear from this figure that POA performance is better at minimizing P_{Loss} compared to other metaheuristic technique$_s$.

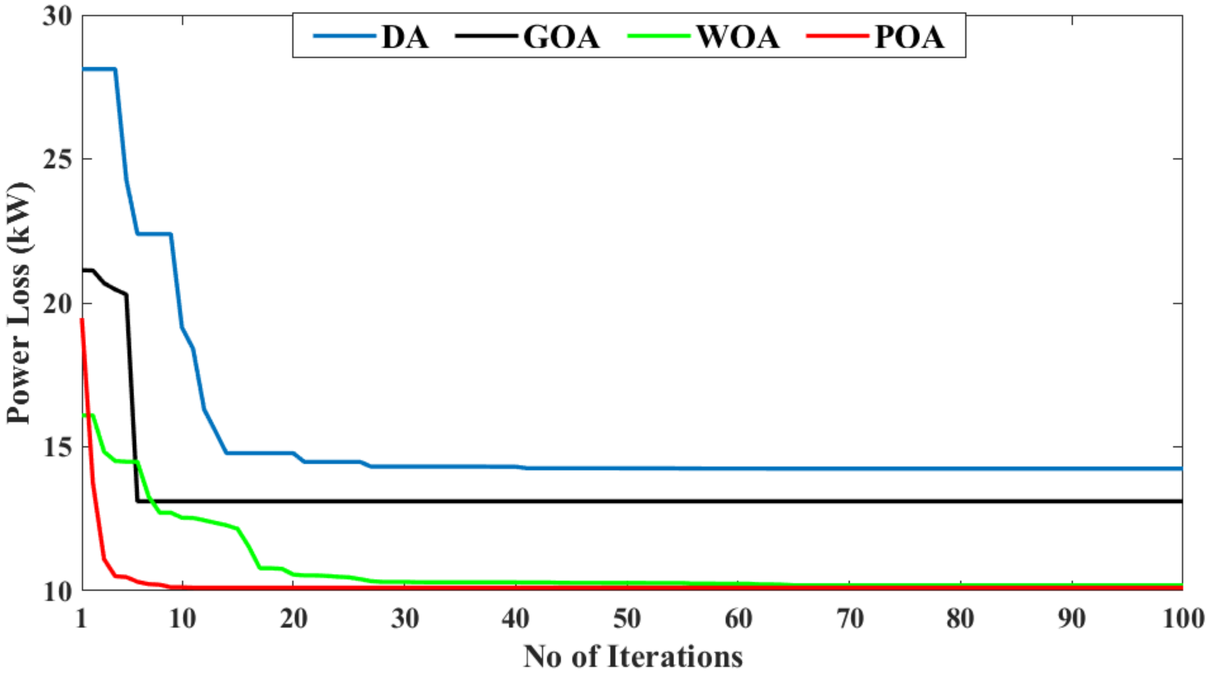

Fig 5.5 Convergence Curve of two wind-based DGs

Case 3: With Three Wind-Based DGs

In this case, the allocation of three wind-based DGs is considered, and the results are tabulated in Table 5.1. As per LSF analysis, bus numbers 11, 17, and 61 are better for three wind-based DGs allocation. It injects kW and kVAr power into the system. The same information was delivered to POA. The results noticed that the VSI, voltage profile and % of reduced P_{Loss} improved in case 3. Fig 5.6 convergence curve shows that POA performs better than other algorithms; it reduces maximum P_{Loss}. The voltage profile and VSI increment are shown in Figures 5.8 and 5.9, and the % of reduced P_{Loss} for every case is illustrated in Fig 5.7; from this figure observed, compared to all other cases, case 3 minimized more P_{Loss}. Based on Table 5.1, statistical results know those three wind DGs give the best results with the help of the POA method. P_{Loss} = 4.067kW, V_{min} = 0.9987 p.u, V_{max} = 0.9947 p.u, % of reducing P_{Loss} = 98.19. The proposed method is compared with the existing algorithms in the literature, and the same is given in Table 5.2. Compared to other methods, POA minimized 98.19% P_{Loss}, and improved voltage profile and stability. It clearly shows that POA performs better in all aspects compared to the other methods.

Table 5.1 Performance analyses of wind-based DGs and compared results with other methods

Different Cases	**Different OTs**	**Bus Number**	**Wind DG Sizes (kW/kVAr)**	**P_{Loss} (kW)**	**V_{min} (p.u)**	**VSI_{min} (p.u)**
Base Case		NA	NA	225.0014	0.9678	0.8773
Case 1	DA	61	1828.47/1300.612	24.1798	0.9724	0.8943
	GOA	61	1828.478/1300.637	23.1588	0.9838	0.9368
	WOA	61	1827.775/1301.584	23.0146	0.9722	0.8934
	POA	**61**	**1828.418/1300.729**	**22.1488**	**0.9838**	**0.9368**
Case 2	DA	11 61	872.1218/789.6246 1684.108/1303.349	14.2437	0.9823	0.9312
	GOA	11 61	885.4453/609.8202 1674.299/1195.619	13.1078	0.9966	0.9864
	WOA	11 61	809.5635/597.8259 1684.069/1218.91	10.1887	0.9845	0.9395
	POA	**11** **61**	**883.2982/609.0988** **1670.704/1194.508**	**10.1082**	**0.9965**	**0.9862**
Case 3	DA	11 17 61	493.5211/304.1673 380.6125/354.1572 1236.033/1236.033	5.2559	0.9999	0.9943
	GOA	11 17 61	494.3808/352.6491 379.1516/251.9374 1674.297/1195.696	4.2664	0.9986	0.99444
	WOA	11 17 61	586.4385/317.6449 343.095/304.266 1663.173/1177.288	4.4243	0.9943	0.9539
	POA	**11** **17** **61**	**513.7702/398.7177** **457.1899/234.2604** **1641.874/1178.444**	**4.067**	**0.9987**	**0.9947**

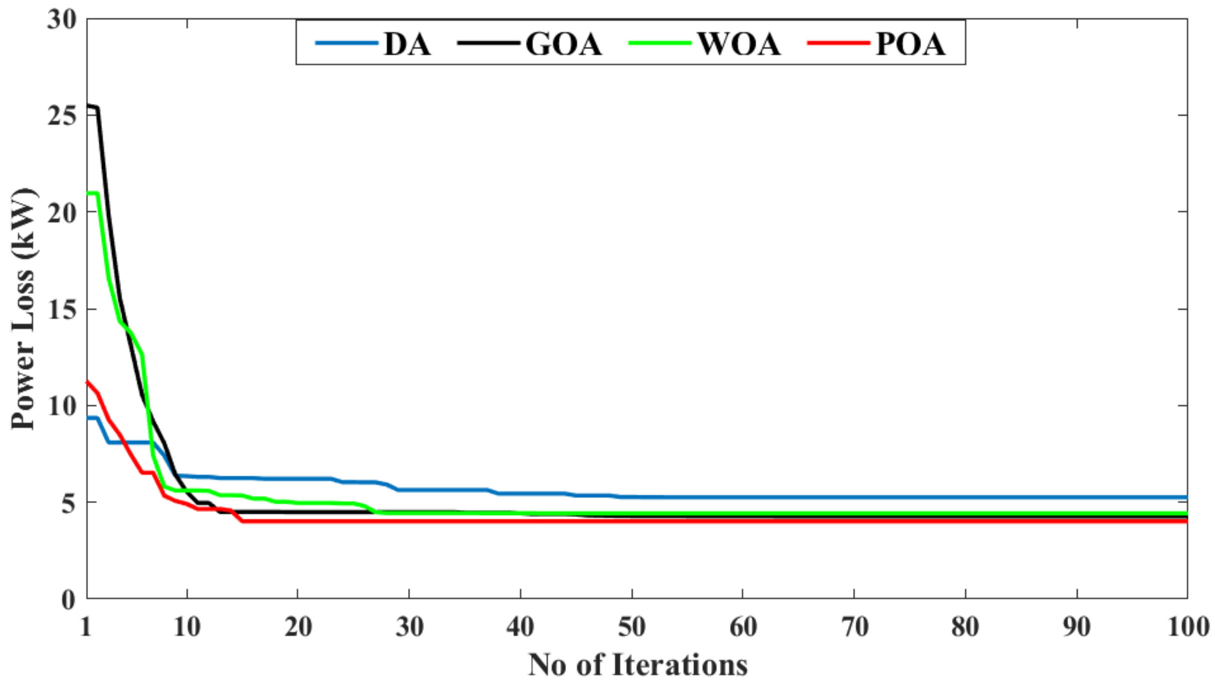

Fig 5.6 Convergence Curve of three wind-based DGs

Table 5.2 POA performance comparison with other existing algorithms

Optimization Method	**SFSA[19]**	**IMPA[85]**	**BWO-2 [86]**	**POA Method**
Size of DG	495.8/357.2(11) 392.9/259.4(18) 1685.5/1195.5(61)	552.96(17)/575.07(12) 719.35(50)/564.35(49) 1754(61)/1187.31(62)	495(11)/334(12) 379(18)/207(21) 1674(61)/1206(61)	513.7702/398.7177(11) 457.1899/234.2604(17) 1641.874/1178.444(61)
Base Case P_{Loss} (kW)	225	225.74	225	225.0014
Multi wind DGs P_{Loss} (kW)	4.285	5.8037	4.300	4.067
% of Minimized P_{Loss} (kW)	98.10	97.42	98.09	98.19

Table 5.3 mean, median and standard deviation of POA comparison with other OTs

Different methods	Mean	Median	Standard Deviation	Time
DA	5.338712	5.2698	0.137766437	16.596
GOA	4.2664	4.2664	0.269159	23.300
WOA	6.754762	6.53905	1.630634	11.174
POA	**4.4434**	**4.4236**	**0.1190**	**11.006**

In addition, the performance of POA is evaluated against that of other OTs using several different parameters, including the mean, the median, and the standard deviation, the same given in Table 5.3. POA standard deviation and time taken to achieve the best solution is low; POA performed well compared to other algorithms. The results show that POA is superior in every case compared. A comparison of all the case studies has been conducted in Figs. 5.7, 5.8, and 5.9 concerning the P_{Loss}, voltage profile, and VSI. From the figures, it is clear that the combined approach of LSF and POA gives significant results.

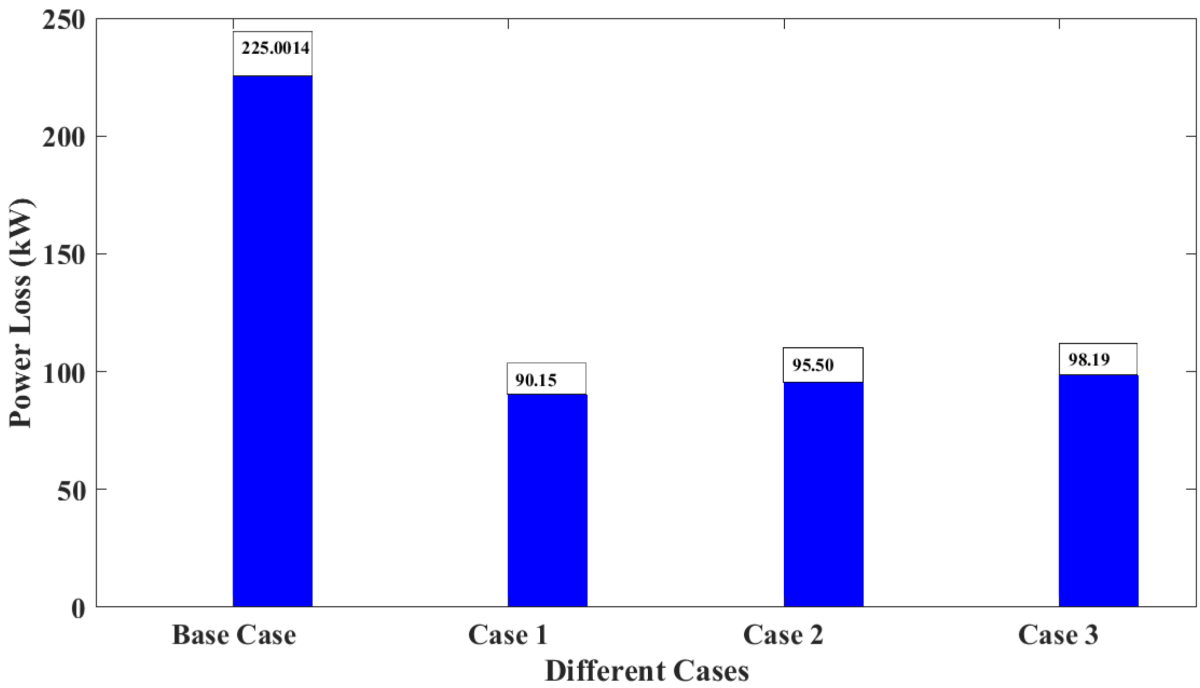

Fig 5.7 Percentage of Reduced P_{Loss} comparison for different cases

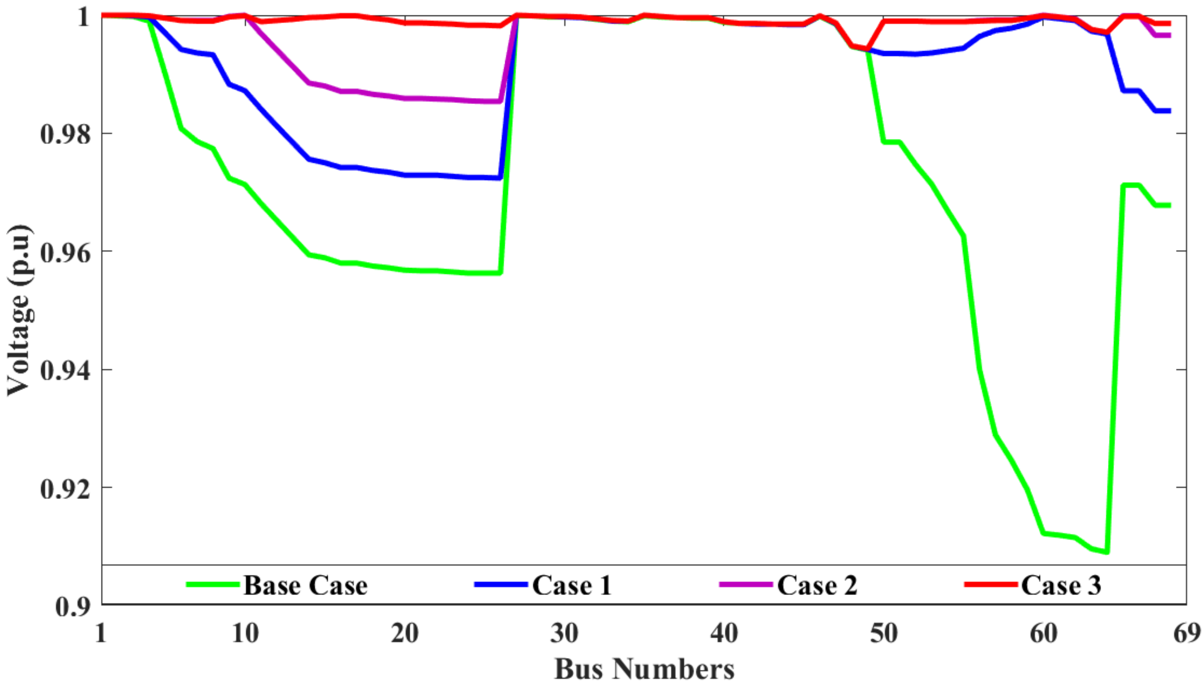

Fig 5.8 Voltage Profile of 69 buses for different cases

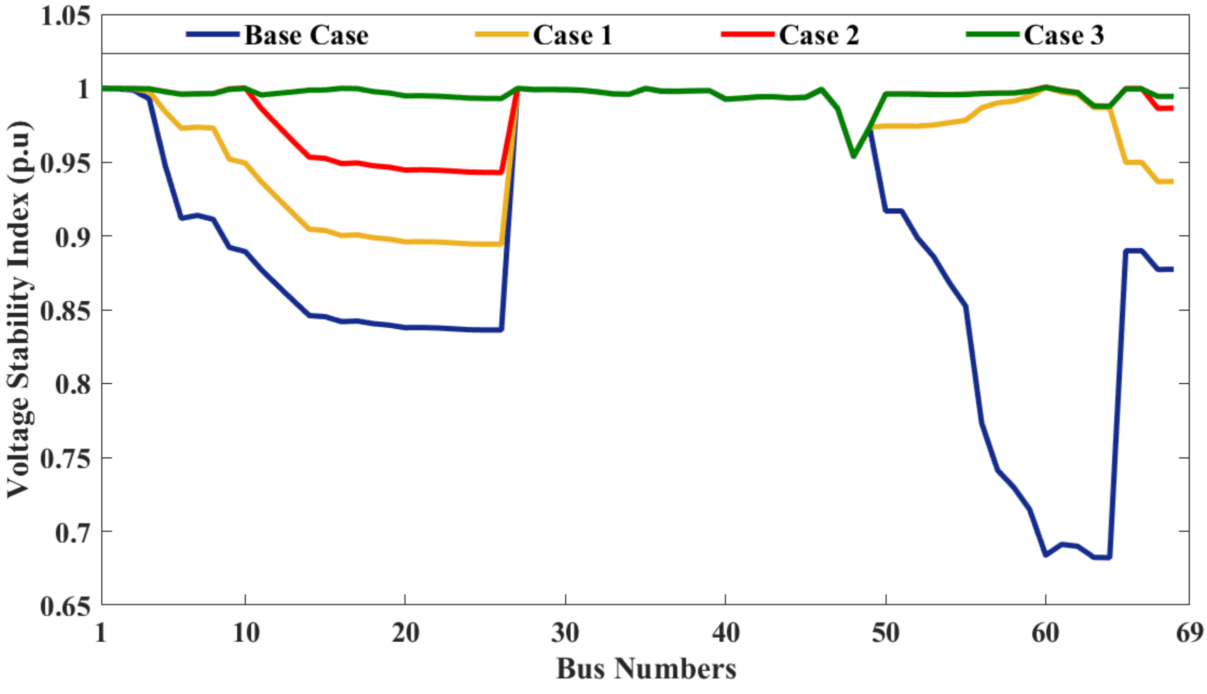

Fig 5.9 VSI comparison of 69 buses for different cases

5.5 Dynamic Load variations:

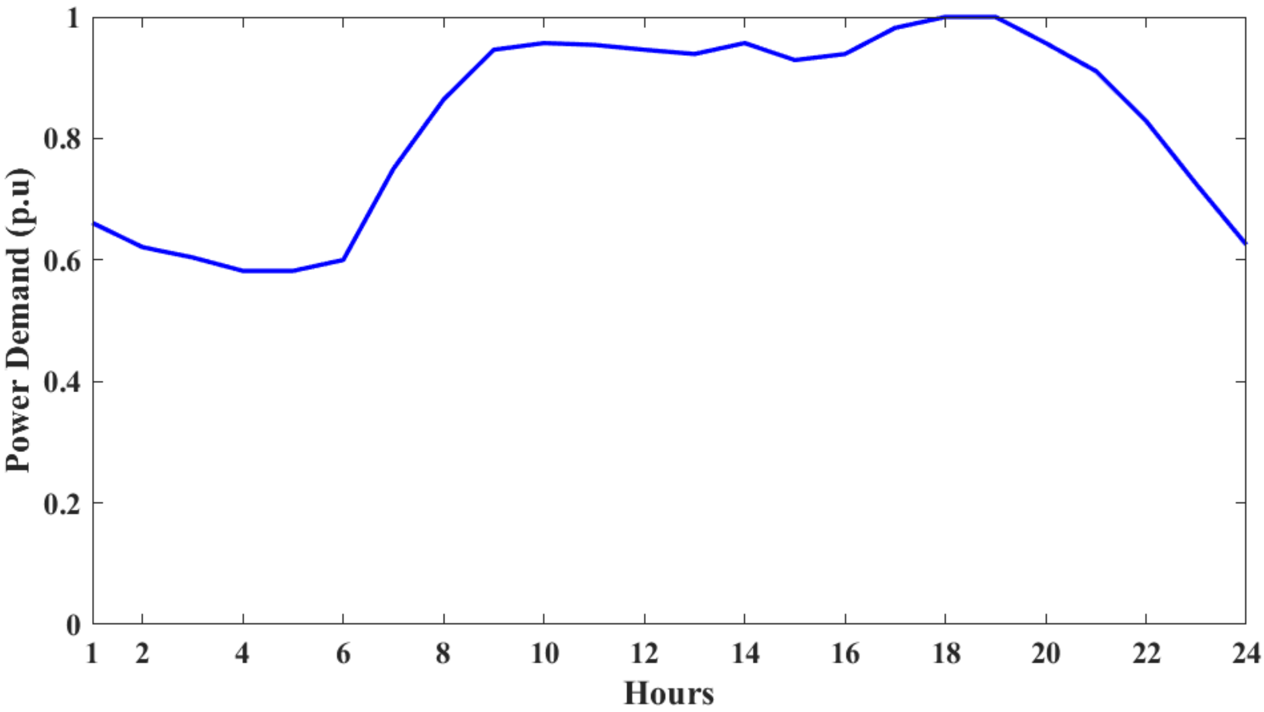

Fig 5.10 power demand curve for typical day (Dynamic load variation)

The load fluctuates from hour to hour, and it's critical to examine the system's dynamic changes. Fig 5.10 depicts a typical 24-hour load curve. Using the combined technique of LSF and POA, the analysis described in four cases is expanded for a typical 24-hour simulation in this section. The load flow is simulated with dynamic changes in system demand, and the LSF approach is used to decide the best placements of DGs and EVCS for all hours. In general, wind DGs will be immovable resources in any system. As a result, the determined place should be unique for all dynamic changes in system demand. The optimal sites for all dynamic load changes have been determined as 11, 17 and 61. Table 5.5 shows the ideal wind DG sizes for the dynamic instances, whereas Table 5.4 shows the P_{Loss}, V_{min}, and VSI_{min} determined using the POA. V_{min} and VSI_{min} are clearly within permitted limits for the whole 24-hour period. Fig 5.11 shows P_{Loss} reduction, and Fig 5.12 and 5.13 show voltage profile and stability improvement compared to the base case

Table 5.4 Variation of P_{Loss}, V_{min} and VSI_{min} for 24 hours

Hours	**Base Case P_{Loss} (kW)**	**Single Wind DG P_{Loss} in (kW)**	**Two Wind DGs P_{Loss} in (kW)**	**Three Wind DGs P_{Loss} in (kW)**	**V_{min} (p.u)**	**VSI_{min} (p.u)**
1	92.6006	9.997045	4.519181	2.276183	0.996091	0.972718
2	81.18967	8.810782	3.952247	1.940631	0.990377	0.961675
3	76.58996	8.329916	3.714869	3.245156	0.987622	0.932116
4	70.85562	7.728043	3.48907	1.627471	0.996672	0.97597
5	70.85562	7.728021	3.501084	1.94945	0.996708	0.976112
6	75.52911	8.218693	3.675057	2.691778	0.996606	0.975375
7	121.0302	12.91228	5.721425	3.317157	0.979198	0.918898
8	163.856	17.20864	7.590665	3.505874	0.99506	0.964395
9	199.362	20.69286	9.095625	4.914155	0.994596	0.961057
10	204.4367	21.18529	9.279934	5.803846	0.994016	0.960594
11	203.0453	21.05046	9.231347	8.009476	0.991465	0.960736
12	199.362	20.69253	9.067148	3.935073	0.994597	0.961059
13	196.1716	20.38204	8.948162	5.107165	0.994629	0.961316
14	204.4367	21.18554	9.260836	4.207328	0.994525	0.960577
15	191.6663	19.94285	8.729324	4.247343	0.974601	0.901652
16	196.1716	20.38205	9.021864	4.069282	0.994672	0.961484
17	216.2509	22.32727	9.877972	4.473015	0.992671	0.959515
18	225.0014	23.16885	10.22055	4.06701	0.994266	0.958766
19	225.0014	23.16892	10.12966	4.06701	0.992177	0.958727

20	204.4367	21.18514	9.314608	4.670326	0.994518	0.960548
21	183.7105	19.16464	8.450706	4.104741	0.994771	0.962393
22	149.9173	15.82167	6.952368	3.57543	0.986681	0.947772
23	112.6126	12.05476	5.433865	2.756878	0.995849	0.970076
24	82.29349	8.926598	3.998644	2.033058	0.996496	0.974479

Table 5.5 Hourly variations of DG size with POA

Hours	**DG_1 (kW)/(kVAr)**	**DG_2 (kW)/(kVAr)**	**DG_3 (kW)/(kVAr)**
1	217.9224/203.7849	337.6442/162.4097	1185.136/800.1176
2	293.6933/257.4669	308.8829/113.1694	987.1071/739.7394
3	120.3167/247.6641	177.893/90.88348	911.9219/816.6972
4	320.9424/288.4534	203.2423/74.9171	965.872/724.6339
5	422.7612/107.3373	153.2742/105.6348	974.5425/674.2156
6	200.7126/204.8863	403.3375/125.222	911.814/711.7699
7	535.1451/316.6117	356.996/211.1493	1182.701/844.8092
8	444.8836/376.8069	354.1446/244.9106	1445.339/1083.592
9	447.9403/403.0867	473.9171/260.7297	1692.056/1136.525
10	613.4937/675.2423	460.9932/151.4237	1506.079/1077.562
11	593.3931/144.8021	210.2473/473.5673	1614.708/895.2707
12	441.027/310.2777	371.8009/234.6754	1635.035/1110.001
13	416.8635/110.4302	472.9843/259.3227	1489.986/1062.311
14	540.7196/344.9702	328.2295/240.4958	1636.778/1220.389

15	531.9128/480.1428	281.3932/207.688	1475.541/1114.379
16	311.7132/357.941	405.0204/237.1805	1532.327/1130.649
17	556.9982/234.8221	403.4687/330.4298	1605.1/1185.733
18	522.5397/599.7671	375.3394/204.7038	1650.187/1208.746
19	655.4726/398.4323	285.0367/195.1887	1573.829/1194.533
20	598.7829/563.7414	312.7205/247.1394	1558.957/1087.777
21	363.3431/222.6481	407.6534/219.809	1550.137/1012.793
22	364.4389/389.215	309.564/256.6737	1380.975/1063.478
23	411.7252/245.1421	279.5643/170.8645	1321.747/860.3539
24	324.9857/215.2468	224.8424/184.2448	1111.327/667.5987

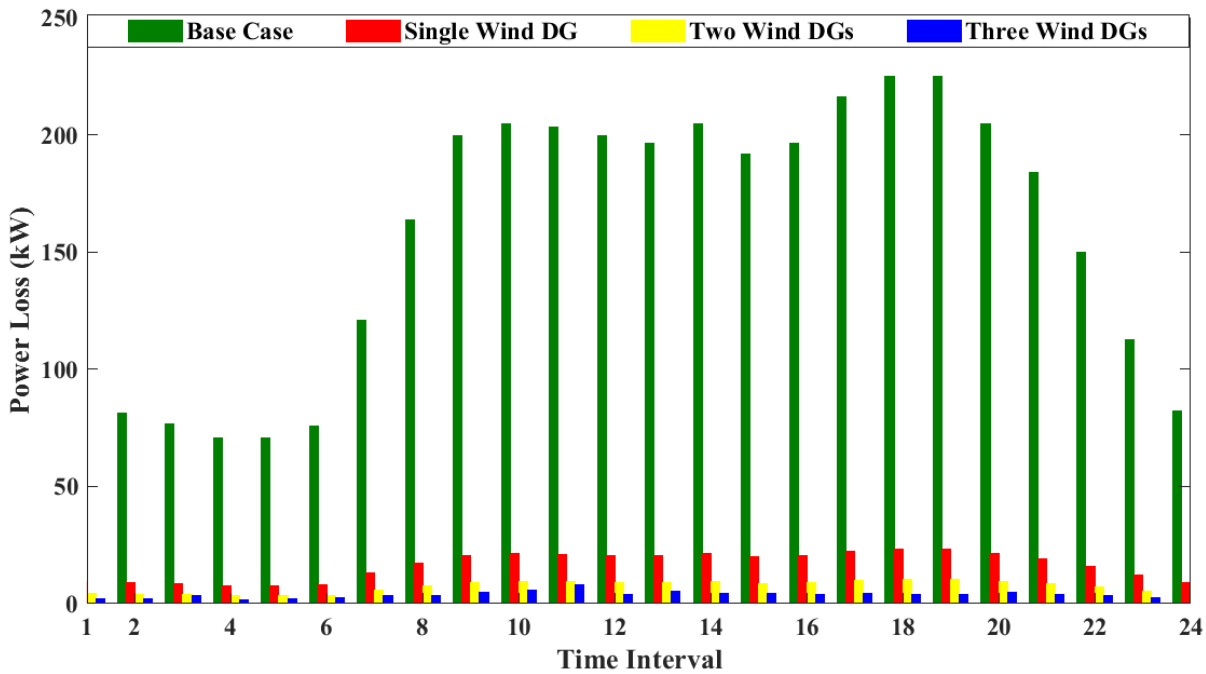

Fig 5.11 P_{Loss} comparison with different cases

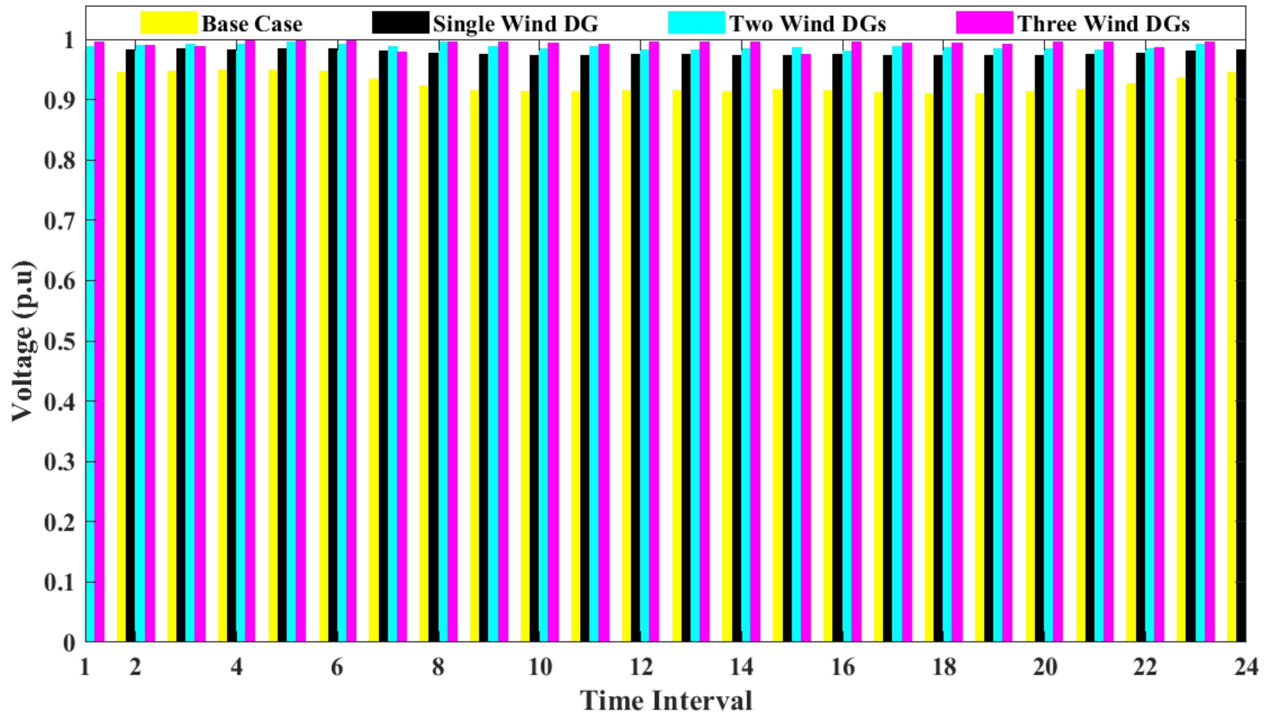

Fig 5.12 Voltage profile comparison with different cases

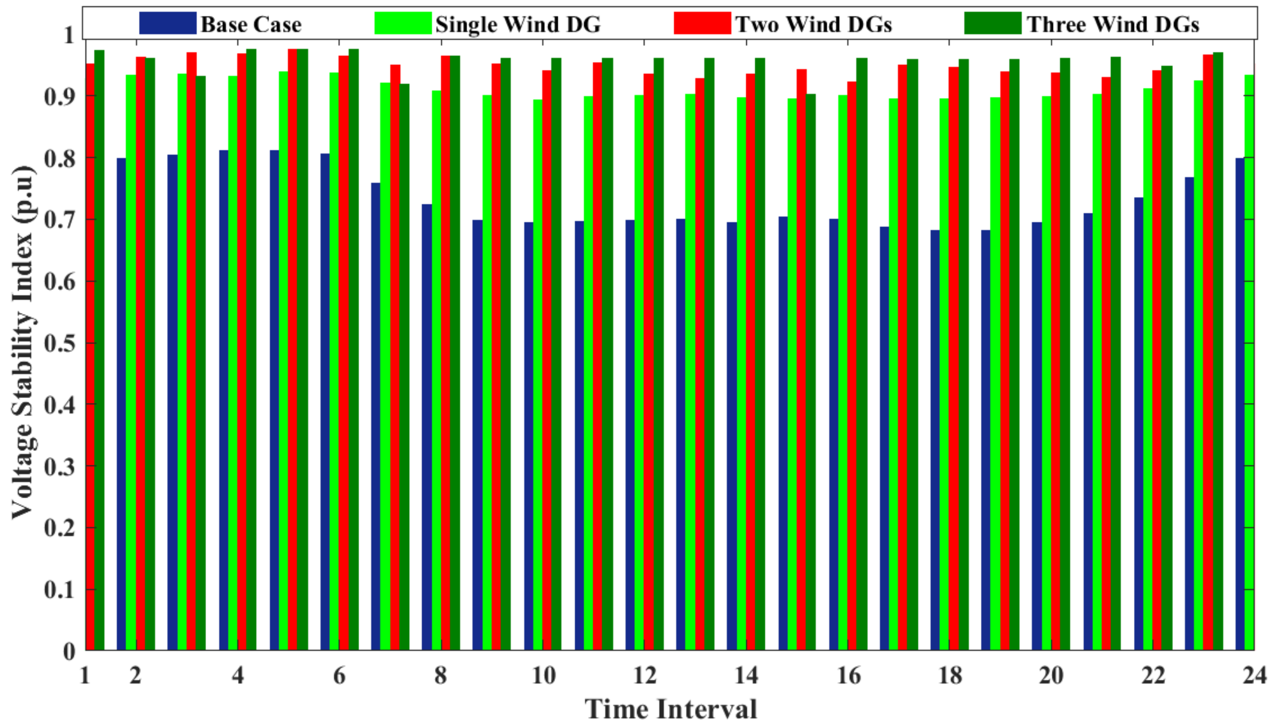

Fig 5.13 Voltage stability Index comparison with different cases

5.6 Various EV Charging Methods:

Chapter 4, sections 4.7, 4.7.1 and 4.7.2 discussed different charging methods of CCM and OEV, according to those methods simulated Table 5.6 results. IEEE 69 bus base case P_{Loss} = 3746.3833 kW for a typical day. Using CCM or OCM approaches, if we connect only EV to the system, P_{Loss} increases compared to the base case. Using the CCM (G2V) method, when we integrate both DGs and EVs into the system, 68.57% of P_{Loss} decreases. With OCM (G2V) strategy, when we incorporate both DGs and EVs at a time, 68.60 % of P_{Loss} minimizes. The same is represented in Fig 5.14.

Table 5.6 Comparison of different EV charging methods P_{Loss}

Different Approaches		**P_{Loss} (kW)**
Base Case P_{Loss} (kW)		3746.3833
Conventional Charging Method (G2V)	Only With EVs	3768.6595
	With DGs + EVs	1177.3658
Optimized Charging Method (G2V)	Only With EVs	3758.233
	With DGs + EVs	1176.0615

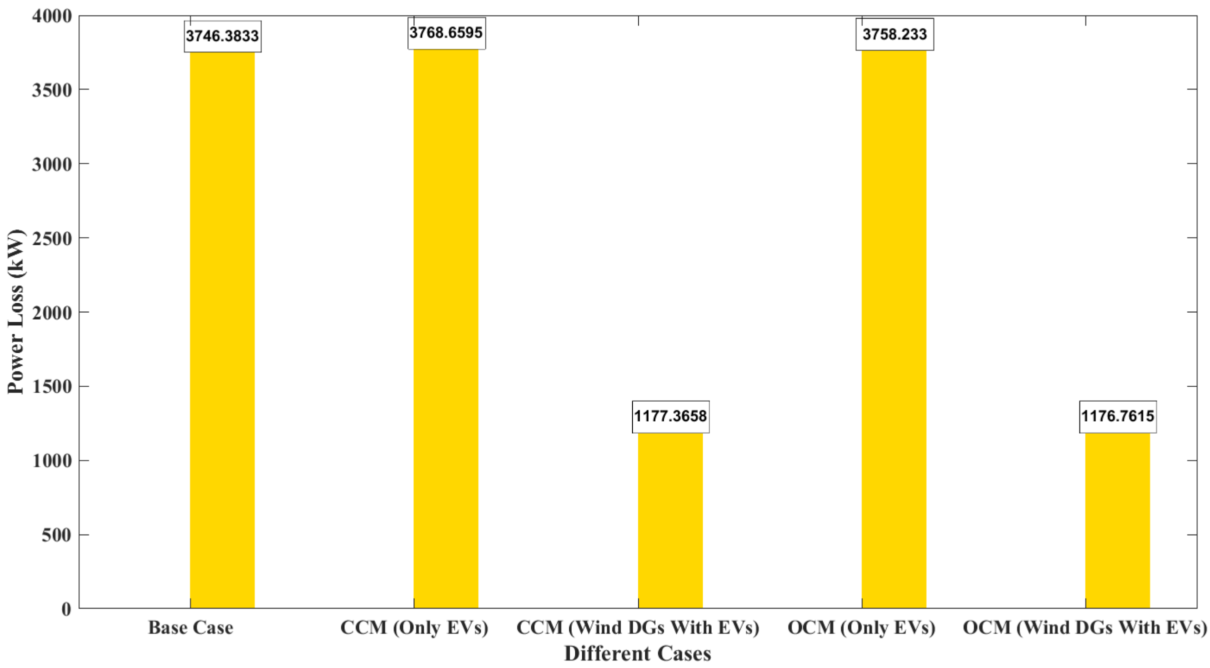

Fig. 5.14 69 bus P_{Loss} comparison with different methods

5.7 P_{Loss} Comparison for wind DGs with different EV charging methods

This section determined 28 real bus test system results for 24hrs. The base case P_{Loss} =1147.1245 kW. Without considering EVs, three wind-based DGs P_{Loss} = 706.5225 kW. Here, we considered different charging approaches CCM (G2V), OCM (G2V), and G2V plus V2G. It is observed from Fig 5.15 G2V plus V2G method reduced significant P_{Loss} = 699.0734 kW, which means 39.058%. It's better than CCM and OCM methods the same depicted in Table 5.7.

Table 5.7 28 Indian test system compared different EV charging methods P_{Loss} for dynamic load variation.

Hours	Base Case P_{Loss} (KW)	3-Wind DGs P_{Loss} (kW)	Conventional Method (3-Wind With EVs) P_{Loss} (kW)	Optimized Method (3-Wind With EVs) P_{Loss} (kW)	G 2V + V2G Method (3 – Wind DGs With EVs) P_{Loss} (kW)
1	28.4096	14.3654	14.3654	14.3654	14.3654
2	24.9163	12.6471	12.6471	12.6471	12.6471
3	23.5076	11.9522	11.9522	11.9522	11.9522
4	21.751	11.082	11.082	11.3619	11.3619
5	21.751	11.0936	11.0936	11.4064	11.4064
6	23.1827	11.8086	11.8086	12.1429	11.8086
7	37.1053	18.6665	18.6665	18.6665	18.6665
8	50.1845	25.3506	25.3506	25.3506	25.3506
9	61.0107	30.7108	30.7108	30.7108	30.7108
10	62.5568	30.9975	30.9975	30.9975	30.9975
11	62.1329	30.6008	30.6008	30.6008	30.6008
12	61.0107	30.0558	30.0558	30.0558	30.0558

13	60.0386	32.8669	32.8669	32.8669	32.8669
14	62.5568	37.4599	37.4599	37.4599	37.4599
15	58.6655	35.4042	35.4042	35.4042	35.4042
16	60.0386	33.7786	33.7786	33.7786	33.7786
17	66.1549	34.5214	36.5082	34.5214	34.5214
18	68.8189	50.6292	55.2317	50.6292	46.8552
19	68.8189	53.3025	58.2218	53.3025	49.0347
20	62.5568	57.8982	57.8982	57.8982	57.8982
21	56.2403	49.9164	49.9164	49.9164	49.9164
22	45.9301	38.4768	38.4768	38.4768	38.4768
23	34.5317	26.5298	26.5298	26.5298	26.5298
24	25.2543	16.4077	16.4077	16.4077	16.4077
Total P_{Loss}	**1147.1245**	**706.5225**	**718.0311**	**707.4495**	**699.0734**

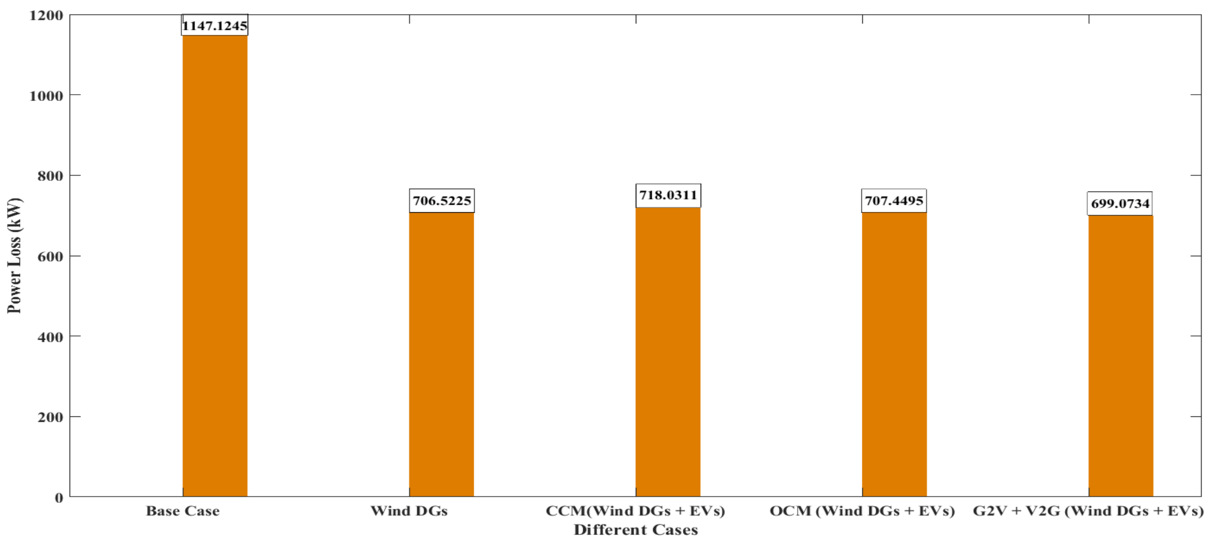

Fig. 5.15 P_{Loss} Comparison of Different cases for dynamic variation (28-bus system)

5.8 Summary:

This chapter proposes an integrated approach (LSF and POA) to solve the allocation of DGs, EVCS and combined DGs and EVCS problems in DS. Further, different load levels are considered, solving the objective function P_{Loss}. Dynamic load variation was considered, determining the sizes of these sources and calculating the objective function. To test the efficacy of the proposed system, IEEE 69 and 28 Indian practical DS are considered. Further, various cases are considered, such as single wind DG, multiple wind-based DGs and EVCS, and the results are represented. From the results, the exact allocation of multiple wind-based DGs alleviates the P_{Loss} from 225.0014 kW (base case) to 4.067 kW (three wind DGs), with a good voltage profile and VSI improvement. 98.19% of P_{Loss} reduced. The efficacy of the POA algorithm is tested and compared with GOA, DA and WOA algorithms. Compared to other algorithms, the POA algorithm reduces the P_{Loss} to the maximum extent. 98.19% of P_{Loss} reduced.

CHAPTER 6

Integration of solar and wind-based Distributed Generators and Electric vehicles into the Distribution System

6.1 Introduction:

This chapter presents a method for efficiently addressing allocation problems affecting RDERs and EV charging stations (EVCS) in the DS, with the primary objective of decreasing P_{Loss} and improving the voltage profile. Solar and wind power are the Renewable DGs taken into account here. Probability distribution functions (PDF) are used to model the uncertainty associated with RDGs. The voltage stability index (VSI) and political optimisation algorithm (POA) determine the best placement and size. Conventional and optimized EV charging methodologies (CCM and OCM, respectively) are considered to further investigate the method's effectiveness. The developed strategy is analyzed using the Indian 28-bus system. Single RDGs, multiple RDGs, and a combination of solar and wind DGs and EVCS cases are all considered. The voltage profile is significantly improved, and P_{Loss} is reduced considerably because of the strategic placement of several RDGs and smart scheduling on the part of the EVCS. Finally, the proposed technique is compared to existing algorithms, and the POA method is found to be better in all areas based on the simulation findings. Schematic diagram integrated solar, wind based DGs and EVs into the DS given in Fig 1.15.

6.2 Problem Formulation:

The proposed method's primary objective is to allocate DGs (solar & wind) and EVCS in the DS in its most effective ways to reduce P_{Loss} and improve the voltage profile.

6.2.1 Objective Function:

The objective P_{Loss} reduction is

$$min \sum_{n=1}^{24} P_{loss}(n) \tag{6.1}$$

Where

$$P_{Loss}(n) = \sum_{n=1}^{24} I_n^2 R_n \tag{6.2}$$

The following are the main constraints related to the objective function

Power balance constraints:

$$\sum_{n=1}^{24} P^{S_{DG}}(n) + \sum_{n=1}^{24} P^{W_{DG}}(n) = \sum_{n=1}^{24}[P^{Demand}(n) \pm\ P^{EV}(n) +\ P_{Loss}(n)] \qquad (6.3)$$

Where, $P^{G}(n)$= n^th^ hour power generator, $P^{Demand}(n)$= n^th^ hour power demand, $P^{EV}(n)$= during an n^th^ hour, EV supplied/consumed power.

Bus Voltage Profile Constraints:

DS's voltage profile must always be within the specified ranges.

$$V_{k,n}^{min} \leq V_{k,n} \leq V_{k,n}^{max} \qquad (6.4)$$

Where, $V_{k,n}$ = k^th^ bus voltage at the n^th^ hour.

6.2.2 Based on DS Load demand, the best installation of RDGs and EVCS

Using VSI on each bus, the suitable installation location of DGs and EVCS can be found. This approach takes into account the total system load demand for each hour and chooses the best placement. [87] Introduced for the first time the VSI, which is utilized in this research with some modifications. The comprehensive analysis of Eq. 6.5 can be determined by finding the content in [87]. All buses are rated and evaluated on the obtained value of VSI, and a bus is regarded to be stronger if the value of VSI is close to 1. Any bus is considered weak if the estimated value is close to 0. This technique selects the stronger buses for EV installation, while the weaker buses are evaluated for RDGs allocation. In this manner, the suitable place for installing renewable DGs and EVs is being considered. Fig 6.1 represents the step-by-step procedure for the optimal location of RDGs and EVs with VSI. Fig 6.2 shows the step-by-step flow to find the size of RDGs with the POA method with the help of VSI.

$$VSI = 2V_s^2V_r^2 - V_r^4 - 2V_r^2(PR + QX) - (P^2 + Q^2)|Z|^2 \qquad (6.5)$$

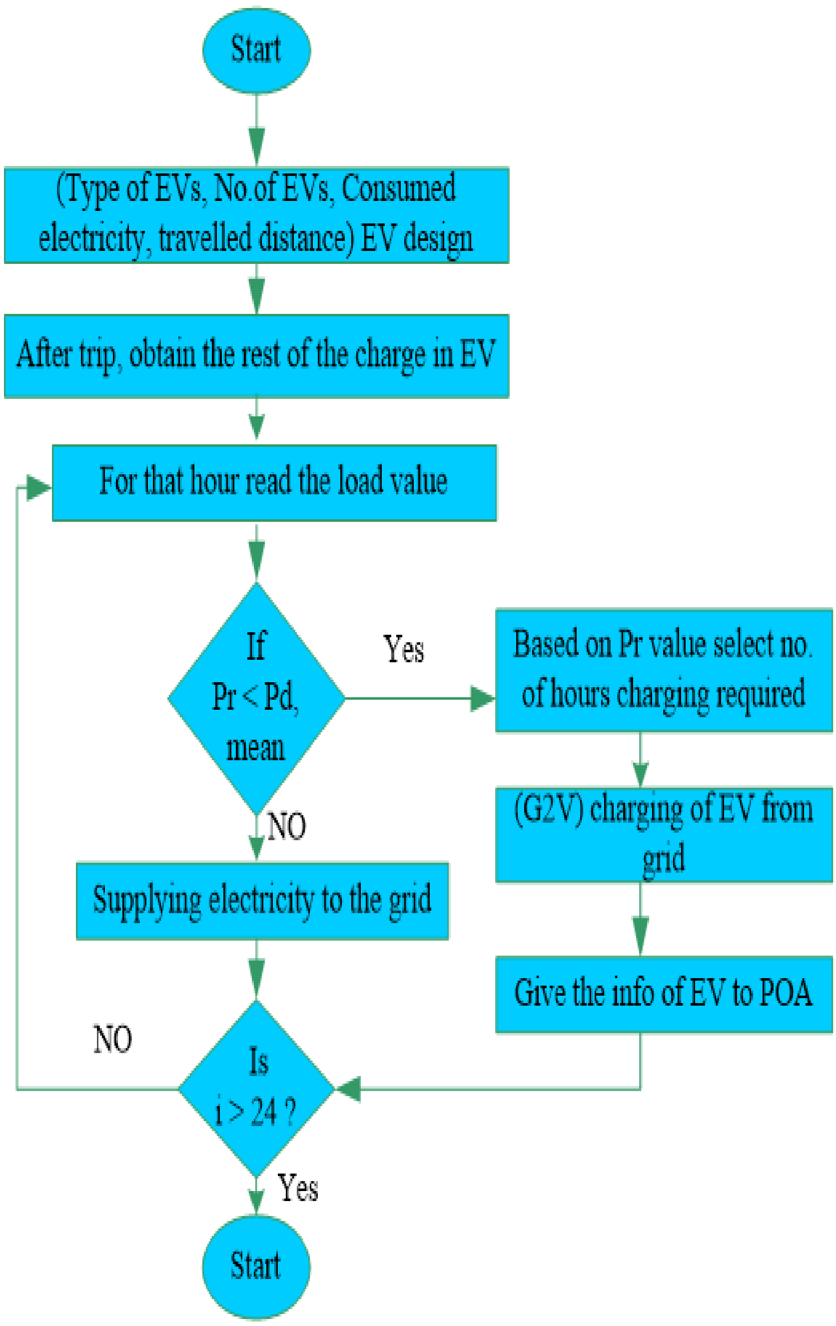

Fig. 6.1 procedure for placement of renewable RDGs and EVCS with VSI

6.2.3 Steps to obtain suitable sizes of RDGs with POA:

Step 1: Read the line & bus data of DS

Step 2: Run the base case load flow

Step3: Finding the suitable location of RDGs, and EVCS with the VSI technique

Step 4: Suitable installation of RDGs, and EVCS determined using VSI the info shared with POA

Step 5: According to equation 4.9, all residents are divided into ‘n’ political parties, and each and every party has ‘n’ members using eq. 4.10.

Step 6: Equation 4.14 determines the party’s leader, while Equation 4.15 determines each constituency’s representative.

Step 7: compared current values to position values from the past

Step 8: Temporary fitness values and placements are established at the start of algorithm loops.

Step 9: Equations 4.17 and 4.18 reflect the second phase of the election campaign, and all political party members’ values and views are updated using these EQs.

Step 10: Each candidate in the switching phase runs individually in Eq. 4.19, which depicts the election campaign following the phase.

Step 11: Constituency champs were determined using equation 4.20.

Step 12: The algorithm displays all parliamentary location champions in this phase, also known as the period of parliament affairs.

Step 13: The upgrading of all fitness values (P_{Loss}) and placements, such as the finest RDGs and SCs, is the last phase.

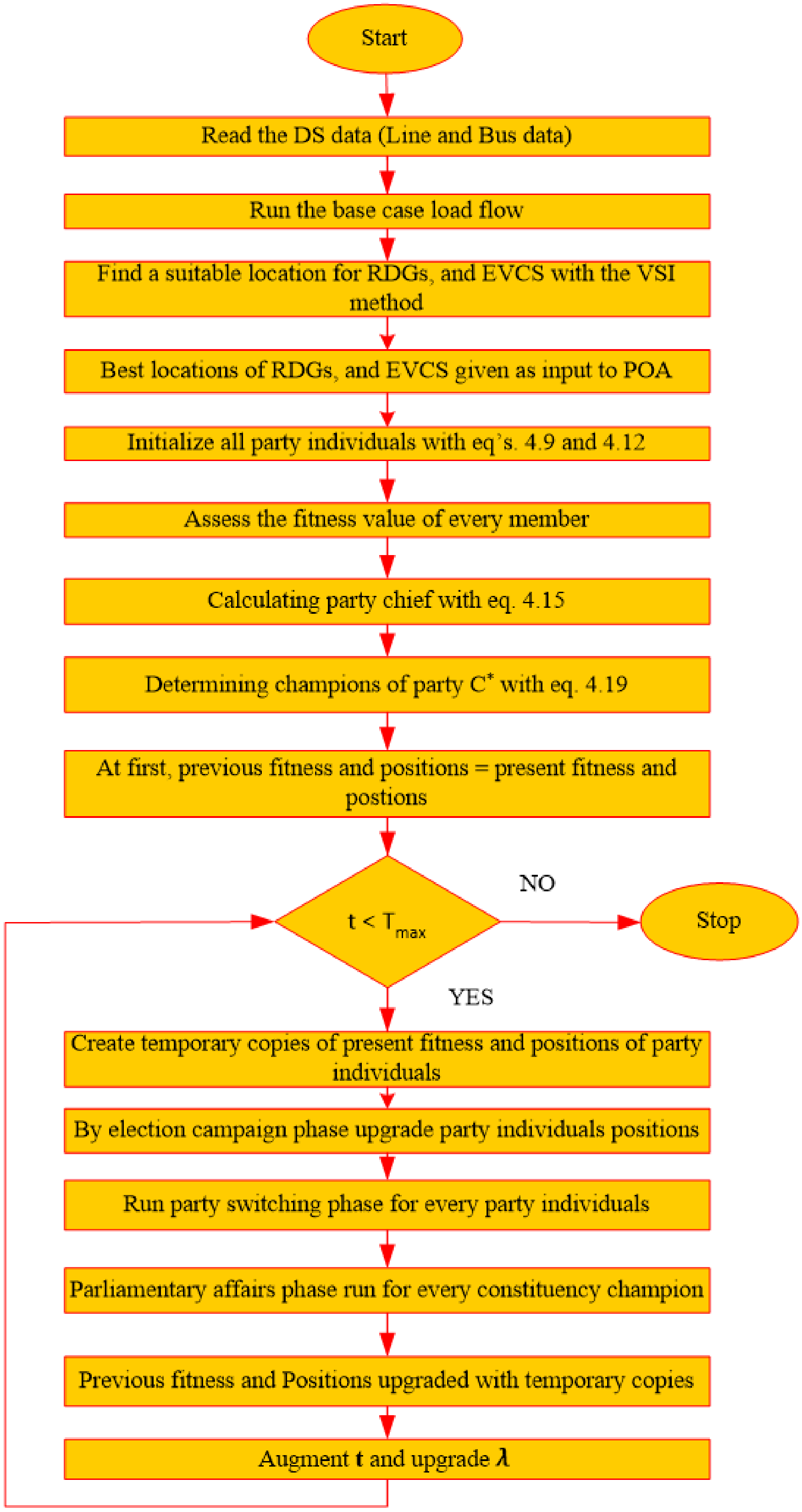

Fig.6.2 Flow Chart of POA with VSI

6.3 Results and Discussion

The influence of RDGs and EVCS on the DS is studied by addressing different operating cases, and the results are given in this section. A combined approach for P_{Loss} reduction and augmenting voltage profile in a DS in the presence of solar and wind-based RDGs and various types of EV groups with unique operating patterns are adopted to address the optimization issue. This strategy combines the proposed optimized EV charging technology with the POA. The 28 Indian real test systems were used throughout the research study and the single line diagram of the test system represented in Fig 6.3.

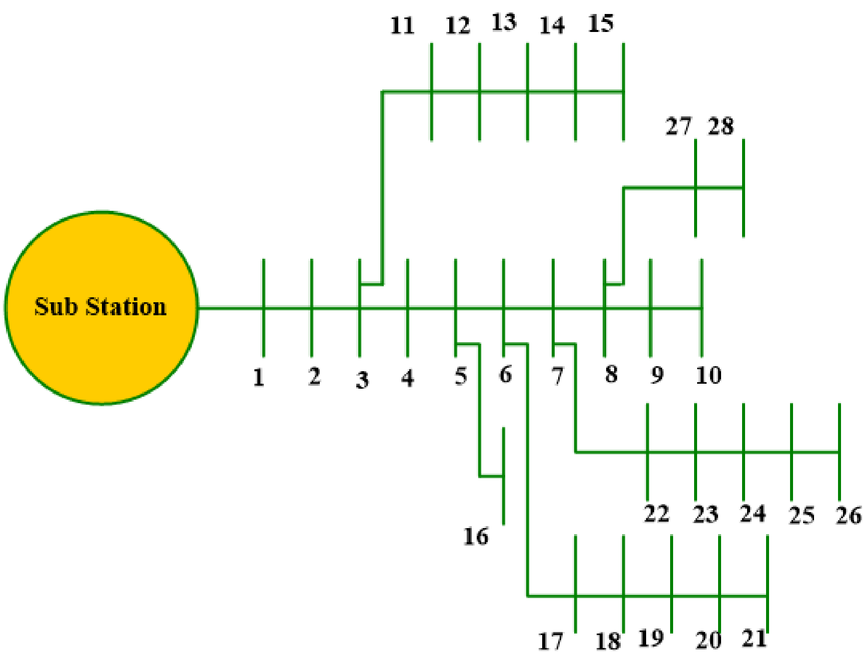

Fig 6.3 Single line diagram of 28 Indian real test system

Initially, the proposed approach is applied and tested for various cases, like the location of a single RDG, two RDGs, and three RDGs. Table 6.2, 6.3 and 6.4 summarizes all the findings. According to the findings, the placement of three RDGs resulted in minimal P_{Loss}, an enhancement in voltage profile, and an increase in VSI. Due to system capacity and load constraints, going above 3 RDGs for the proposed DS is not possible. The system's performance will suffer if the number of RDGs is increased above 3.

To test the effectiveness of the suggested technique, the assessment is now done for different load levels, like half 0.5 per unit (p.u.), full (1.0 p.u.), and heavy (1.1 p.u.). If the DGs are placed in proper places and of suitable size at all load levels, energy loss is significantly reduced, and voltage profile and VSI are enhanced. Table 6.1 shows the calculated P_{Loss}, VSI and voltage profile at various load conditions.

Table 6.1 P_{Loss}, V_{min} and VSI_{min} comparison at different load levels

Different Loads	**Base Case P_{Loss}(kW)**	**With DG P_{Loss}(kW)**	**DG Size (kW)**	**V_{min} (p.u)**	**VSI_{min} (p.u)**	**% Red P_{Loss}**
Half Load(0.5)	15.8508	8.132	162.8245 111.5187 72.5212	0.982	0.9299	48.6965
Full Load (1.0)	68.8189	33.6501	334.2578 230.5428 145.6313	0.9633	0.8611	51.1086
Heavy Load (1.1)	84.7675	41.0029	369.6675 255.3580 160.3221	0.9595	0.8475	51.6289

Base Case:

In this case, without considering solar and wind-based DGs. The base case P_{Loss} = 68.8189 kW, V_{min} = 0.9123 p.u, VS_{Imin} = 0.6927 p.u. The same is mentioned in Table 6.2.

Case 1: With single solar DG:

Following the VSI method, 7 is the apt location to insert a single solar DG; it injects only kW into the DS. The info was passed to POA and found the size was 583.0954 kW, P_{Loss} = 37.00 kW, V_{min} = 0.9615 p.u, VSI_{min}= 0.8545 p.u. With the compared base case, 46.22% of P_{Loss} was reduced.

Case 2: With Single Wind DG:

As per VSI 7^{th} bus is the best location to insert a single wind-based DG; it injects both kW and kVAr into the DS. The location is given as input to the POA method; it determines the ranges of single wind DG_1 in DS. The POA size of wind DGs is 581.0851 kW/577.2126 kVAr, respectively. P_{Loss} = 8.6901 kW, V_{min} = 0.9805 p.u VSI_{min}= 0.9244 p.u compared to the above cases single wind DG performs better in all aspects tabulated values in Table 6.2. Fig 6.4 represents the convergence characteristics of a single wind-based DG.

Table 6.2 28 Indian bus test system P_{Loss} comparison with different cases

Different Cases	**OTs**	**Bus No**	**RDG Size in (kW/kVAr)**	$\mathbf{P_{Loss}}$ **(kW)**	$\mathbf{V_{min}}$ **(p.u.)**	$\mathbf{VSI_{min}}$ **(p.u.)**
Base Case	NA	NA	NA	68.8189	0.9123	0.6927
Case 1	DA	7	583.0955/0	37.0166	0.9614	0.8544
	GOA	7	583.0154/0	37.0216	0.9615	0.8545
	WOA	7	583.0255/0	37.0143	0.9621	0.8566
	POA	**7**	**583.0954/0**	**37.0066**	**0.9615**	**0.8545**
Case 2	DA	7	569.8847/577.2568	8.7501	0.9805	0.9244
	GOA	7	569.0923/578.0599	8.8901	0.9802	0.9241
	WOA	7	569.0823/578.0499	8.8301	0.9804	0.9241
	POA	**7**	**569.9647/577.2126**	**8.6901**	**0.9805**	**0.9244**

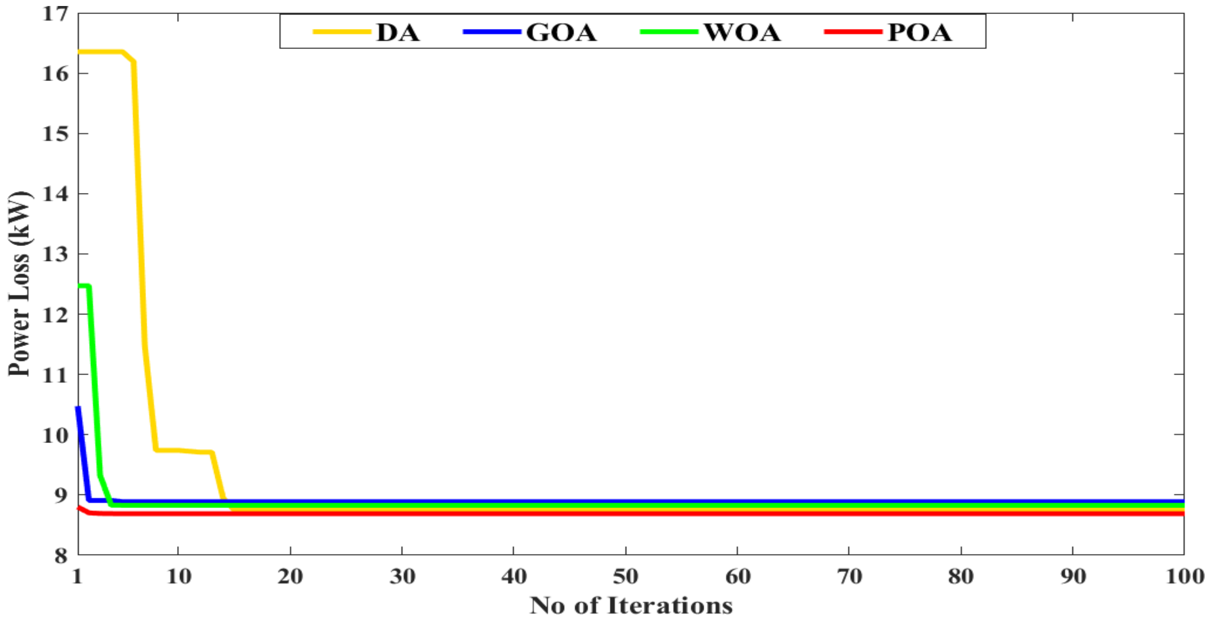

Fig 6.4 POA convergence comparison with other methods

Case 3: With Two Solar DGs:

The optimal allocation of two solar-based DGs, 7 and 12, are the best locations as per the VSI method. The same message was sent to POA. The POA gives the sizes of the two solar DG values tabulated in Table 6.3. 47.93% of P_{Loss} was minimized, and voltage stability and profile augmented.

Case 4: With Two Wind DGs:

The optimal placement of two wind-based DG locations is identified with the VSI method. By VSI, 7 and 12 are suitable for placing two wind-based DGs. The same message was sent to POA, which determines the size of two wind DGs. Compared to the above cases, 91.24% of P_{Loss} was minimized. Voltage profile and voltage stability enhanced. It injects both kW and kVAr into the system. Fig 6.5 represents POA converges significantly less time compared to other meta-heuristic methods. Table 6.3 shows the two wind DGs' P_{Loss}, V_{min}, and VSI_{min}.

Table 6.3 28 Indian real test system P_{Loss} comparison with different Cases

Different Cases	**OTs**	**Bus Numbers**	**RDG Size in (kW/kVAr)**	**P_{Loss} (kW)**	**V_{min} (p.u.)**	**VSI_{min} (p.u.)**
Case 3	DA	7 12	403.2372/0 272.0938/0	35.8397	0.9572	0.8395
	GOA	7 12	403.2372/0 272.0938/0	35.9297	0.9578	0.8392
	WOA	7 12	391.9622/0 288.3318/0	35.8581	0.9568	0.8380
	POA	**7** **12**	**403.2352/0** **272.0916/0**	**35.8297**	**0.9572**	**0.8395**
Case 4	DA	7 12	397.8004/404.0415 256.1763/259.109	6.2561	0.9853	0.9423
	GOA	7 12	397.8004/404.0415 256.1763/259.109	6.6202	0.9857	0.9425
	WOA	7 12	382.7337/335.0179 264.2817/355.0826	6.8206	0.9847	0.9400
	POA	**7** **12**	**467.2699/474.5903** **217.3112/221.1341**	**6.0236**	**0.9908**	**0.9635**

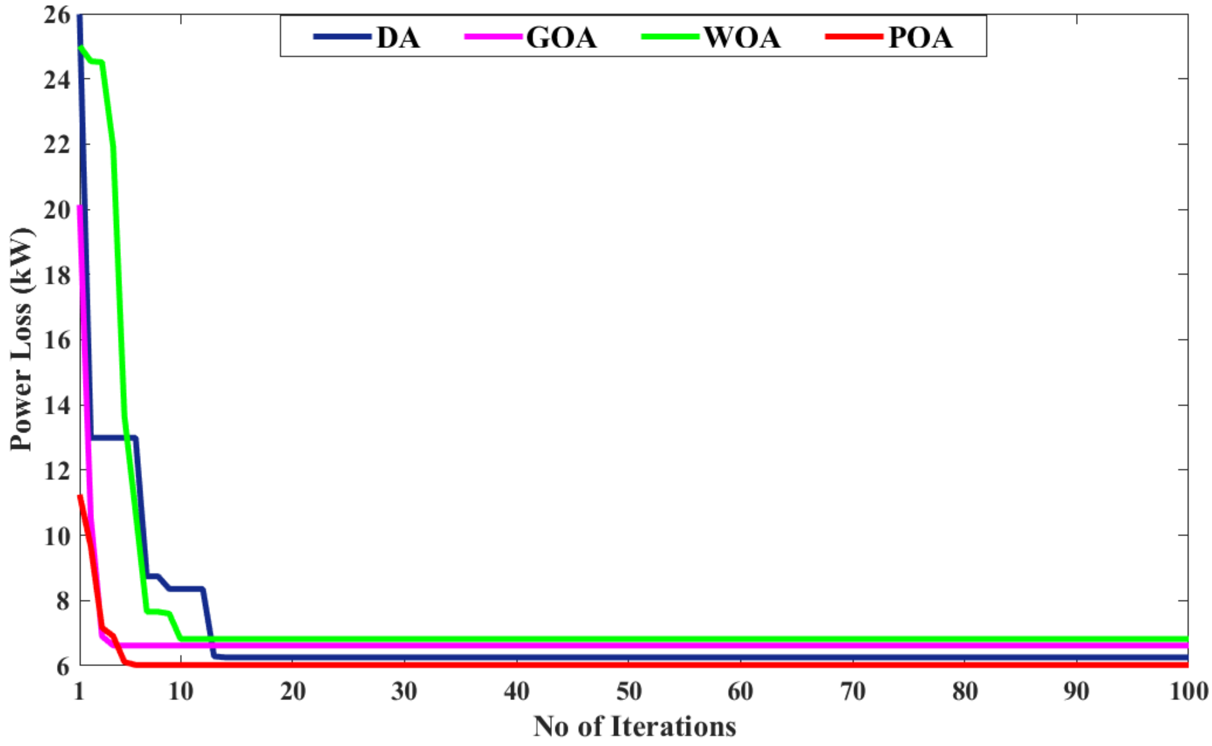

Fig 6.5 POA Comparison with Other methods

Case 5: With Three Solar DGs:

With VSI found, 7, 12 and 22 are suitable locations to install three solar DGs; it injects real power into the system. The same information given to the POA gives sizes of three DGs. Compared to the above cases, three solar DGs analysis shrinking P_{Loss} inflates the voltage profile and stability the same information tabulated in Table 6.4.

Case 6: With Three Wind DGs:

Following VSI, 7, 12 and 22 are the best site to place simultaneous allocation of three wind DGs; it injects both the active (kW) and reactive power (kVAr) into the DS. The same information is given to the POA and found in the three wind DG sizes tabulated in Table 6.4. Fig 6.6 shows the convergence characteristics of the practical 28 test system, proving that, compared to other optimization methods DA, GOA and WOA, POA performance is outstanding in all aspects 95.76% of P_{Loss} was minimized, higher than all other cases. Fig 6.7 shows that compared to all other cases, case 6 (three wind-based DGs) decreased P_{Loss} more. Fig 6.8 and 6.9 represents augmented voltage profile and stability with POA. From all 6 cases, overall performance improved with the three wind DGs.

Table 6.4 Three solar DGs and three wind DGs P_{Loss}, V_{min}, and VSI_{min} comparison with different Cases

Different Case	**OTs**	**Bus No**	**DG Size in (kW)**	**P_{Loss} (kW)**	**V_{min} (p.u.)**	**VSI_{min} (p.u.)**
Case 5	DA	7 12 22	258.8496/0 243.0252/0 207.3577/0	33.7189	0.9629	0.8595
	GOA	7 12 22	258.8496/0 243.0252/0 207.3577/0	33.7289	0.9629	0.8595
	WOA	7 12 22	105.8228/0 238.9345/0 348.1836/0	34.2807	0.9618	0.8558
	POA	**7** **12** **22**	**334.2644/0** **230.5484/0** **145.6193/0**	**33.6501**	**0.9633**	**0.8611**
Case 6	DA	7 12 22	221.2611/325.527 219.3133/196.8555 233.1384/164.1613	3.1973	0.9904	0.9679
	GOA	7 12 22	221.2611/325.527 219.3133/196.8555 233.1384/164.1613	3.9249	0.9903	0.9659
	WOA	7 12 22	476.6020/40.02637 86.16243/86.34596 80.34672/455.5511	3.2912	0.9876	0.9514
	POA	**7** **12** **22**	**320.9047/326.2948** **217.3023/221.1548** **145.2620/147.6875**	**2.9142**	**0.9901**	**0.9632**

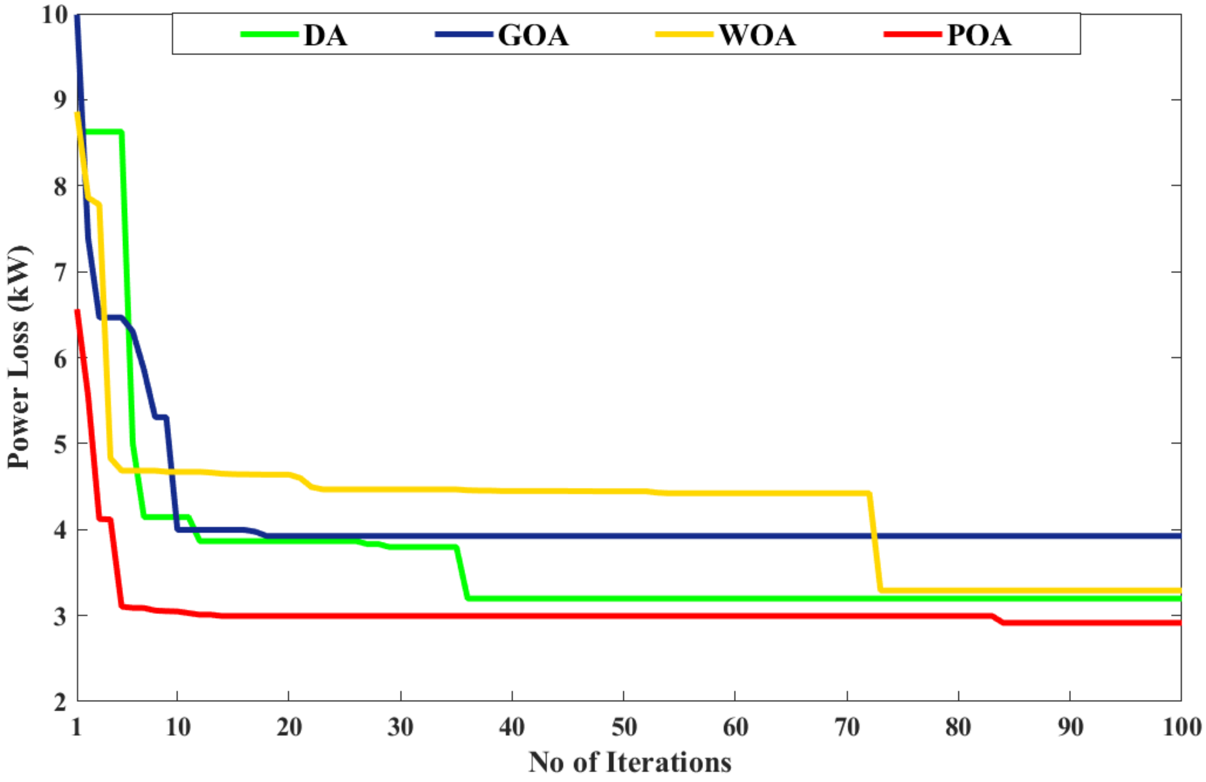

Fig 6.6 POA performance comparison with other methods

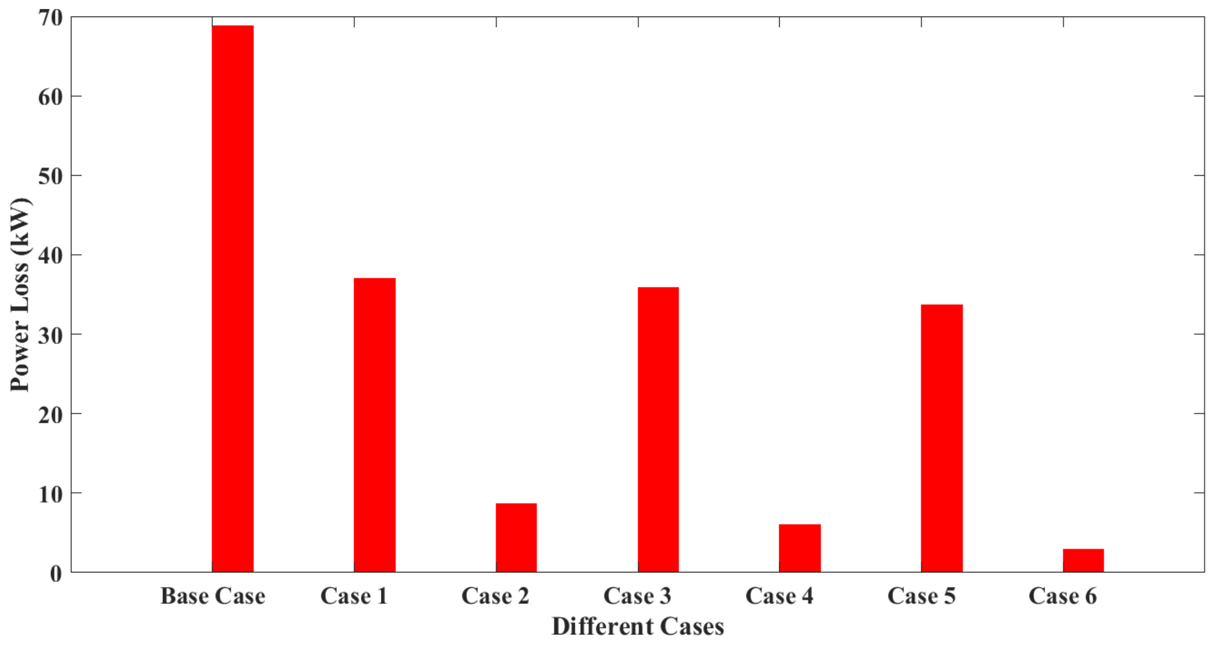

Fig 6.7 P_{Loss} reduction for different cases

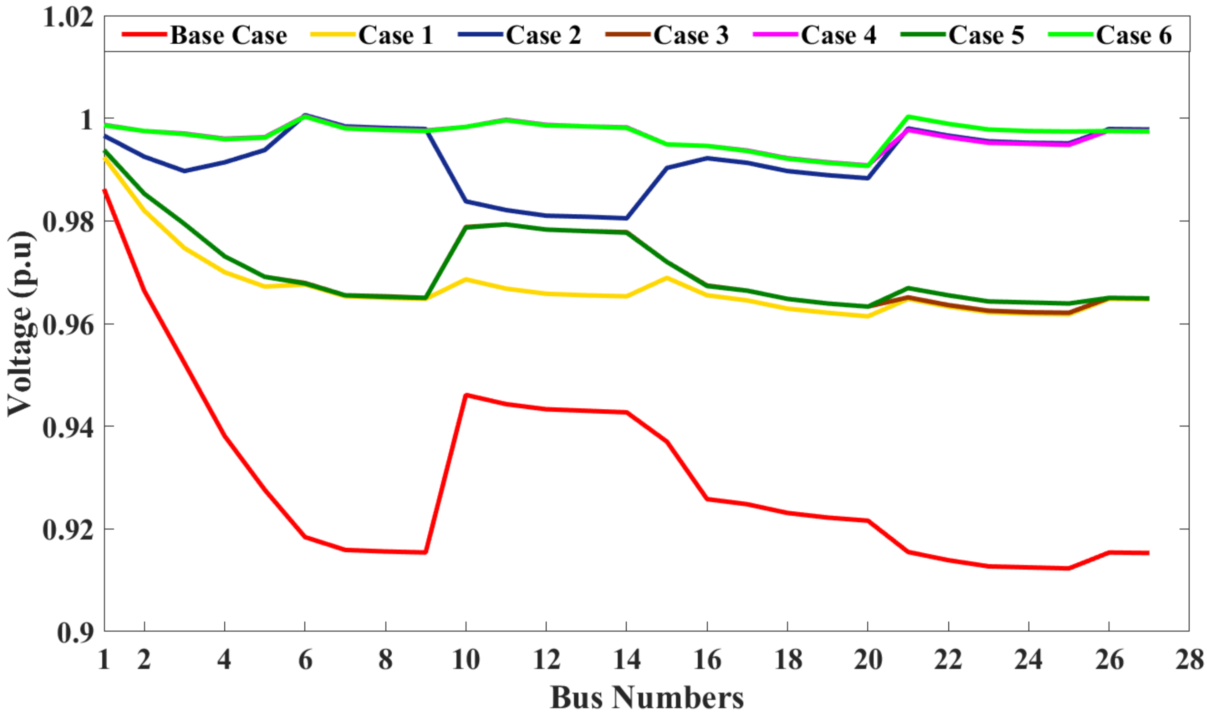

Fig 6.8 Voltage Profile for 28 Test System

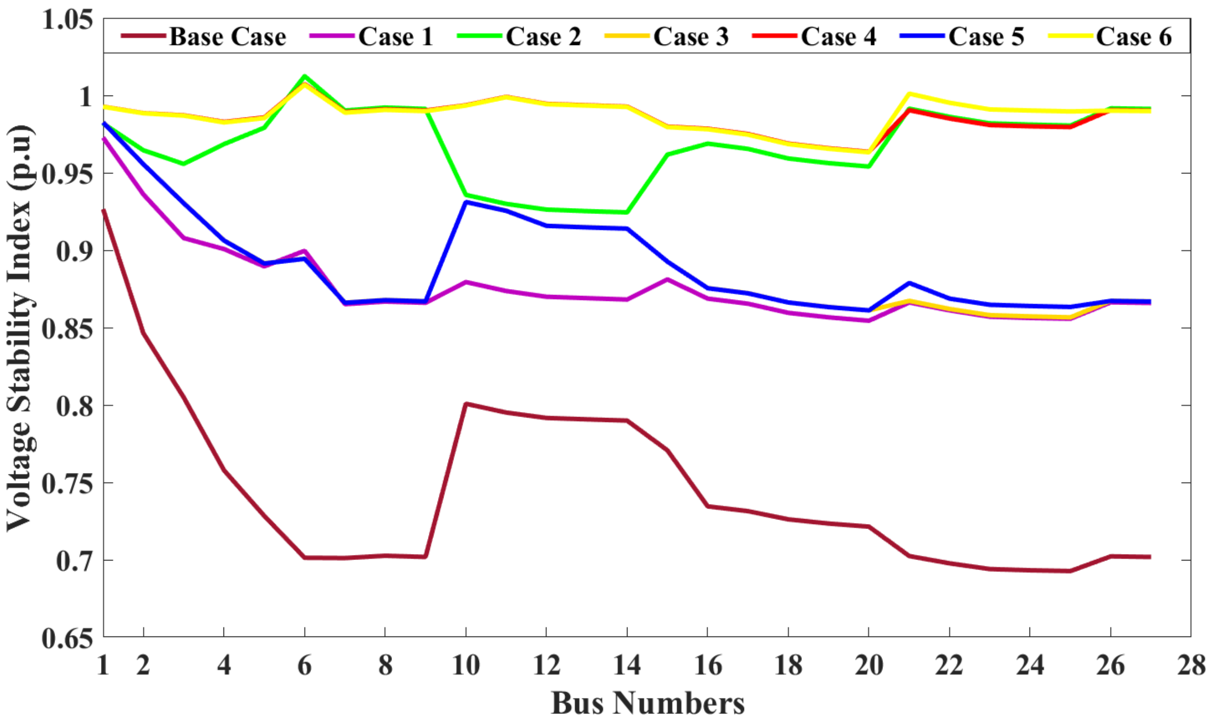

Fig 6.9 Voltage stability Index for 28 Test System

Furthermore, the proposed POA is compared in terms of several criteria to other current optimization approaches, such as grasshopper optimization (GOA), whale optimization (WOA), and dragonfly algorithm (DA). The findings of all optimization methods are shown in Tables 6.2, 6.3, and 6.4 with 50 trials. The P_{Loss} reduction achieved by POA surpasses all other techniques. The suggested POA has a better standard deviation than all other approaches, indicating its dominance over existing methods. The proposed POA method is compared with the existing algorithms in the literature and the same is given in Table 6.5.

Figure 6.6 depicts the convergence curves for several optimizer approaches for the given objective function. Tables 6.2, 6.3 and 6.4 show the RDGs sizes, P_{Loss}, and voltage profiles derived using different methods with identical simulation conditions. POA delivers the best outcomes in all aspects than other techniques. POA is particularly efficient in giving better results in less iteration with less P_{Loss}, voltage profile, and voltage stability enhancement, as shown in Fig 6.7, 6.8 and 6.9. As a result, this POA is implemented throughout the research study as an appropriate optimization method.

Table 6.5 POA performance comparison with other existing algorithms

Optimization Method	**JOA [88]**	**MLC [89]**	**Proposed POA Method**
Location of DGs	18 23 26	7 13 24	7 12 22
Base Case P_{Loss} (kW)	68.81	68.81	68.8189
Renewable DGs P_{Loss} (kW)	38.55	34.68	33.6501
% of Minimized P_{Loss} (kW)	43.97	49.60	51.11

6.4 Dynamic load variation analysis with 28 Indian test system:

The power demand values fluctuates from hour to hour, and it's critical to examine the systems dynamic variations. Fig 6.10 represents the system power demand for 24hrs.

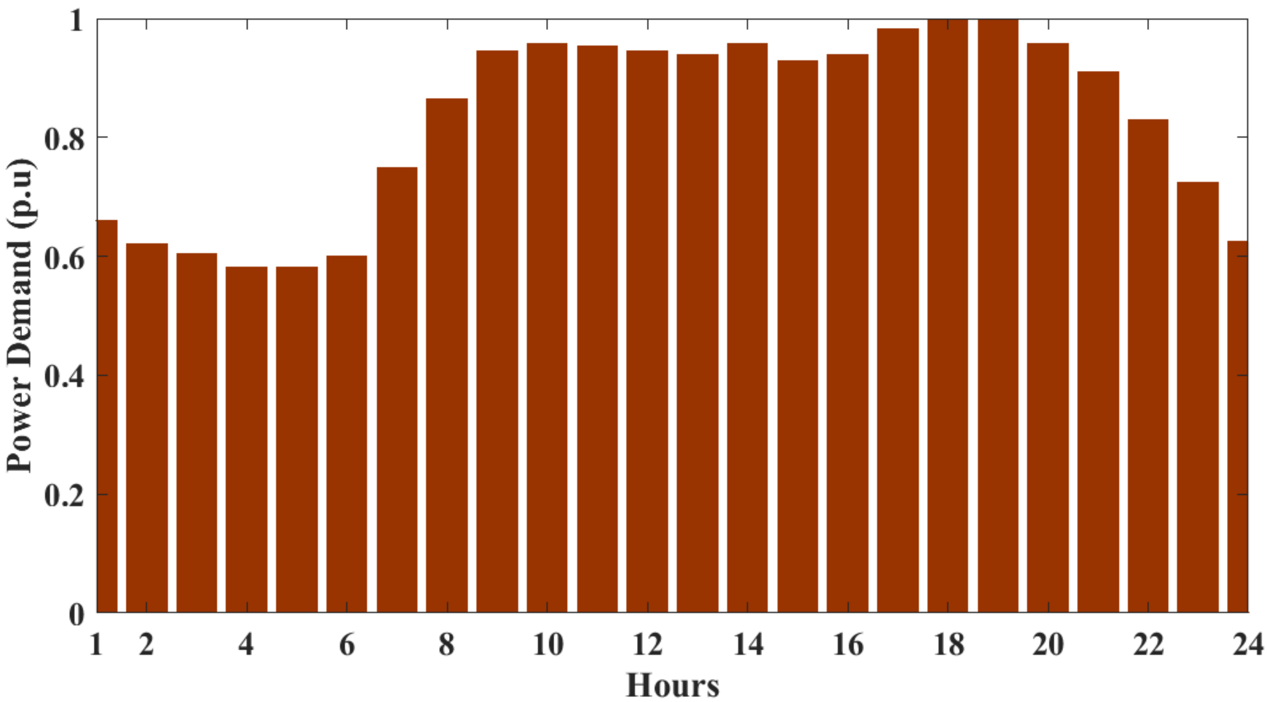

Fig 6.10 system power demand for 24hrs

Table.6.6 RDGs P_{Loss} comparison for a typical day with different cases

Hours	Base case P_{Loss} (kW)	3 Solar DGs P_{Loss} (kW)	Three Wind DGs P_{Loss} (kW)
1	28.4096	14.3654	1.2736
2	24.9163	12.6454	1.1237
3	23.5076	11.949	1.1189
4	21.751	11.0781	0.9868
5	21.751	11.0781	0.9884
6	23.1827	11.7881	1.0514
7	37.1053	18.6057	1.6712
8	50.1845	24.8845	2.1851
9	61.0107	30.0013	2.6349
10	62.5568	30.7265	2.7625
11	62.1329	30.5278	2.6952

12	61.0107	30.0013	2.621
13	60.0386	29.5446	2.5836
14	62.5568	30.7265	2.6783
15	58.6655	28.8987	2.5559
16	60.0386	29.5446	2.5864
17	66.1549	32.409	2.85
18	68.8189	33.6501	2.9644
19	68.8189	33.6501	2.9262
20	62.5568	30.7265	2.6914
21	56.2403	27.7552	2.4322
22	45.9301	22.8544	2.0121
23	34.5317	17.3566	1.539
24	25.2543	12.8123	1.1383
Total P_{Loss}(kW)	**1147.1245**	**567.5798**	**50.0705**

Table 6.7 RDGs sizes under dynamic load profile

Hours	**DG_1(kW)/(kVAr**	**DG_2(kW)/**(kVAr)	**DG_3(kW)/ (kVAr)**
1	210.7206/215.4397	143.4961/146.0035	96.4064/97.3415
2	198.0454/202.0878	134.6688/137.2445	90.4982/91.6464
3	214.6506/128.8066	128.9084/135.2567	68.7568/150.8837
4	189.4424/190.0019	126.0795/128.2829	81.212/85.4957
5	177.238/180.2527	126.8883/129.0058	92.2764/94.1719
6	196.2714/210.1376	129.6972/131.4016	83.2224/75.2002
7	187.8103/243.6103	165.7727/165.8331	155.3168/111.0499
8	275.1772/261.2111	187.8655/192.2673	126.7693/145.7598
9	274.4525/279.5333	208.2886/211.5439	163.1902/165.7982
10	221.0144/329.9158	213.1171/210.209	216.688/125.127
11	254.3625/331.3371	210.3074/210.2636	185.9277/122.2905
12	305.0765/287.3826	205.3285/210.1099	136.2943/158.6894
13	279.6907/296.0798	204.8049/208.0304	155.9552/148.2067
14	314.5124/309.3864	207.6128/211.8118	132.2097/143.8423

15	344.0973/233.0081	198.6467/207.9851	93.3928/199.8106
16	273.5156/299.6057	205.4764/207.4219	161.031/144.6458
17	271.7732/290.8291	215.7283/219.2835	181.657/171.1532
18	277.4357/285.294	220.8872/222.5304	183.8044/185.7095
19	325.435/316.6544	216.9379/221.2959	141.0793/156.4717
20	273.2208/323.2753	209.7685/211.1037	169.0943/130.948
21	266.6413/296.3674	199.82/201.9526	154.4002/135.4794
22	249.891/285.8363	181.4701/182.5449	134.2684/108.2325
23	210.3748/224.045	158.8054/160.6301	124.6813/117.9704
24	199.8273/203.2955	135.5016/138.084	90.6123/92.3085

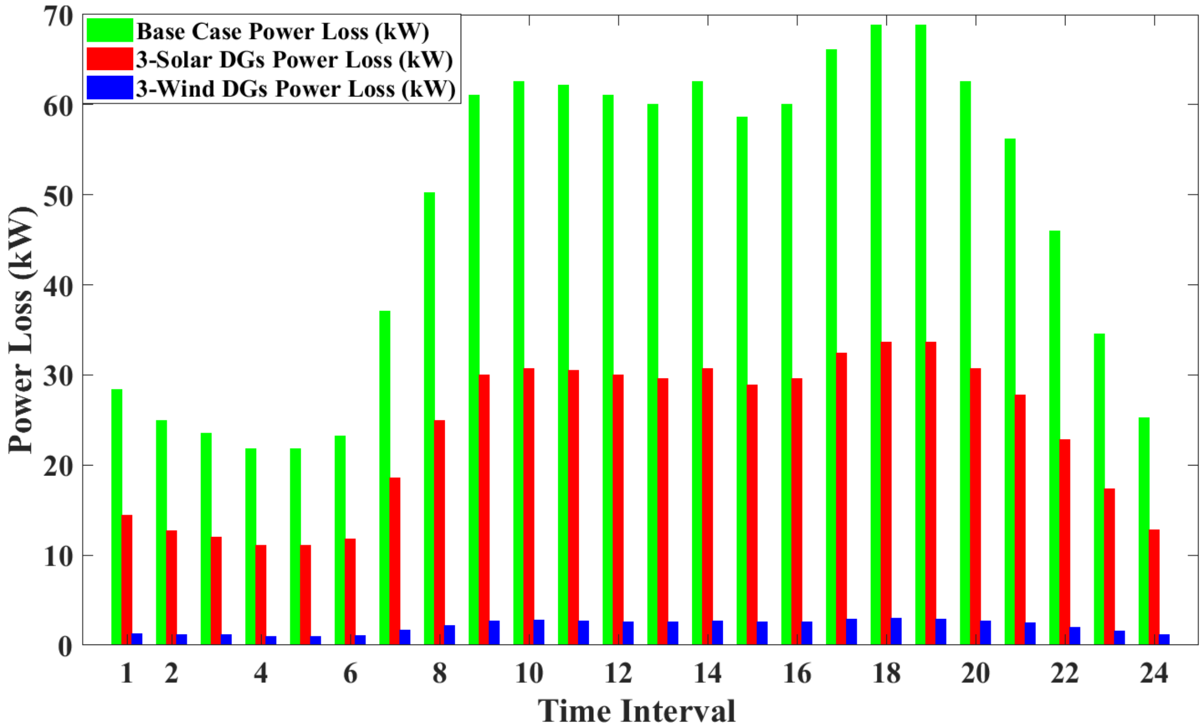

Fig 6.11 28 practical test system P_{Loss} typical day with different cases

Table 6.8 V_{min} and VSI_{min} of comparison for a typical day

Hours	**Voltage profile (p.u)**			**Voltage stability index (p.u)**		
	Base Case	**3-Solar DGs**	**3-Wind DGs**	**Base Case**	**3-Solar DGs**	**3-Wind DGs**
1	0.9438	0.9761	0.9938	0.7934	0.9177	0.9754
2	0.9474	0.9776	0.9942	0.8055	0.9132	0.9769
3	0.9489	0.9782	0.9942	0.8106	0.9155	0.9771
4	0.9508	0.979	0.9946	0.8173	0.9185	0.9783
5	0.9508	0.979	0.9945	0.8173	0.9185	0.9782
6	0.9492	0.9783	0.9944	0.8119	0.916	0.9779
7	0.9357	0.9727	0.9927	0.7666	0.8953	0.9711
8	0.9252	0.9685	0.9919	0.7327	0.8797	0.9678
9	0.9175	0.9654	0.991	0.7085	0.8684	0.9646
10	0.9164	0.9649	0.9908	0.7053	0.8669	0.9636
11	0.9167	0.9651	0.991	0.7062	0.8673	0.9643
12	0.9175	0.9654	0.9911	0.7085	0.8685	0.965
13	0.9181	0.9656	0.9912	0.7106	0.8694	0.965
14	0.9164	0.9649	0.9911	0.7053	0.8669	0.965
15	0.9191	0.966	0.9913	0.7135	0.8708	0.9656
16	0.9181	0.9656	0.9911	0.7106	0.8694	0.9647
17	0.914	0.964	0.9906	0.698	0.8635	0.9627
18	0.9123	0.9633	0.9904	0.6927	0.8611	0.9622
19	0.9123	0.9633	0.9907	0.6927	0.8611	0.9631
20	0.9164	0.9649	0.9909	0.7053	0.8669	0.9641
21	0.9208	0.9667	0.9914	0.7188	0.8732	0.9659
22	0.9284	0.9698	0.9922	0.743	0.8845	0.9692
23	0.938	0.9737	0.9931	0.7741	0.8988	0.9726
24	0.947	0.9774	0.9941	0.8043	0.9125	0.9767

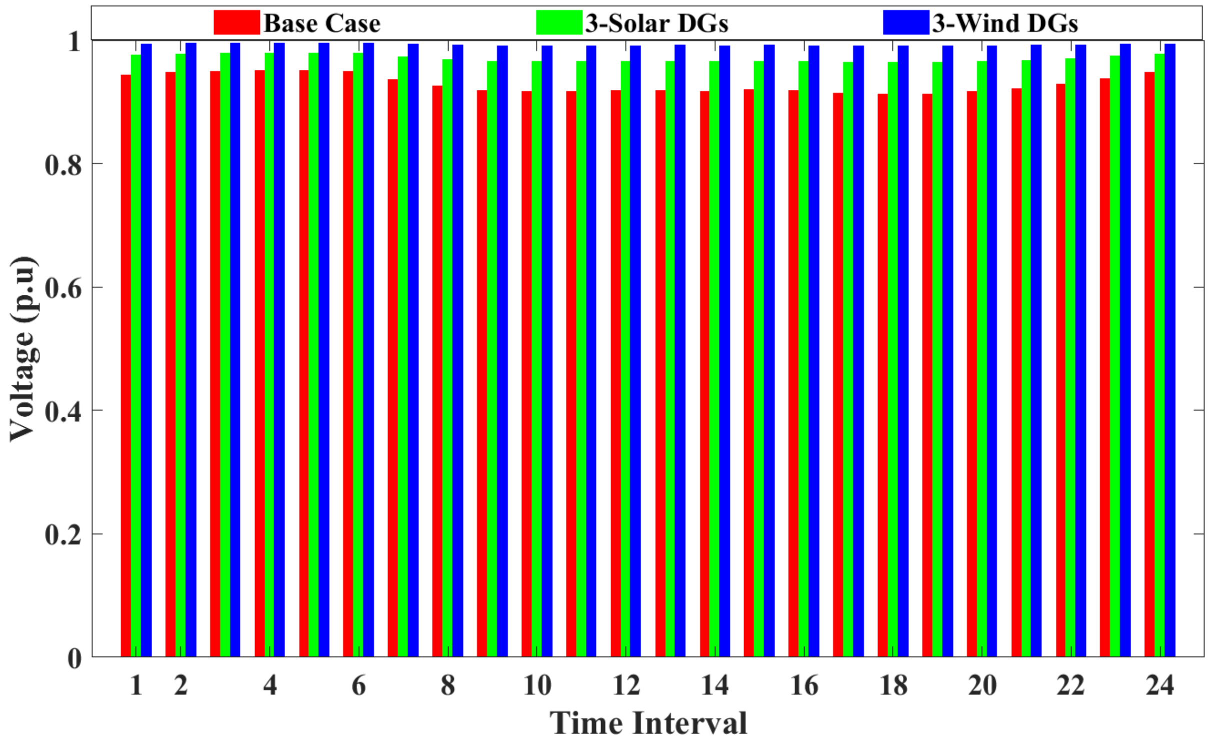

Fig 6.12 Various cases voltage profile comparison for dynamic load

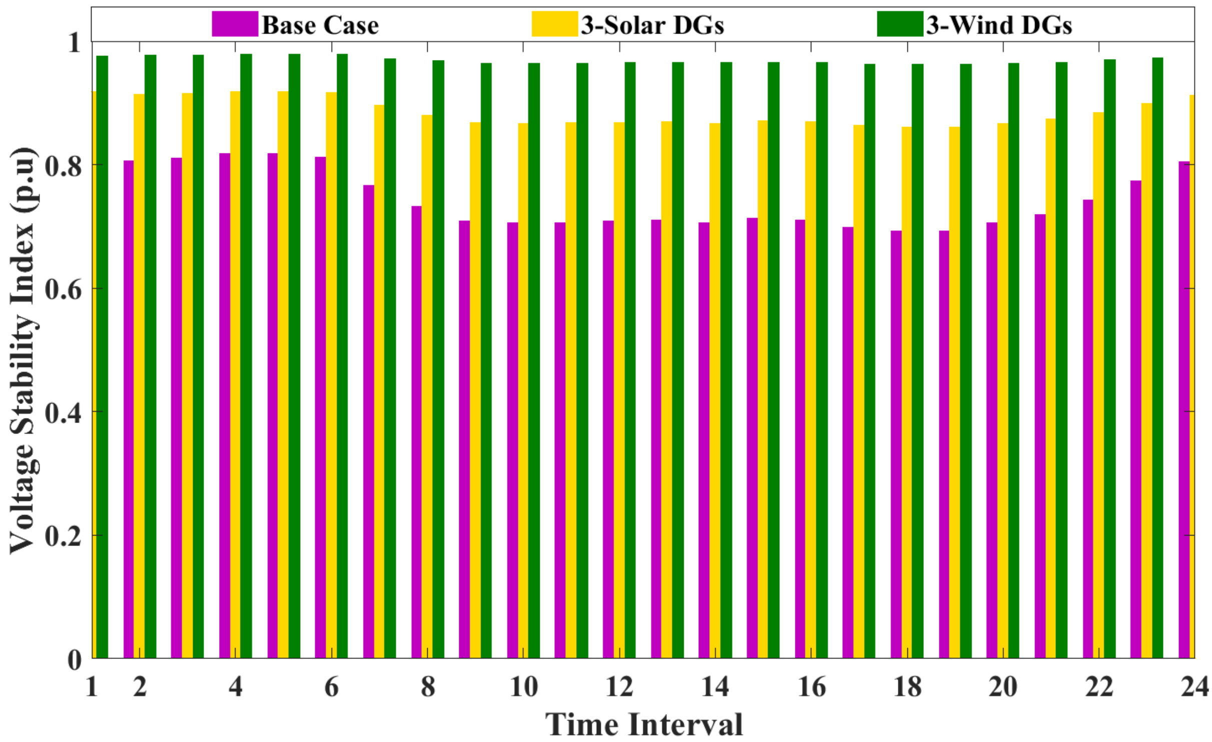

Fig 6.13 Comparison of Dynamic load voltage stability index for different cases

6.5 28 Indian Test System Evaluation with RDGs without EVs:

The VSI approach allocates RDGs to the 7^{th}, 12^{th}, and 22^{nd} buses. Table.6.6 represents RDGs P_{Loss} comparison for a typical day with different cases. Table 6.7 shows the results of POA optimization in deciding the suitable DG size for time-varying load conditions. After installing the RDGs, the P_{Loss}, V_{min}, and VSI_{min} at every hour are determined, and the outcomes are compared to the base case. Fig 6.11 depicts the variation in P_{Loss} achieved before and after RDG placement. Compared to the base case study, there is a considerable decrease in overall P_{Loss}. Fig 6.12 and 6.13 also show the difference in V_{min} VSI_{min} before and after introducing solar and wind-based DGs. Compared to the base case, there is an enormous improvement in voltage profile and VSI.

6.6 28 Indian Test System Evaluation with EVs:

The advantages of placing RDGs in three different modes of operation are discussed in further detail, and the expansion of scheduling EVs is further examined.

The network's operational conditions deteriorate because of the dynamic variations in system demand and the growing adaption of EVs. Consequently, EVs must be scheduled following the changing levels of demand. The Chevy Volt EV, a well-known vehicle on the market, is used as an example in this study. Table 3.5 lists the EV's parameters.

- There are 60 EVs that ride to work, covering an average daily distance of 30 km, departing at 8:00 a.m. and arriving back at 5:00 p.m.
- All EVs must begin their journey with a full charge, and there is no way to recharge between the hours of travel. Furthermore, EVs require significant time to charge their batteries depending on the distance travelled/supplied to the grid.
- The technology is also expected to provide a two-way communication system between EVs & the power grid. This channel permits info between them, allowing for combined EV and DG scheduling. As a result, data is transported without delay from one channel to the next.

6.6.1 Conventional Charging Method (CCM):

In the CCM, EVs are recharged ideally at the 2^{nd}, 5^{th}, and 11^{th} nodes. The VSI approach is used to identify these places. As illustrated in Fig 6.14, the EVs are charged in G2V mode throughout the 18^{th}, 19^{th}, and 20^{th} hours. For each hour, the P_{Loss}, V_{min}, and VSI_{min} are calculated, and the results are shown in Tables 6.9 and 6.10. The voltage profile during 18-20 hr. is impacted due to the increased load on the network; as shown in Table 6.9, the 24hrs P_{Loss} is 835.6594 kW.

6.6.2 Optimised Charging Method (OCM):

The OCM technology takes into account system power demand and calculates the appropriate time to charge the EVs. In an OCM, EVs are optimally located on the 2^{nd}, 5^{th}, and 11^{th} buses. VSI is used to find these places. The EVs are charged in G2V mode between the 4^{th}, 5^{th}, and 6^{th} hrs, as illustrated in Fig 6.14 and 6.15. For each hour, the P_{Loss}, are calculated, and the results are shown in Tables 6.9 and 6.10. Compared to the CCM approach, the total P_{Loss} per day is reduced. The voltage profile has been enhanced and is now superior to the CCM approach.

6.6.3 G2V plus V2G Method:

The assessment is carried out in combination with the OCM. This method allows EVs to charge and send electricity back to the grid (V2G plus G2V)). The OCM approach considers system load demand and calculates the best time to charge the EVs. As illustrated in Fig 6.14 and 6.15, The EVs are charged in G2V mode between the 4^{th} and 5^{th} hours. Between the 18^{th} and 19^{th} hours, the EVs will deliver electricity to the grid. For each hour, the P_{Loss}, are calculated, and the results are shown in Tables 6.9 and 6.10. The total daily P_{Loss} is 813.566 kW and 753.8709 kW. Tables 6.9 and 6.10 contains a comparison of several cases. The voltage profile is considerably better than with the previous approaches. Efficient EV scheduling, combined with appropriate allocation of RDGs, assists in loss minimization and improving voltage profile.

Table 6.9 Comparison of P_{Loss} for different operation conditions

Hours	Base Case P_{Loss} (KW)	(2-Solar + 1-Wind) DGs P_{Loss} (kW)	Conventional method (2-Solar DGs +1-Wind DG With EVs) P_{Loss} (kW)	Optimized method (2-Solar DGs +1-Wind DG With EVs) P_{Loss} (kW)	(G2V + V2G) Method (2-Solar + 1-Wind DG With EVs) P_{Loss} (kW)
1	28.4096	17.9573	17.9573	17.9573	17.9573
2	24.9163	16.1636	16.1636	16.1636	16.1636
3	23.5076	15.392	15.392	15.392	15.392
4	21.751	14.3217	14.3217	16.5088	16.5088
5	21.751	14.8205	14.8205	17.1457	17.1457

6	23.1827	14.5505	14.5505	16.6181	14.5505
7	37.1053	22.4727	22.4727	22.4727	22.4727
8	50.1845	29.9445	29.9445	29.9445	29.9445
9	61.0107	35.3964	35.3964	35.3964	35.3964
10	62.5568	34.8334	34.8334	34.8334	34.8334
11	62.1329	33.227	33.227	33.227	33.227
12	61.0107	32.6859	32.6859	32.6859	32.6859
13	60.0386	35.5933	35.5933	35.5933	35.5933
14	62.5568	40.2087	40.2087	40.2087	40.2087
15	58.6655	39.6139	39.6139	39.6139	39.6139
16	60.0386	41.929	41.929	41.929	41.929
17	66.1549	47.0788	51.5117	47.0788	47.0788
18	68.8189	61.0836	66.9075	61.0836	55.9324
19	68.8189	62.346	68.2826	62.346	57.0849
20	62.5568	60.7269	60.7269	60.7269	60.7269
21	56.2403	53.7249	53.7249	53.7249	53.7249
22	45.9301	42.9118	42.9118	42.9118	42.9118
23	34.5317	31.1939	31.1939	31.1939	31.1939
24	25.2543	21.2897	21.2897	21.2897	21.2897
Total P_{Loss} (kW)	**1147.1245**	**819.466**	**835.6594**	**826.0459**	**813.566**

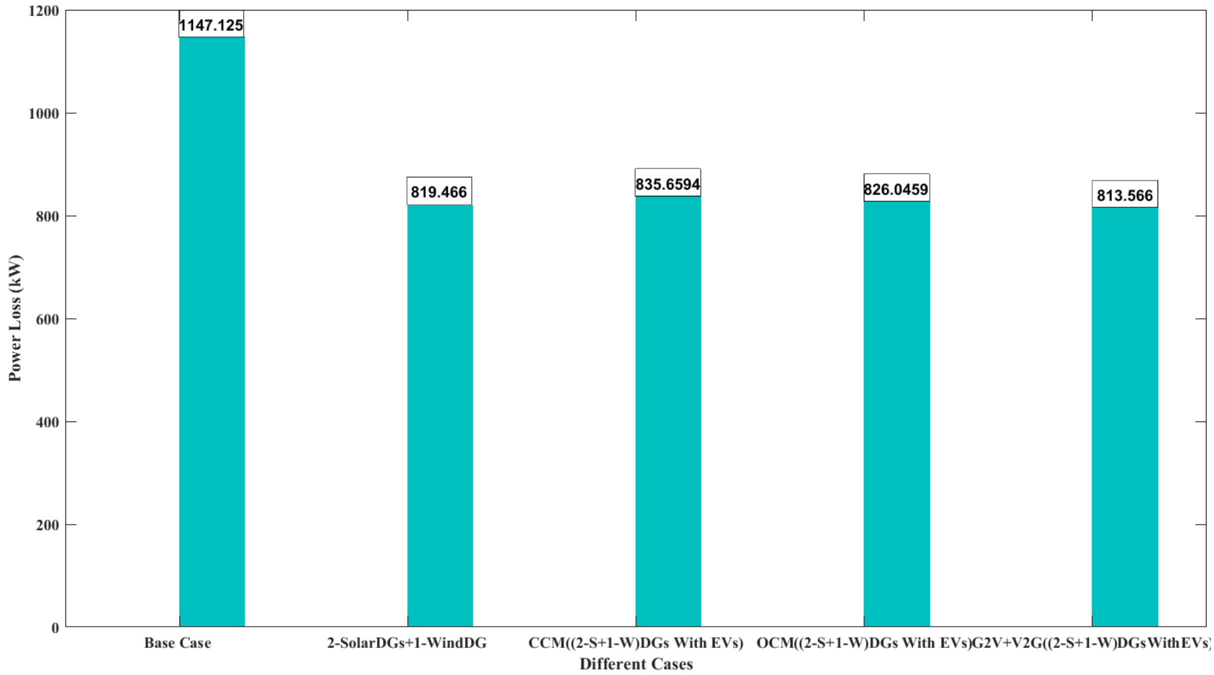

Fig 6.14 Comparison of P_{Loss} for different cases with combination of RDGs and EVs

Table 6.10 Comparison of P_{Loss} for different operation conditions

Hours	**Base Case P_{Loss} (KW)**	**(2-Wind + 1-Solar) DGs P_{Loss} (kW)**	**Conventional method (2-Wind DGs +1-Solar DG With EVs) P_{Loss} (kW)**	**Optimized method (2-Wind DGs +1-Solar DG With EVs) P_{Loss} (kW)**	**(G2V + V2G) Method (2-Wind + 1-Solar DG With EVs) P_{Loss} (kW)**
1	28.4096	15.048	15.048	15.048	15.048
2	24.9163	13.4387	13.4387	13.4387	13.4387
3	23.5076	12.7703	12.7703	12.7703	12.7703
4	21.751	11.8761	11.8761	12.7913	12.7913
5	21.751	12.2542	12.2542	13.436	13.436
6	23.1827	12.6455	12.6455	13.7616	12.6455
7	37.1053	20.2663	20.2663	20.2663	20.2663
8	50.1845	27.5291	27.5291	27.5291	27.5291
9	61.0107	32.9941	32.9941	32.9941	32.9941
10	62.5568	32.6984	32.6984	32.6984	32.6984
11	62.1329	31.3334	31.3334	31.3334	31.3334
12	61.0107	30.6333	30.6333	30.6333	30.6333

13	60.0386	34.4124	34.4124	34.4124	34.4124
14	62.5568	39.0762	39.0762	39.0762	39.0762
15	58.6655	37.851	37.851	37.851	37.851
16	60.0386	38.3294	38.3294	38.3294	38.3294
17	66.1549	40.9142	44.0938	40.9142	40.9142
18	68.8189	56.8144	62.0351	56.8144	52.2525
19	68.8189	58.711	64.1471	58.711	53.9386
20	62.5568	59.6402	59.6402	59.6402	59.6402
21	56.2403	52.2444	52.2444	52.2444	52.2444
22	45.9301	41.1574	41.1574	41.1574	41.1574
23	34.5317	29.2972	29.2972	29.2972	29.2972
24	25.2543	19.173	19.173	19.173	19.173
Total P_{Loss}(kW)	**1147.1245**	**761.1082**	**774.9446**	**764.3213**	**753.8709**

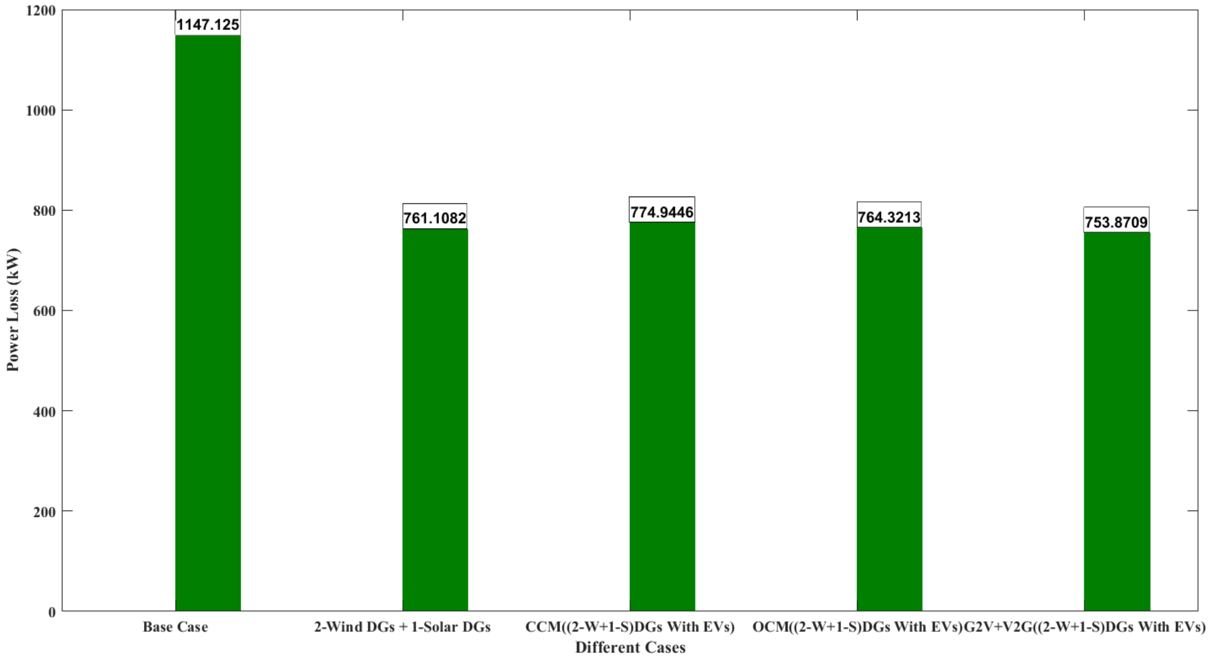

Fig 6.15 Comparison of P_{Loss} for different cases with Integration of RDGs and EVs

6.7 Summary of the Chapter

The presented method aims to achieve minimal P_{Loss} and a better voltage profile with optimal allocation of RDGs and scheduling EVs in DS. The combination of the VSI-POA method is proposed to find the suitable location to install RDGs and charging EV locations and determine the size of RDGs. The proposed VSI-POA analysis was performed on 28 Indian real test systems. Compared to POA performance with other existing methods, POA gives better results with less iteration. Simultaneous allocation of RDGs with EVCS enhanced voltage profile and reduced RES uncertainty in DS compared to a single allocation system.

CHAPTER 7

CONCLUSION AND FUTURE SCOPE

7.1 Conclusion:

The primary aim of this study is to address the RDGs, EVCS, and simultaneously RDGs and EVCS allocation problems to decrease P_{Loss} and improve voltage profile DS. The LSF-POA and VSI-POA methods are utilized in this work to calculate the optimal location and sizes for DERs. Further, the location of EVCS found out using LSF and VSI methods. The suggested technique was validated using the standard IEEE 33, 69 buses, and the 28 Indian test system while taking into account a different load levels and various cases. The findings make it abundantly evident that the simultaneous allocation of RDGs, which injects both real and reactive power along with EVs, may decrease the system losses and improve the voltage profile to the highest possible level. Additionally, the location of DG systems powered by solar and wind energy while considering generation uncertainty is very significant. Appropriate probability distribution functions efficiently describe this. Solar panel exact output power is calculated with the beta probability distribution function (PDF). Beta PDF is more suitable for statistical analysis to model solar irradiance. The uncertainty related to wind speed is adequately simulated before placing these sources in DS. Weibull PDF has been utilized for these. The optimal combination of various kinds of RDGs with EVCS located in the DS improves the system's performance by decreasing the amount of active P_{Loss} and increasing the voltage profile. The allocation of single RDGs came first, followed by allocating these sources in combination with EVs. Several cases are taken into consideration throughout the investigation.

EVs are making tremendous strides in the DS, and this trend is expected to continue. This work presents a different approach to scheduling EVs and RDGs in a DS. A system of optimal charging that helps successfully reduce peak demand and takes into account the travel patterns of EVs has been established. The results demonstrate that it is vital to reduce peak congestion and overall P_{Loss} efficiently. In addition, when conducting a comparative assessment of EVs' various modes of operation, it is essential to consider the various travel patterns of EVs and its impact on DS is assessed. It is possible to deduce that the successful scheduling of EVs and RDGs contributes to enhancing the overall effectiveness of the DS. If EV owners can schedule their vehicles according to the system's consumption pattern, they may earn income using the V2G mode. This study has the potential to be improved further by taking into account the variable nature of the RES and considering different charging and discharging patterns of EVs. The static and dynamic load variations are considered to study the performance. Different cases, such as single RDG, multiple RDGs, only EVs and the combination of RDGs plus EVs, are considered to check the method's effectiveness. Furthermore, different EV charging methods, such as conventional charging method (CCM), optimized charging method (OCM) and different modes such as Grid 2Vehicle (G2V) plus vehicle 2 Grid (V2G) are considered for the assessment. From the simulated results, it is observed G2V plus V2G method gives the best results. The obtained results verified that proper placement of RDGs and effective charging strategies for EVs reduce the P_{Loss} considerably. The developed technique is compared with other methods that are already present in the existing literature. Using LSF - POA method validated results on IEEE 33 test system using multi solar DGs with static load variation of 64.93%, with dynamic load variation of 64.38% and using different EV charging methods (G2V + V2G) 63.39% of P_{Loss} reduced and enhanced both voltage profile and stability. The same procedure was followed for 28 Indian bus system with multi-solar DGs and EVs 17.48% of P_{Loss} decreased. With the IEEE 69 test system using multi-wind DGs with static load variation of 98.19%, dynamic load variation 87.31% and optimized charging method of 58.38% of P_{Loss} minimized and improved voltage profile and voltage stability. Considering the same method for 28 test system using multi-wind DGs with EVs for 24hrs decreased 39.05% of P_{Loss}.

Implementing VSI – POA method simulated results on 28 Indian bus system with static load variation considering multi solar DGs 51.10% and multi wind DGs 95.76% of P_{Loss} minimized. Dynamic load variation using multi solar DGs 50.52% and with multi wind DGs 95.63% P_{Loss} decreased. Different EV charging methods combination of two solar DGs + 1 wind DG with EVs (G2V + V2G) 29.07% and combination of two wind DGs + 1 solar DG with EVs (G2V + V2G) 34.28% of P_{Loss} reduced.

The findings that were obtained demonstrate its effectiveness in every case that was taken into consideration. Therefore, it is concluded that the proposed approach effectively solved the problem of allocating RDGs and EVCS in the DS without violating any of the constraints of the DS.

7.2 Future Scope:

- Techno-economic analysis with the integration of RDGs and EVCS in DS
- Reliability analysis considering RDGs along with the uncertainties and EVCS in DS
- Simultaneous allocation of RDGs, DSTATCOM, battery energy storage system (BESS) and EVCS in DS
- Assessment of DS with the integration of RES, EVCS and BESS to minimize losses and improve voltage profile and stability
- Energy Management System for Efficient use of RDGs in DS
- Enhancing DS Reliability Through Efficient PEV Parking Lot Allocation with V2G
- In addition, the same study analysis can be used for various large scale test systems and different hybrid metaheuristic algorithms

REFERENCES:

[1] A. Shaheen, A. Elsayed, A. Ginidi, R. El-Sehiemy, and E. Elattar, “Improved Heap-Based Optimizer for DG Allocation in Reconfigured Radial Feeder Distribution Systems,” *IEEE Syst. J.*, pp. 1–10, 2022, doi: 10.1109/JSYST.2021.3136778.

[2] H. A. Taha, M. H. Alham, and H. K. M. Youssef, “Multi-Objective Optimization for Optimal Allocation and Coordination of Wind and Solar DGs, BESSs and Capacitors in Presence of Demand Response,” *IEEE Access*, vol. 10, pp. 16225–16241, 2022, doi: 10.1109/ACCESS.2022.3149135.

[3] V. Suresh, N. Pachauri, and T. Vigneysh, “Decentralized control strategy for fuel cell/PV/BESS based microgrid using modified fractional order PI controller,” *Int. J. Hydrogen Energy*, vol. 46, no. 5, pp. 4417–4436, 2021, doi: 10.1016/j.ijhydene.2020.11.050.

[4] Y. Abd El Aziz, “Renewables 2022 Global Status Report Asia Factsheet,” 2022.

[5] Y. Abd El Aziz, “Renewables 2022 Global Status Report India Factsheet,” pp. 2019–2021, 2022.

[6] MNRE, “Ministry of New and Renewable Energy, Goverment of India: Annual report 2020-2021,” vol. 53, no. 9, pp. 1689–1699, 2021.

[7] C. E. T. P. Time, “Trends in India Facts from the Renewables in Cities 2021 Global Status Report Key,” no. March, pp. 2–4, 2021.

[8] IEA and NITI Aayog, “Renewables Integration report in India,” *Iea*, pp. 1–93, 2021.

[9] International Energy Agency, “IEA (2021), World Energy Investment 2021,” *Iea*, pp. 1–56, 2021.

[10] P. Prakash and D. K. Khatod, “Optimal sizing and siting techniques for distributed generation in distribution systems: A review,” *Renew. Sustain. Energy Rev.*, vol. 57, pp. 111–130, 2016, doi: 10.1016/j.rser.2015.12.099.

[11] IEA, “Global EV Outlook 2022 Securing supplies for an electric future,” *Iea*, p. 221, 2022.

[12] H. S. Das, M. M. Rahman, S. Li, and C. W. Tan, “Electric vehicles standards, charging infrastructure, and impact on grid integration: A technological review,” *Renew. Sustain.*

Energy Rev., vol. 120, no. February, 2020, doi: 10.1016/j.rser.2019.109618.

[13] G. N. S, D. K. Khatod, and M. P. Sharma, “Optimal Allocation of Distributed Generation in Distribution System for Loss Reduction,” *IACSIT Coimbatore Conf.*, vol. 28, pp. 42–46, 2012.

[14] S. Abdi and K. Afshar, “Application of IPSO-Monte Carlo for optimal distributed generation allocation and sizing,” *Int. J. Electr. Power Energy Syst.*, vol. 44, no. 1, pp. 786–797, 2013, doi: 10.1016/j.ijepes.2012.08.006.

[15] M. Sedighizadeh, M. Esmaili, and M. Esmaeili, “Application of the hybrid Big Bang-Big Crunch algorithm to optimal reconfiguration and distributed generation power allocation in distribution systems,” *Energy*, vol. 76, pp. 920–930, 2014, doi: 10.1016/j.energy.2014.09.004.

[16] S. N. Gopiya Naik, D. K. Khatod, and M. P. Sharma, “Analytical approach for optimal siting and sizing of distributed generation in radial distribution networks,” *IET Gener. Transm. Distrib.*, vol. 9, no. 3, pp. 209–220, 2015, doi: 10.1049/iet-gtd.2014.0603.

[17] T. T. Nguyen, A. V. Truong, and T. A. Phung, “A novel method based on adaptive cuckoo search for optimal network reconfiguration and distributed generation allocation in distribution network,” *Int. J. Electr. Power Energy Syst.*, vol. 78, no. June 2016, pp. 801–815, 2016, doi: 10.1016/j.ijepes.2015.12.030.

[18] R. Sanjay, T. Jayabarathi, T. Raghunathan, V. Ramesh, and N. Mithulananthan, “Optimal allocation of distributed generation using hybrid grey Wolf optimizer,” *IEEE Access*, vol. 5, pp. 14807–14818, 2017, doi: 10.1109/ACCESS.2017.2726586.

[19] T. P. Nguyen and D. N. Vo, “A novel stochastic fractal search algorithm for optimal allocation of distributed generators in radial distribution systems,” *Appl. Soft Comput. J.*, vol. 70, pp. 773–796, 2018, doi: 10.1016/j.asoc.2018.06.020.

[20] H. Li, H. Cui, and C. Li, “Distribution network power loss analysis considering uncertainties in distributed generations,” *Sustain.*, vol. 11, no. 5, pp. 1–17, 2019, doi: 10.3390/su11051311.

[21] F. C. R. Coelho, I. C. da Silva Junior, B. H. Dias, W. Peres, V. H. Ferreira, and A. L. M. Marcato, “Optimal distributed generation allocation in unbalanced radial distribution

networks via empirical discrete metaheuristic and steepest descent method," *Electr. Eng.*, vol. 103, no. 1, pp. 633–646, 2020, doi: 10.1007/s00202-020-01106-3.

[22] M. Naguib, W. A. Omran, and H. E. A. Talaat, "Performance Enhancement of Distribution Systems via Distribution Network Reconfiguration and Distributed Generator Allocation Considering Uncertain Environment," *J. Mod. Power Syst. Clean Energy*, vol. 10, no. 3, pp. 647–655, 2021, doi: 10.35833/mpce.2020.000333.

[23] Y. G. Werkie and H. A. Kefale, "Optimal allocation of multiple distributed generation units in power distribution networks for voltage profile improvement and power losses minimization," *Cogent Eng.*, vol. 9, no. 1, 2022, doi: 10.1080/23311916.2022.2091668.

[24] A. S. Machava, K. K. Kaberere, and G. A. Vilanculo, "A Method for Optimal Distributed Generation Allocation Considering Load Demand Uncertainties," *Int. J. Electr. Electron. Eng. Telecommun.*, vol. 11, no. 3, pp. 210–217, 2022, doi: 10.18178/ijeetc.11.3.210-217.

[25] M. Jamil and S. Kirmani, "Optimal allocation of SPV based DG system for loss reduction and voltage improvement in radial distribution systems using approximate reasoning," *India Int. Conf. Power Electron. IICPE*, pp. 1–5, 2012, doi: 10.1109/IICPE.2012.6450387.

[26] D. K. Khatod, V. Pant, and J. Sharma, "Evolutionary Programming Based Optimal Placement of Renewable Distributed Generators," *Ieee Trans. Power Syst. Vol. 28, No. 2,May 2013*, vol. 28, no. 2, pp. 683–695, 2013.

[27] S. Montoya-Bueno, J. I. Muñoz, and J. Contreras, "Optimal expansion model of renewable distributed generation in distribution systems," *Proc. - 2014 Power Syst. Comput. Conf. PSCC 2014*, 2014, doi: 10.1109/PSCC.2014.7038348.

[28] P. Kayal and C. K. Chanda, "Optimal mix of solar and wind distributed generations considering performance improvement of electrical distribution network," *Renew. Energy*, vol. 75, pp. 173–186, 2015, doi: 10.1016/j.renene.2014.10.003.

[29] V. Kalkhambkar, R. Kumar, and R. Bhakar, "Joint optimal allocation methodology for renewable distributed generation and energy storage for economic benefits," *IET Renew. Power Gener.*, vol. 10, no. 9, pp. 1422–1429, 2016, doi: 10.1049/iet-rpg.2016.0014.

[30] E. S. Ali, S. M. Abd Elazim, and A. Y. Abdelaziz, "Ant Lion Optimization Algorithm for optimal location and sizing of renewable distributed generations," *Renew. Energy*, vol. 101,

pp. 1311–1324, 2017, doi: 10.1016/j.renene.2016.09.023.

[31] A. Naeem, N. U. Hassan, and C. Yuen, “Power Loss Minimization in Power Distribution Systems Using Wind and Solar Complementarity,” *Int. Conf. Innov. Smart Grid Technol. ISGT Asia 2018*, pp. 1165–1170, 2018, doi: 10.1109/ISGT-Asia.2018.8467939.

[32] K. S. Sambaiah and T. Jayabarathi, “Optimal reconfiguration and renewable distributed generation allocation in electric distribution systems,” *Int. J. Ambient Energy*, vol. 42, no. 9, pp. 1018–1031, 2019, doi: 10.1080/01430750.2019.1583604.

[33] H. M. H. Farh, A. M. Al-Shaalan, A. M. Eltamaly, and A. A. Al-Shamma’A, “A Novel Crow Search Algorithm Auto-Drive PSO for Optimal Allocation and Sizing of Renewable Distributed Generation,” *IEEE Access*, vol. 8, pp. 27807–27820, 2020, doi: 10.1109/ACCESS.2020.2968462.

[34] A. Rathore and N. P. Patidar, “Optimal sizing and allocation of renewable based distribution generation with gravity energy storage considering stochastic nature using particle swarm optimization in radial distribution network,” *J. Energy Storage*, vol. 35, no, p. 102282, 2021, doi: 10.1016/j.est.2021.102282.

[35] B. Sun, Y. Li, Y. Zeng, J. Chen, and J. Shi, “Optimization planning method of distributed generation based on steady-state security region of distribution network,” *Energy Reports*, vol. 8, pp. 4209–4222, 2022, doi: 10.1016/j.egyr.2022.03.078.

[36] M. Purlu and B. E. Turkay, “Optimal Allocation of Renewable Distributed Generations Using Heuristic Methods to Minimize Annual Energy Losses and Voltage Deviation Index,” *IEEE Access*, vol. 10, pp. 21455–21474, 2022, doi: 10.1109/ACCESS.2022.3153042.

[37] R. Baghipour and S. M. Hosseini, “Placement of DG and Capacitor for Loss Reduction, Reliability and Voltage Improvement in Distribution Networks Using BPSO,” *Int. J. Intell. Syst. Appl.*, vol. 4, no. 12, pp. 57–64, 2012, doi: 10.5815/ijisa.2012.12.08.

[38] S. Gopiya Naik, D. K. Khatod, and M. P. Sharma, “Optimal allocation of combined DG and capacitor for real power loss minimization in distribution networks,” *Int. J. Electr. Power Energy Syst.*, vol. 53, pp. 967–973, 2013, doi: 10.1016/j.ijepes.2013.06.008.

[39] S. Devi and M. Geethanjali, “Optimal location and sizing determination of Distributed

Generation and DSTATCOM using Particle Swarm Optimization algorithm," *Int. J. Electr. Power Energy Syst.*, vol. 62, pp. 562–570, 2014, doi: 10.1016/j.ijepes.2014.05.015.

[40] N. A. Khan, S. P. Ghoshal, and S. Ghosh, "Optimal allocation of distributed generation and shunt capacitors for the reduction of total voltage deviation and total line loss in radial distribution systems using binary collective animal behavior optimization algorithm," *Electr. Power Components Syst.*, vol. 43, no. 2, pp. 119–133, 2015, doi: 10.1080/15325008.2014.975384.

[41] A. Khodabakhshian and M. H. Andishgar, "Simultaneous placement and sizing of DGs and shunt capacitors in distribution systems by using IMDE algorithm," *Int. J. Electr. Power Energy Syst.*, vol. 82, pp. 599–607, 2016, doi: 10.1016/j.ijepes.2016.04.002.

[42] M. Dixit, P. Kundu, and H. R. Jariwala, "Incorporation of distributed generation and shunt capacitor in radial distribution system for techno-economic benefits," *Eng. Sci. Technol. an Int. J.*, vol. 20, no. 2, pp. 482–493, 2017, doi: 10.1016/j.jestch.2017.01.003.

[43] L. Zhang, C. Shen, Y. Chen, S. Huang, and W. Tang, "Coordinated allocation of distributed generation, capacitor banks and soft open points in active distribution networks considering dispatching results," *Appl. Energy*, vol. 231, no. December 2017, pp. 1122–1131, 2018, doi: 10.1016/j.apenergy.2018.09.095.

[44] A. Bayat and A. Bagheri, "Optimal active and reactive power allocation in distribution networks using a novel heuristic approach," *Appl. Energy*, vol. 233–234, no. August 2019, pp. 71–85, 2019, doi: 10.1016/j.apenergy.2018.10.030.

[45] K. Balu and V. Mukherjee, "Siting and Sizing of Distributed Generation and Shunt Capacitor Banks in Radial Distribution System Using Constriction Factor Particle Swarm Optimization," *Electr. Power Components Syst.*, vol. 48, no. 6–7, pp. 697–710, 2020, doi: 10.1080/15325008.2020.1797935.

[46] T. Yuvaraj *et al.*, "Optimal integration of capacitor and distributed generation in distribution system considering load variation using bat optimization algorithm," *Energies*, vol. 14, no. 12, 2021, doi: 10.3390/en14123548.

[47] M. M. Sayed, M. Y. Mahdy, S. H. E. Abdel Aleem, H. K. M. Youssef, and T. A. Boghdady, "Simultaneous Distribution Network Reconfiguration and Optimal Allocation of Renewable-Based Distributed Generators and Shunt Capacitors under Uncertain

Conditions," *Energies*, vol. 15, no. 6, 2022, doi: 10.3390/en15062299.

[48] Z. Liu, F. Wen, and G. Ledwich, "Optimal planning of electric-vehicle charging stations in distribution systems," *IEEE Trans. Power Deliv.*, vol. 28, no. 1, pp. 102–110, 2012, doi: 10.1109/TPWRD.2012.2223489.

[49] C. L. Su, R. C. Leou, J. C. Yang, and C. N. Lu, "Optimal electric vehicle charging stations placement in distribution systems," *IECON Proc. (Industrial Electron. Conf.*, pp. 2121–2126, 2013, doi: 10.1109/IECON.2013.6699459.

[50] I. Niazazari, H. Askarian Abyaneh, M. Javad Farah, F. Safaei, and H. Nafisi, "Voltage profile and power factor improvement in Prev charging station using a probabilistic model and flywheel," *2014 19th Conf. Electr. Power Distrib. Networks, EPDC 2014*, vol. 2014-January, no. October 2019, pp. 100–105, 2014, doi: 10.1109/EPDC.2014.6867506.

[51] N. Banol A., J. F. Franco, M. Lavorato, M. J. Rider, and R. Romero, "Plug-in electric vehicle charging coordination in electrical distribution systems using a tabu search algorithm," *2015 IEEE 15th Int. Conf. Environ. Electr. Eng. EEEIC 2015 - Conf. Proc.*, pp. 1510–1515, 2015, doi: 10.1109/EEEIC.2015.7165395.

[52] N. B. Arias, R. Romero, J. F. Franco, and M. L. De Oliveira, "GRASP algorithm for charging coordination of plug-in electric vehicles in electrical distribution systems," *2016 IEEE PES Transm. Distrib. Conf. Expo. Am. PES T D-LA 2016*, 2016, doi: 10.1109/TDC-LA.2016.7805624.

[53] A. Arias, M. Granada, and C. A. Castro, "Optimal probabilistic charging of electric vehicles in distribution systems," *IET Electr. Syst. Transp.*, vol. 7, no. 3, pp. 246–251, 2017, doi: 10.1049/iet-est.2016.0072.

[54] L. Gong, W. Cao, K. Liu, J. Zhao, and X. Li, "Spatial and temporal optimization strategy for plug-in electric vehicle charging to mitigate impacts on distribution network," *Energies*, vol. 11, no. 6, 2018, doi: 10.3390/en11061373.

[55] V. Suresh, S. Sudabattula, and S. H. C. Cherukuri, "Coordinated power loss minimization technique for Distribution systems in the presence of Electric Vehicles," *2019 Natl. Power Electron. Conf. NPEC 2019*, pp. 1–5, 2019, doi: 10.1109/NPEC47332.2019.9034757.

[56] A. Amin *et al.*, "An integrated approach to optimal charging scheduling of electric vehicles

integrated with improved medium-voltage network reconfiguration for power loss minimization," *Sustain.*, vol. 12, no. 21, pp. 1–15, 2020, doi: 10.3390/su12219211.

[57] M. Usman *et al.*, "A coordinated charging scheduling of electric vehicles considering optimal charging time for network power loss minimization," *Energies*, vol. 14, no. 17, 2021, doi: 10.3390/en14175336.

[58] M. S. Kumar Reddy and K. Selvajyothi, "Investment analysis for optimal planning of electric vehicle charging station on a reconfigured unbalanced radial distribution system," *Electr. Eng.*, vol. 104, no. 3, pp. 1725–1739, 2022, doi: 10.1007/s00202-021-01404-4.

[59] O. Hafez and K. Bhattacharya, "Optimal PHEV charging in coordination with distributed generation operation in distribution systems," *IEEE Power Energy Soc. Gen. Meet.*, pp. 1–7, 2012, doi: 10.1109/PESGM.2012.6345320.

[60] E. Mohammadi, A. Foroughi, M. Rashidinejad, R. Fadaeinedjad, and G. Moschopoulos, "Optimal allocation of parking lots and PV systems in distribution system for energy loss reduction and voltage profile improvement," *Can. Conf. Electr. Comput. Eng.*, vol. 3, no. 2, pp. 31–34, 2013, doi: 10.1109/CCECE.2013.6567709.

[61] F. Fazelpour, M. Vafaeipour, O. Rahbari, and M. A. Rosen, "Intelligent optimization to integrate a plug-in hybrid electric vehicle smart parking lot with renewable energy resources and enhance grid characteristics," *Energy Convers. Manag.*, vol. 77, pp. 250–261, 2014, doi: 10.1016/j.enconman.2013.09.006.

[62] H. Modi, D. Saxena, and R. K. Chauhan, "Impact of Wind Distributed Generation on Distribution Systems Embedded with Electric Vehicles," *Proc. - 2015 Int. Conf. Control. Autom. Power Signal Process. CAPS 2021*, vol. 6, no. 1, pp. 79–87, 2015, doi: 10.1109/CAPS52117.2021.9730724.

[63] S. Shojaabadi, S. Abapour, M. Abapour, and A. Nahavandi, "Simultaneous planning of plug-in hybrid electric vehicle charging stations and wind power generation in distribution networks considering uncertainties," *Renew. Energy*, vol. 99, pp. 237–252, 2016, doi: 10.1016/j.renene.2016.06.032.

[64] N. B. Arias, J. F. Franco, M. Lavorato, and R. Romero, "Metaheuristic optimization algorithms for the optimal coordination of plug-in electric vehicle charging in distribution systems with distributed generation," *Electr. Power Syst. Res.*, vol. 142, pp. 351–361, 2017,

doi: 10.1016/j.epsr.2016.09.018.

[65] Y. Liu, X. Zhao, G. Li, Y. Liu, and H. Yin, "Research on the Optimization Plan Method based on Electric Vehicles' Scheduling Strategy in Active Distribution Network with Wind/Photovoltaic/Energy Storage Hybrid Distribution System," *IOP Conf. Ser. Mater. Sci. Eng.*, vol. 366, no. 1, 2018, doi: 10.1088/1757-899X/366/1/012025.

[66] S. Cheng and Z. Li, "Multi-objective network reconfiguration considering v2g of electric vehicles in distribution system with renewable energy," *Energy Procedia*, vol. 158, pp. 278–283, 2019, doi: 10.1016/j.egypro.2019.01.089.

[67] S. R. Gampa, K. Jasthi, P. Goli, D. Das, and R. C. Bansal, "Grasshopper optimization algorithm based two stage fuzzy multiobjective approach for optimum sizing and placement of distributed generations, shunt capacitors and electric vehicle charging stations," *J. Energy Storage*, vol. 27, no. November 2019, 2020, doi: 10.1016/j.est.2019.101117.

[68] V. Janamala, U. Kamal Kumar, and T. K. S. Pandraju, "Future search algorithm for optimal integration of distributed generation and electric vehicle fleets in radial distribution networks considering techno-environmental aspects," *SN Appl. Sci.*, vol. 3, no. 4, pp. 1–17, 2021, doi: 10.1007/s42452-021-04466-y.

[69] H. Shokouhandeh, M. Ahmadi Kamarposhti, F. Asghari, I. Colak, and K. Eguchi, "Distributed Generation Management in Smart Grid with the Participation of Electric Vehicles with Respect to the Vehicle Owners' Opinion by Using the Imperialist Competitive Algorithm," *Sustain.*, vol. 14, no. 8, 2022, doi: 10.3390/su14084770.

[70] P. V. K. Babu, K. Swarnasri, and P. Vijetha, "Multi-Objective Optimal planning of Renewable Energy Sources & Electric Vehicle Charging Stations in Unbalanced Radial Distribution Systems using Harris Hawk Optimization Algorithm," *Int. J. Renew. Energy Res.*, vol. 12, no. 1, pp. 58–69, 2022, doi: 10.20508/ijrer.v12i1.12653.g8373.

[71] S. H. Karaki, R. B. Chedid, and R. Ramadan, "Probabilistic performance assessment of autonomous solar-wind energy conversion systems," *IEEE Trans. Energy Convers.*, vol. 14, no. 3, pp. 766–772, 1999, doi: 10.1109/60.790949.

[72] Y. M. Atwa, E. F. El-Saadany, M. M. A. Salama, and R. Seethapathy, "Optimal renewable resources mix for distribution system energy loss minimization," *IEEE Trans. Power Syst.*,

vol. 25, no. 1, pp. 360–370, 2010, doi: 10.1109/TPWRS.2009.2030276.

[73] N. Acharya, P. Mahat, and N. Mithulananthan, “An analytical approach for DG allocation in primary distribution network,” *Int. J. Electr. Power Energy Syst.*, vol. 28, no. 10, pp. 669–678, 2006, doi: 10.1016/j.ijepes.2006.02.013.

[74] K. Prakash and M. Sydulu, “Particle swarm optimization based capacitor placement on radial distribution systems,” in *2007 IEEE Power Engineering Society General Meeting, PES*, 2007. doi: 10.1109/PES.2007.386149.

[75] H. M. Ayres, L. C. P. Da Silva, W. Freitas, M. C. De Almeida, and V. F. Da Costa, “Evaluation of the impact of distributed generation on power losses by using a sensitivity-based method,” *2009 IEEE Power Energy Soc. Gen. Meet. PES ’09*, pp. 1–6, 2009, doi: 10.1109/PES.2009.5275237.

[76] A. Borji, “A new global optimization algorithm inspired by parliamentary political competitions,” *Lect. Notes Comput. Sci. (including Subser. Lect. Notes Artif. Intell. Lect. Notes Bioinformatics)*, vol. 4827 LNAI, pp. 61–71, 2007, doi: 10.1007/978-3-540-76631-5_7.

[77] Q. Askari, I. Younas, and M. Saeed, “Political Optimizer: A novel socio-inspired meta-heuristic for global optimization,” *Knowledge-Based Syst.*, vol. 195, p. 105709, 2020, doi: 10.1016/j.knosys.2020.105709.

[78] A. Zhu, Z. Gu, C. Hu, J. Niu, C. Xu, and Z. Li, *Political optimizer with interpolation strategy for global optimization*, vol. 16, no. 5 May. 2021.

[79] A. Khodabakhshian and M. H. Andishgar, “Simultaneous placement and sizing of DGs and shunt capacitors in distribution systems by using IMDE algorithm,” *Int. J. Electr. Power Energy Syst.*, vol. 82, pp. 599–607, 2016, doi: 10.1016/j.ijepes.2016.04.002.

[80] S. Shyamkant, H. Rajesh, and A. Atul, “Locating , Optimal Sizing and Reliability Analysis of Solar Based DGs in Radial Distribution System,” *J. Inst. Eng. Ser. B*, no. 0123456789, 2022, doi: 10.1007/s40031-022-00826-3.

[81] S. Velamuri, S. H. C. Cherukuri, S. K. Sudabattula, N. Prabaharan, and E. Hossain, “Combined Approach for Power Loss Minimization in Distribution Networks in the Presence of Gridable Electric Vehicles and Dispersed Generation,” *IEEE Syst. J.*, vol. 16,

no. 2, pp. 3284–3295, 2022, doi: 10.1109/JSYST.2021.3123436.

[82] D. Das, H. S. Nagi, and D. P. Kothari, “Novel method for solving radial distribution networks,” *IEE Proc. Gener. Transm. Distrib.*, vol. 141, no. 4, pp. 291–298, 1994, doi: 10.1049/ip-gtd:19949966.

[83] A. P. Hota, S. Mishra, and D. P. Mishra, “Power/energy loss allocation in deregulated power distribution system with load factor and load power factor variation,” *Int. J. Syst. Assur. Eng. Manag.*, vol. 13, no. 1, pp. 250–266, 2022, doi: 10.1007/s13198-021-01227-3.

[84] N. C. Sahoo and K. Prasad, “A fuzzy genetic approach for network reconfiguration to enhance voltage stability in radial distribution systems,” *Energy Convers. Manag.*, vol. 47, no. 18–19, pp. 3288–3306, 2006, doi: 10.1016/j.enconman.2006.01.004.

[85] A. Eid, S. Kamel, and L. Abualigah, “Marine predators algorithm for optimal allocation of active and reactive power resources in distribution networks,” *Neural Comput. Appl.*, vol. 33, no. 21, pp. 14327–14355, 2021, doi: 10.1007/s00521-021-06078-4.

[86] Z. H. Leghari, S. Hussain, A. Memon, A. H. Memon, and A. A. Baloch, “Parameter-Free Improved Best-Worst Optimizers and Their Application for Simultaneous Distributed Generation and Shunt Capacitors Allocation in Distribution Networks,” *Int. Trans. Electr. Energy Syst.*, vol. 2022, 2022, doi: 10.1155/2022/6833488.

[87] R. Ranjan, B. Venkatesh, and D. Das, “Voltage stability analysis of radial distribution networks,” *Electr. Power Components Syst.*, vol. 31, no. 5, pp. 501–511, 2003, doi: 10.1080/15325000390127011.

[88] P. Venkatareddy, K. S. Sambaiah, and N. Samanvita, “Optimal Mix and allocation of Solar and Wind Energy Sources in Active Distribution System Using Jaya Optimization Algorithm,” *Int. Conf. Trends Electr. Electron. Comput. Eng. TEECCON 2022*, pp. 45–49, 2022, doi: 10.1109/TEECCON54414.2022.9854843.

[89] A. P. Hota, S. Mishra, and D. P. Mishra, “Power/energy loss allocation in deregulated power distribution system with load factor and load power factor variation,” *Int. J. Syst. Assur. Eng. Manag.*, vol. 13, no. 1, pp. 250–266, 2022, doi: 10.1007/s13198-021-01227-3.

APPENDICES

A.1.1 IEEE 33 System Data [73, 79].

S.NO	Sending End	Receiving End	Resistance (Ω)	Reactance (Ω)	Nominal Load at Receiving Bus	
					P (kW)	Q (kVAr)
1	1	2	0.0922	0.0477	100	60
2	2	3	0.493	0.2511	90	40
3	3	4	0.366	0.1864	120	80
4	4	5	0.3811	0.1941	60	30
5	5	6	0.819	0.707	60	20
6	6	7	0.1872	0.6188	200	100
7	7	8	0.7114	0.2351	200	100
8	8	9	1.03	0.74	60	20
9	9	10	1.04	0.74	60	20
10	10	11	0.1966	0.065	45	30
11	11	12	0.3744	0.1238	60	35
12	12	13	1.468	1.155	60	35
13	13	14	0.5416	0.7129	120	80
14	14	15	0.591	0.526	60	10
15	15	16	0.7463	0.545	60	20
16	16	17	1.289	1.721	60	20
17	17	18	0.732	0.574	90	40
18	2	19	0.164	0.1565	90	40
19	19	20	1.5042	1.3554	90	40
20	20	21	0.4095	0.4784	90	40
21	21	22	0.7089	0.9373	90	40
22	3	23	0.4512	0.3083	90	50
23	23	24	0.898	0.7091	420	200
24	24	25	0.896	0.7011	420	200
25	6	26	0.203	0.1034	60	25
26	26	27	0.2842	0.1447	60	25
27	27	28	1.059	0.9337	60	20
28	28	29	0.8042	0.7006	120	70
29	29	30	0.5075	0.2585	200	600
30	30	31	0.9744	0.963	150	70
31	31	32	0.3105	0.3619	210	100
32	32	33	0.341	0.5302	60	40

A.1.2 IEEE 69 Data [73, 79].

S.NO	Sending End	Receiving End	Resistance (Ω)	Reactance (Ω)	Nominal Load at Receiving Bus	
					P (kW)	Q (kVAr)
1	1	2	0.0005	0.0012	0	0
2	2	3	0.0015	0.0036	0	0
3	3	4	0.0251	0.0294	0	0
4	4	5	0.366	0.1864	0	0
5	5	6	0.3811	0.1941	2.6	2.2
6	6	7	0.0922	0.047	40.4	30
7	7	8	0.0493	0.0251	75	54
8	8	9	0.819	0.2707	30	22
9	9	10	0.1872	0.0691	28	19
10	10	11	0.7114	0.2351	145	104
11	11	12	1.03	0.34	145	104
12	12	13	1.044	0.345	8	5.5
13	13	14	1.058	0.3496	8	5.5
14	14	15	0.1966	0.065	0	0
15	15	16	0.3744	0.1238	45.5	30
16	16	17	0.0047	0.0016	60	35
17	17	18	0.3276	0.1083	60	35
18	18	19	0.2106	0.069	0	0
19	19	20	0.3416	0.1129	1	0.6
20	20	21	0.014	0.0046	114	81
21	21	22	0.1591	0.0526	5.3	3.5
22	22	23	0.3463	0.1145	0	0
23	23	24	0.7488	0.2745	28	20
24	24	25	0.3089	0.1021	0	0
25	25	26	0.1732	0.0572	14	10
26	26	27	0.0044	0.0108	14	10
27	27	28	0.064	0.1565	26	18.6
28	28	29	0.3978	0.1315	26	18.6
29	29	30	0.0702	0.0232	0	0
30	30	31	0.351	0.116	0	0
31	31	32	0.839	0.2816	0	0
32	32	33	1.708	0.5646	14	10
33	33	34	1.474	0.4673	19.5	14
34	34	35	0.0044	0.0108	6	4
35	35	36	0.064	0.1565	26	18.55
36	36	37	0.1053	0.123	26	18.55

Continuned..

37	37	38	0.0304	0.0355	0	0
38	38	39	0.0018	0.0021	24	17
39	39	40	0.7283	0.8509	24	17
40	40	41	0.31	0.3623	1.2	1
41	41	42	0.041	0.0478	0	0
42	42	43	0.0092	0.0116	6	4.3
43	43	44	0.1089	0.1373	0	0
44	44	45	0.0009	0.0012	39.22	26.3
45	45	46	0.0034	0.0084	39.22	26.3
46	46	47	0.0851	0.2083	0	0
47	47	48	0.2898	0.7091	79	56.4
48	48	49	0.0822	0.2011	384.7	274.5
49	49	50	0.0928	0.0473	384	274.5
50	50	51	0.3319	0.1114	40.5	28.3
51	51	52	0.174	0.0886	3.6	2.7
52	52	53	0.203	0.1034	4.35	3.5
53	53	54	0.2842	0.1447	26.4	19
54	54	55	0.2813	0.1433	24	17.2
55	55	56	1.59	0.5337	0	0
56	56	57	0.7837	0.263	0	0
57	57	58	0.3042	0.1006	0	0
58	58	59	0.3861	0.1172	100	72
59	59	60	0.5075	0.2585	0	0
60	60	61	0.0974	0.0496	1244	888
61	61	62	0.145	0.0738	32	23
62	62	63	0.7105	0.3619	0	0
63	63	64	1.041	0.5302	227	162
64	64	65	0.2012	0.0611	59	42
65	65	66	0.0047	0.0014	18	13
66	66	67	0.7394	0.2444	18	13
67	67	68	0.0047	0.0016	28	20
68	68	69	0.0005	0.0012	28	20

A. 1.3. 28 Indian Bus Data [80-81]

S.NO	Sending End	Receiving End	Resistance (Ω)	Reactance (Ω)	Nominal Load at Receiving Bus	
					P (kW)	P (kVAr)
1	1	2	1.197	0.82	35.28	35.99266
2	2	3	1.796	1.231	14	14.2828
3	3	4	1.306	0.895	35.28	35.99266
4	4	5	1.851	1.268	14	14.2828
5	5	6	1.524	1.044	35.28	35.99266
6	6	7	1.905	1.305	35.28	35.99266
7	7	8	1.197	0.82	35.28	35.99266
8	8	9	0.653	0.447	14	14.2828
9	9	10	1.143	0.783	14	14.2828
10	10	11	2.823	1.172	56	57.1312
11	11	12	1.184	0.491	35.28	35.99266
12	12	13	1.002	0.416	35.28	35.99266
13	13	14	0.455	0.189	14	14.2828
14	14	15	0.546	0.227	35.28	35.99266
15	15	16	2.55	1.058	35.28	35.99266
16	16	17	1.366	0.567	8.96	9.140992
17	17	18	0.819	0.34	8.96	9.140992
18	18	19	1.548	0.642	35.28	35.99266
19	19	20	1.366	0.567	35.28	35.99266
20	20	21	3.552	1.474	14	14.2828
21	21	22	1.548	0.642	35.28	35.99266
22	22	23	1.092	0.453	8.96	9.140992
23	23	24	0.91	0.378	56	57.1312
24	24	25	0.455	0.189	8.96	9.140992
25	25	26	0.364	0.151	35.28	35.99266
26	26	27	0.546	0.226	35.28	35.99266
27	27	28	0.273	0.113	35.28	35.99266

LIST OF PUBLICATIONS

INTERNATIONAL JOURNALS

[1] **N. Dharavat *et al*.**, "Optimal Allocation of Renewable Distributed Generators and Electric Vehicles in a Distribution System Using the Political Optimization Algorithm," *Energies*, vol. 15, no. 18, 2022, doi: 10.3390/en15186698. **Impact Factor: 3.252.**

[2] **N. Dharavat *et al*.**, "Impact of plug-in electric vehicles on grid integration with distributed energy resources: A review," *Front. Energy Res.*, vol. 10, no. January, pp. 1–13, 2023, doi: 10.3389/fenrg.2022.1099890. **Impact Factor: 3.858.**

[3] **N. Dharavat**, S. K. Sudabattula, and V. Suresh, "Optimal Integration of Distributed Generators (DGs) Shunt Capacitors (SCs) and Electric Vehicles (EVs) in a Distribution System (DS) using Marine Predator Algorithm," *Int. J. Renew. Energy Res.*, vol. 12, no. 3, pp. 1637–1650, 2022, doi: 10.20508/ijrer.v12i3.13230.g8550.

[4] **N. Dharavat**, S. K. Sudabattula, and V. Suresh, "Optimal Allocation of Multiple Distributed Generators and Shunt Capacitors in a Distribution System Using Political Optimization Algorithm," *Int. J. Renew. Energy Res.*, vol. 11, no. 4, pp. 1479–1488, 2021, doi: 10.20508/ijrer.v11i4.12240.g8349.

[5] S. Gupta, A. M. Singh, S. Mishra, P. Vishnuram, **N. Dharavat**, S. Kalyan, K. M. Aboras, N. K. Sharma, and M. Bajaj, "Estimation of solar radiation and diminish of solar radiation due to anthropogenic substances at any location — A review," *Sustainability,* pp. 1–32, 2023. **Accepted for Publication**, **Impact Factor: 3.889.**

[6] R. Thakur, S. Mishra, S. K. Sudabattula, and **N. Dharavat**, N. K. Sharma "Modeling and Simulation of Hydropower Plant in Islanded Mode for Different Operating Conditions," *IEEE Access*. **Communicated**, **Impact Factor: 3.476.**

[7] NK. Golla, **N. Dharavat**, S. K. Sudabattula,V. Suresh, MVVP. Kantipudi, H. Kotb, Y. Y. Ghadi, R. Djidimbele "Techno-Economic Analysis of Distribution System with Integration of Distributed Generators and Electric Vehicles," *Frontiers in Energy Research*. **Under Review**, **Impact Factor: 3.858.**

INTERNATIONAL CONFERENCES

[1] **N. Dharavat**, S. K. Sudabattula, and S. Velamuri, “Integration of Distributed Generation and Electric vehicles in a distribution network using Political Optimizer,” *2021 4th Int. Conf. Recent Dev. Control. Autom. Power Eng. RDCAPE 2021*, vol. 3, pp. 521–525, 2021, doi: 10.1109/RDCAPE52977.2021.9633448.

[2] **N. Dharavat**, S. K. Sudabattula, and S. Velamuri, “Review on the Integration of Distributed Generations (Solar, Wind) and Electric Vehicles Connected to the Distribution System to Minimize Power Loss and Voltage Profile Enhancement,” *AIP Conf. Proc.*, vol. 2455, no. October, 2022, doi: 10.1063/5.0100957.

[3] V. Kumar, S. K. Sudabattula, and **N. Dharavat**, “Optimal integration of renewable distributed generators and electric vehicles in a radial distributed network,” *J. Phys. Conf. Ser.*, vol. 2327, no. 1, 2022, doi: 10.1088/1742-6596/2327/1/012010.

[4] A. Shaik, S. K. Sudabattula, and S. Mishra, and **N. Dharavat** “Optimal Placement of Solar and Wind Distributed Generators in Radial Distribution System,” *AIP Conf. Proc.*2023. **Accepted for Publication**.

BOOK CHAPTERS

[1] **N. Dharavat**, S. K. Sudabattula, and N. K. Golla, “Optimal Integration of Distributed Generators and Electric Vehicle Charging Stations in the Distribution System Using a Hybrid Approach,” *Intelligent System and Applications. Lecture Notes in Electrical Engineering. Springer, Singapore*. **Accepted For Publication**.

COPYRIGHT

Filed copyright ID-67157, on Title:

Assessment of distribution system with integration of distributed energy resources and electric vehicles